unesp UNIVERSIDADE ESTADUAL PAULISTA
"JÚLIO DE MESQUITA FILHO"
CAMPUS DE GUARATINGUETÁ

THERMODYNAMIC, ECONOMIC AND EMISSIONS ANALYSIS OF A MICRO GAS TURBINE COGENERATION SYSTEM OPERATING ON BIOFUELS

Guaratinguetá - São Paulo
BRAZIL
2015

unesp UNIVERSIDADE ESTADUAL PAULISTA
"JÚLIO DE MESQUITA FILHO"
CAMPUS DE GUARATINGUETÁ

BENJAMIN KUNTE

Thermodynamic, Economic and Emissions Analysis of a Micro Gas Turbine Cogeneration System operating on Biofuels

Guaratinguetá - SP
2015

UNESP
Universidade Estadual Paulista "Júlio de Mesquito Filho"
Campus de Guaratinguetá

Benjamin Kunte

Thermodynamic, Economic and Emissions Analysis of a Micro Gas Turbine Cogeneration System operating on Biofuels

Dissertation submitted to the Faculty of Engineering of Guaratinguetá, São Paulo State University, to obtain the title of Master in Mechanical Engineering in the field of Energy.

Supervisor: Prof. Dr. José Alexandre Matelli
Co-Supervisor: Prof. Dr. José Luz Silveira

Guaratinguetá - SP
2015

Kunte, Benjamin
K96t Thermodynamic, economic and emissions analysis of a micro gas turbine cogeneration system operating on biofuels / Benjamin Kunte – Guaratinguetá, 2015.
101 f. : il.
Bibliografia : f. 96-101

Dissertação (Mestrado) – Universidade Estadual Paulista, Faculdade de Engenharia de Guaratinguetá, 2015.
Orientador: Prof. Dr. José Alexandre Matelli
Coorientador: Prof. Dr. José Luz Silveira

1. Biocombustíveis 2. Turbinas a gás 3. Biogás I. Título

CDU 620.91 (043)

unesp

UNIVERSIDADE ESTADUAL PAULISTA
CAMPUS DE GUARATINGUETÁ

BENJAMIN KUNTE

ESTA DISSERTAÇÃO FOI JULGADA ADEQUADA PARA A OBTENÇÃO DO TÍTULO DE
"MESTRE EM ENGENHARIA MECÂNICA"

PROGRAMA: ENGENHARIA MECÂNICA
ÁREA: Energia

APROVADA EM SUA FORMA FINAL PELO PROGRAMA DE PÓS-GRADUAÇÃO

Prof. Dr. Edson Cocchieri Botelho
Coordenador

BANCA EXAMINADORA:

Prof. Dr. JOSÉ ALEXANDRE MATELLI
UNESP/FEG

Prof. Dr. CELSO EDUARDO TUNA
UNESP/FEG

Prof. Dr. PEDRO TEIXEIRA LACAVA
ITA

Dezembro de 2015

CURRICULUM VITAE

Benjamin Kunte

BIRTH	14.05.1991 – HEIDELBERG / GERMANY
PARENTS	Christian Herbert Werner Kunte Bettina Susanne Kunte
2007-2010	High School Graduation: Ludwig-Frank-Gymnasium Mannheim, GERMANY
2010-2014	Bachelor of Science in Mechanical Engineering, at the University of Applied Sciences, Hochschule Mannheim, GERMANY
2014-2015	Master of Science in Mechanical Engineering, at Faculty of Engineering of Guaratinguetá, São Paulo State University, BRAZIL.

in particular, to my fiancée Natalia, for giving me the motivation to finish this work, and my parents Christian and Susanne for always supporting me.

ACKNOWLEDGEMENTS

To my supervisor, Prof. Dr. José Alexandre Matelli who never stopped encouraging me. Without his guidance, dedication and assistance, the presented study would not have been possible.

To Prof. Dr. José Luz Silveira and Prof. Dr. Celso Eduardo Tuna for their time, feedback, ideas and support.

“I am not a product of my circumstances. I am a product of my decisions.”

Stephen R. Covey

“Everything should be made as simple as possible, but not simpler.”

Albert Einstein

KUNTE, B. **Thermodynamic, economic and emissions analysis of a micro gas turbine cogeneration system operating on biofuels.** 2015. 101 p. Dissertation (Master in Mechanical Engineering) - Faculty of Engineering of Guaratinguetá, São Paulo State University, Guaratinguetá, 2015.

ABSTRACT

The most promising methods to reduce greenhouse gases as well as counteract against the imminent depletion of fossil fuels are: a) the use of alternative fuels obtained from biomass, such as biogas or bio-syngas; b) enhancing the power plant efficiency by decreasing the percentage of useful energy lost to the environment. Whereas efficiency optimisation of a particular machine in a power plant, e.g. gas turbine or compressor, is a very longsome development, cogeneration can quickly and significantly increase the overall efficiency of a power plant. In this work, energetic, exergetic, emissions and economic analyses of a cogeneration system consisting of a 200 kW micro gas turbine combined with a heat recovery steam generator are introduced and conducted. Furthermore, biogas and syngas operation are compared to natural gas operation, to investigate the adequacy of these two alternative fuels for use in micro gas turbines. The proposed cogeneration plant proved to be technically feasible for all fuels, because the selected micro gas turbine Capstone C200 is available in various, fuel-specific versions with optimised fuel injection systems. The plant presented overall energetic efficiencies of 50.9%, 48.6% and 47.9% for natural gas, biogas and syngas operation, respectively. Due to very high natural gas and syngas prices, the cogeneration plant presented economic feasibility only in case of biogas operation, with short payback periods of approximately 2.8 years and high expected annual saving. Moreover, biogas has the highest ecologic efficiency and was therefore found to be the best alternative to fossil fuels.

KEYWORDS: Biogas. Cogeneration. Exergetic Analysis. Micro Gas Turbine. Syngas.

KUNTE, B. **Análise termodinâmica, econômica e de emissões de sistemas de cogeração baseados em microturbinas operando com biocombustíveis.** 2015. 101 f. Dissertação (Mestrado em Engenharia Mecânica) – Faculdade de Engenharia do Campus de Guaratinguetá, Universidade Estadual Paulista, Guaratinguetá, 2015.

RESUMO

Os métodos mais promissores para reduzir gases de efeito estufa, bem como combater o iminente esgotamento das reservas de energia fóssil, são: a) o uso de combustíveis alternativos obtidos a partir da biomassa, como o biogás ou gás de síntese (syngas); b) o aumento da eficiência do sistema através da redução da percentagem de energia útil perdido para o ambiente. Enquanto a otimização da eficiência de uma determinada máquina da central elétrica, por exemplo, turbina a gás ou compressor, é um desenvolvimento muito demorado, a cogeração pode rápida e significativamente aumentar a eficiência global da central. Neste trabalho, análise termodinâmica, econômica e de emissões de um sistema de cogeração baseado em uma microturbina a gás de 200 kW combinado com uma caldeira de recuperação são conduzidas. Além disso, a operação de biogás e syngas é comparada com a operação de gás natural para investigar a pertinência destes dois combustíveis alternativos para o uso em micro turbinas a gás. A central de cogeração proposta mostrou-se tecnicamente viável para todos os combustíveis, porque a microturbina selecionada é disponível em várias versões, específicas para cada combustível, com sistemas de injeção de combustível otimizados. A central apresentou eficiências energéticas globais de 50,9%, 48,6% e 47,9% para operação com gás natural, biogás e syngas, respectivamente. Devido aos preços muito elevados do gás natural e do syngas, a central de cogeração apresentou viabilidade econômica apenas no caso de operação com biogás, com curtos períodos de retorno de aproximadamente 2,8 anos e alta economia anual esperada. Além disso, o biogás tem a maior eficiência ecológica e, portanto, apresentou-se como a melhor alternativa aos combustíveis fósseis.

PALAVRAS-CHAVE: Biogás. Cogeração. Análise Exergética. Microturbina a Gás. Syngas.

LIST OF FIGURES

LIST OF TABLES

LIST OF ABBREVIATIONS AND ACRONYMS

BRL	Brazilian Real
CHP	Combined Heat and Power
CG	Combustion Gases
EES	Engineering Equation Solver
HRSG	Heat Recovery Steam Generator
LHV	Lower Heating Value
MGT	Micro Gas Turbine
NG	Natural Gas
USD	United States Dollar
WWTP	Wastewater Treatment Plant

LIST OF SYMBOLS

a	Altitude	[m]
C_{el}	Power production costs	[USD/kWh]
CF_{Eff}	Correction factor for Efficiency	[-]
CF_P	Correction factor for Power output	[-]
C	Cost or Price	[USD/kWh]
$C_{M,cb}$	Maintenance and operation costs of conventional boiler system	[USD/kWh]
$C_{M,gts}$	Maintenance and operation costs of MGT system	[USD/kWh]
$(CO_2)_e$	CO_2-equivilent of exhaust gases	[kg/kg]
(CO_2)	Mass of CO_2 in exhaust gases per mass of fuel	[kg/kg]
(SO_2)	Mass of SO_2 in exhaust gases per mass of fuel	[kg/kg]
(NO_x)	Mass of NO_x in exhaust gases per mass of fuel	[kg/kg]
C_{spc}	Conventional boiler steam production costs	[USD/kWh]
C_{st}	Steam production costs	[USD/kWh]
c_p	Specific heat at constant pressure	[kJ/kg K]
E_{el}	Power generated by MGT	[kW]
$Effec_{rec}$	Effectiveness of recuperator	[-]
E_{fuel}	Energy supplied by fuel per unit of time	[kW]
EM	Mass of pollutant in combustion emissions per mass of fuel	[kg/kg]
E_R	Heat flow recovered from exhaust gases	[kW]
E_{los}	Energy losses per unit of time	[kW]
E_{st}	Heat flow effectively transferred into water / steam in HRSG	[kW]
ex_i	Specific exergy at point i	[kJ/kg]
Ex	Exergy	[kJ]
$\dot{E}x_i$	Exergy flow rate at point i	[kW]
f	Annuity factor	[$year^{-1}$]
f_{cAlt}	Correctional coefficient for local altitude	[-]
f_{cT}	Correctional coefficient for local temperature	[-]
f_{cUe}	Correctional coefficient for local humidity	[-]
g	Gravitational acceleration	[m/s^2]
H	Hours of operation per year	[h/year]
H_i	Total enthalpy at point i per unit of time	[kW]
h_i	Specific enthalpy at point i	[kJ/kg]
h_p	Specific enthalpy of the saturated liquid in HRSG	[kJ/kg]
HR	Heat Rate	[kJ/kWh]
I_j	Irreversibility of component j	[kW]
I_{HRSG}	Investment in the HRSG	[USD]
I_{MGT}	Investment in the MGT	[USD]
I_{gts}	Investment in the gas turbine system	[USD]
k	Payback, amortisation period of the investment	[years]
k_{civ}	Factor for civil engineering and transportation cost	[-]
k_{import}	Factor for import and tax cost	[-]
LHV	Lower heating value (natural gas, biogas or syngas)	[kJ/kg]

M	Molar mass	[g/mol]
$\dot{m}_{air}$	Inlet air flow	[kg/s]
$\dot{m}$	Mass flow	[kg/s]
$\dot{m}_{st,ai}$	Steam flow in HRSG calculated using initial exhaust temp. T_{7ai}	[kg/s]
$\dot{m}_{st}$	Steam flow in HRSG adjusted by *pinch point*	[kg/s]
N	Number of moles	[mol]
n_{H2S}	Mass of H_2S in the fuel per mass of fuel	[kg/kg]
P_0	Average sea-level pressure	[kPa]
P_a	Local atmospheric pressure	[kPa]
P_{el}	Electric energy price	[USD/kWh]
P_{oil}	Price of fuel oil used in conventional steam generators	[USD/kWh]
p_s	Process steam pressure	[kPa]
p_i	Pressure at point i	[kPa]
PR	Pressure ratio of the compressor	[-]
q	Interest rate quotient	[-]
r	Annual interest rate	[%]
R	Gas constant	[kJ/kg K]
R_u	Universal gas constant	[kJ/kg K]
Re	Expected annual saving	[USD]
s_i	Specific entropy at point i	[kJ/kg K]
T_0	Ambient temperature	[°C]
T_{7ai}	Initially adopted exhaust gas temperature at point 7	[°C]
T_i	Temperature at point i	[°C]
T_p	Temperature of exhaust gases at dew point in HRSG	[°C]
T_S	Saturation temperature corresponding to p_S	[°C]
U_e	Specific humidity	[%]
U_{rel}	Relative humidity	[%]
W	Work / Power	[kW]
w_{CO2}	Mol of CO_2 in exhaust gases per mol of fuel.	[mol/mol]
W_{elGT}	Power output of MGT	[kW]
W_{shaft}	Power in turbine transferred into electric generator	[kW]
%EA	Amount of excess air	[%]

Greek letters:

β	Power to heat ratio of cogeneration plant	[-]
δ	Specific heat ratio (c_p / c_v)	[-]
Δp	Pressure losses	[-]
ΔT_{pp}	Pinch point temperature difference	[°C]
Δh^0	Enthalpy of formation	[kJ/mol]
ε	Exergetic efficiency (second-law efficiency)	[-]
ε_{eco}	Ecologic efficiency	[-]
Πg	Pollution indicator	[kg/MJ]
η	Energetic efficiency	[-]

η_{isoTG}	Isentropic efficiency of gas turbine	[-]
ρ_{air}	Air density	[kg/m³]
φ	Ratio of chemical exergy to LHV of fuel	[-]
ψ_j	Rational efficiency of component j	[-]

Subscripts:

0	Reference or ambient state (25°C, 101.325 kPa)
a	Combustion air per mass of fuel
air	Air
as	Stoichiometric combustion air per mass of fuel
back	Back pressure
BIO	Biogas
c	compressor
cb	Conventional boiler for steam generation
cc	Combustion chamber
cg	Combustion gases
comp	Compressor
el	Electricity / Power
FPO	Cost related to the fuel per plant output
fuel	Fuel (natural gas, biogas or syngas)
GB	Gas booster (compressor) for biogas and syngas compression
ger	Power generator
GT	Gas turbine
gts	Gas turbine system
HRSG	Heat recovery steam generator
i	At point i (1, ... , 10)
inlet	Inlet pressure drop caused by air filtering
INV	Costs related to the initial investment in the plant
ISO	At ISO conditions
M	Maintenance and operation
MGT	Micro gas turbine
NG	Natural gas
P	Products of combustion
pp	Pinch point
rec	Recuperator (air pre-heater)
R	Reactants of combustion
s	Sensible enthalpy
shaft	Turbine shaft (to electric generator)
scp	Steam production cost using amortised conventional boilers burning fuel oil
st	Steam
SYN	Syngas
u	Universal

Superscripts:

‘	Not yet adjusted to local conditions
CH	Chemical exergy
KIN	Kinetic exergy
PH	Physical exergy
PT	Potential exergy

TABLE OF CONTENTS

1 INTRODUCTION

1.1 GENERAL INFORMATION

One of the most important – if not the single most important – challenges that scientists and engineers of our time are facing around the world is the reduction of global warming. Moreover, mankind as a whole, including politicians, scientists, engineers and others, must rapidly increase its efforts to diminish greenhouse gases as well as pollution and preserve the world we live in. Thus, minimisation of greenhouse gases released into the atmosphere has become a major goal in the field of power generation.

Nevertheless, fuel-fired power plants will remain the predominant source for power generation in the foreseeable future, because alternative energies such as nuclear power, solar power, wind power and hydropower all underlie their own limitations and problems such as environmental impacts, disproportionately high costs, fluctuating generating conditions and regional restrictions, to only name a few. Therefore, the most promising methods to reduce the greenhouse gases in the atmosphere are the use of alternative fuels such as biogas or syngas (obtained from biomass) and enhancing the power plant efficiency by decreasing the percentage of useful energy lost to the environment. The main advantage of biogas and syngas, besides being renewable energy sources, is that their use in thermal power plants is considered cleaner than natural gas (NG) use, in regard to the whole life cycle of the carbons. As a result, the carbon-dioxide-equivalents of the emissions released into the atmosphere are lower, which reduces the environmental impacts, especially regarding global warming. Additionally, the use of biogas or syngas can counteract against the imminent depletion of fossil fuels. Furthermore, whereas efficiency optimisation of a particular machine in a power plant, e.g. gas turbine or compressor, is a very longsome development, cogeneration is a relatively simple and quickly applicable method to significantly increase the overall efficiency of any thermal power plant. Cogeneration is defined as the simultaneous generation of mechanical energy and useful heat, e.g. power and saturated steam.

Biogas is obtained by anaerobic digestion of organic matter and consists mainly of methane and carbon dioxide. There are many studies regarding its obtainment and there are various types of digesters around the world that use human or animal residues as well as sugar or starch crops for the production of the gas. Most of the time, the digesters are installed along with wastewater treatment plants (WWTP), which makes this a source of renewable energy replacing fossil fuel sources (CORONADO, 2007). Among all fossil fuels, NG is the least

polluting. According to Somehsaraei et al. (2014), electrical efficiency of micro gas turbine (MGT) systems decreases together with the percentage of methane in the fuel. However, biogas use is encouraged because the reduction in energy efficiency is less than 1% when comparing NG (90% methane) and biogas (45% methane) firing (SOMEHSARAEI et al., 2014).

Syngas, also known as synthesis gas, is produced by gasification of biomass or other solid fuels. Similar to biogas, the crude gas must pass through cleaning and filtering processes before being effectively useable in power generation. Furthermore, syngas also has great importance in researches and in the pursuit of renewable energy sources. Although its obtaining technique was already well known, it ceased to matter after World War II and only returned to relevance in the late 20th and early 21st century due to the oil crisis, environmental problems and the imminent depletion of fossil fuels (SIEDLECKI; DE JONG; VERKOOIJEN, 2011). In Brazil, the use of synthesis gas is very attractive due to the large production of biomass in the form of bagasse from sugarcane mills. In this sense, the gasification of biomass presents an important alternative to fuel MGTs generating power and useful heat. Likewise, the technology of obtaining biogas through anaerobic digestion at WWTPs is also highly recommendable, since it uses a material as a source which is found in large quantity and was previously not taken advantage of.

Besides the search for renewable and cleaner energy sources, another focal point is the rational use of primary energy. The higher the percentage of fuel energy converted into useable energy, the greater the overall efficiency of the system – even more so, if taking into account the effects on the environment. In this context of efficiency optimisation lays the importance of implementing cogeneration plants. Cogeneration consists of the combined generation of mechanical energy and useful heat by recovering thermal energy from the exhaust gases. The mechanical energy can be used to drive equipment or to generate power, while the heat can be directly applied into a process (e.g. to heat the digesters in WWTPs) or indirectly used to produce steam, hot water or chilled water. According to Silveira (1994), the efficiency of thermal power plants increases from a range of 34 - 50% to 50 - 90% by implementing cogeneration, since heat previously lost into the atmosphere is recovered and made useful.

In Brazil, after commencing the use of the great hydro potential to generate electricity in the 1950s, the use of thermoelectric plants and the interest to invest in cogeneration plants decreased. This topic only recently regained importance due to the presented advantages and the imminent depletion of fossil fuel reserves. For Coronado, Yoshioka and Silveira (2011),

cogeneration has proven to be the best alternative considering the optimal fuel consumption and high overall plant efficiency.

Cogeneration is already widely used in the industrial sector. For the tertiary sector, however, the implementation is not always feasible. Thus, MGTs are chosen for the cogeneration system due to the small size of the machines, enabling increased mobility and easy maintenance. In the literature, several studies researching and describing cogeneration systems operating in different conditions can be found (SILVEIRA; WALTER; LUENGO, 1997; BRIZI et al., 2014).

1.2 OBJECTIVE

The objective of this dissertation is to conduct energetic, exergetic, emissions and economic analyses of a cogeneration system consisting of a MGT generating power combined with a heat recovery steam generator (HRSG) producing saturated steam. Moreover, biogas and syngas firing are compared to NG firing to investigate how suitable these two renewable fuels are for the use in MGTs.

In the energetic analysis, the ISO-condition-data of the gas turbine Capstone C200 obtained from its manufacturer are adjusted to the climatic conditions of Guaratinguetá. Hereupon, the important energetic data are calculated for the principle points of the system to obtain the energetic efficiencies of all the single components, and of the plant as a whole.

The exergy analysis determines the exergies at each point and the irreversibilities and exergetic efficiencies of each component. Additionally, the total irreversibility and the overall exergetic efficiency are calculated.

Through the emissions analysis, plant CO_2-equivalent for each fuel, pollution indicator and ecologic efficiency are all determined.

Finally, the economic analysis calculates and compares the power generation and steam production costs of the proposed plant with traditional production costs to predict the annual saving and payback period of the system.

1.3 PROPOSED COGENERATION PLANT

The proposed cogeneration plant consists of a MGT system including compressor, combustion chamber and power generator, as well as a HRSG. The selected MGT is the

Capstone C200 with a nominal power output of 200 kW (see Figure 1). A schematic overview of the complete cogeneration plant is shown in Figure 12.

Figure 1 - Capstone C200 MGT

Source: (CAPSTONE TURBINE CORPORATION, 2015).

1.4 STRUCTURE

The chapter “literature review” presents information and fundamentals about the proposed MGT cogeneration system as well as the analysed fuels NG, biogas and syngas. In chapter three, titled “material and method”, energetic, exergetic, emissions and economic analyses are introduced, described and conducted for the proposed system. Subsequently, the results of the aforementioned analyses are illustrated and discussed. The last chapter is the conclusion, rounding of the work, summarising the meaning of the results and proposing further studies.

2 LITERATURE REVIEW

This chapter presents information and fundamentals about the proposed MGT cogeneration system, as well as the analysed fuels NG, biogas and syngas.

2.1 MICRO GAS TURBINES AND COGENERATION

Gas turbines with a power output of up to several hundred kW are usually labelled as MGTs – but as there is no official definition, each author can define the range more or less arbitrarily. The MGT mainly considered in this dissertation is the Capstone C200 with a power output of 200 kW. Some of the advantages of MGTs are their fuel flexibility and low maintenance costs. The most interesting application of these small turbines lies in distributed power generation. One of the principal advantages that several small plants have over a single larger power plant is the reduction in transmission losses.

The military and aerospace industries were the first to invest in MGTs. In these two sectors, the importance of compact, light-weight and high-powered generators traditionally outweighs the high requirements of MGTs in terms of development and production costs (PILAVACHI, 2002). Starting from there, the manufacturers developed the turbines into one of the primary power generation systems. A typical micro turbine is single-stage and single-shaft with a comparably low pressure ratio. Optionally, the turbine system can include a recapture of the exhaust gases to preheat the compressed air – in this case, it is called a regenerative gas turbine. This increases the electric efficiency of the system, while decreasing the potential to generate useful heat through cogeneration.

To support the understanding of turbines, Figure 2 shows an inside view of the MGT Capstone C65. Just like most MGTs, the C65 is single shaft, meaning that the turbine, compressor and generator are installed on a single shaft. The inlet air, depending on the model, can be used to cool the power generator. After being compressed, the air is pre-heated in the recuperator. Subsequently, the air enters the combustion chamber and is mixed with the fuel. After combustion, the high-temperature and high-pressure combustion gases are expanded in the turbine and transfer parts of their energy onto the shaft. This energy is used to drive the compressor and generate power using the generator. Leaving the turbine, the gases pass through the recuperator, transferring part of their thermal energy into the compressed air.

Finally, the exhaust gases leave the turbine through the outlet – steel hot enough to be further utilised.

Figure 2 - Cutaway view of a Capstone C65 MGT

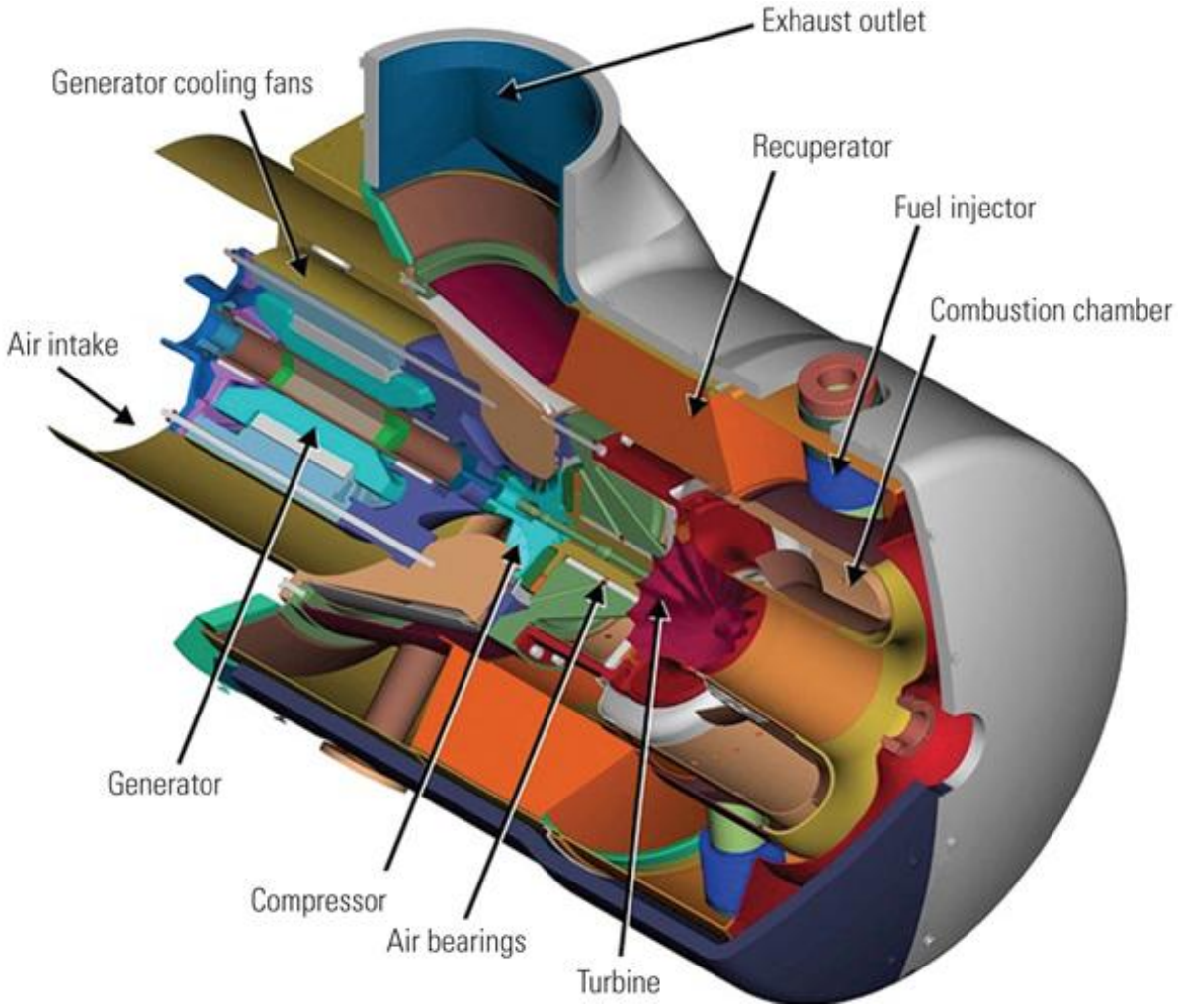

Source: (GILLETTE, 2010).

MGTs are traditionally designed for NG burning. The use of biofuels usually requires costly engine modifications. This is mainly due to the fact that biofuels have significantly smaller lower heating values (LHV) than NG. Therefore, the fuel flow rate has to be drastically increased to maintain the same energy input. The main component that needs to be modified to the higher fuel flow rate is the combustion chamber, but also the fuelling system (fuel injectors, fuel valve etc.) needs to be adjusted. Nikpey et al. (2014) researched the possibility of using a NG and biogas mixture, to avoid turbine modifications and to use NG as a fallback option in case of biogas shortage or a change in the biogas composition, to increase availability. Various mixtures (from 0% biogas up to 39% biogas) were tested for the whole

range of power output. As the load increases, the highest usable percentage of biogas decreases – at full load, the limit was found to be 26%. The use of this mixture reportedly reduces CO_2 emissions by about 19% at full load. The paper also states that the mixture neither has a significant influence on the electrical efficiency nor on the operating parameters.

The higher the percentage of fuel energy converted into useable energy, the greater the overall efficiency of the system – even more so, if taking into account the effects on the environment. In this context of efficiency optimisation lays the importance of implementing cogeneration plants. Cogeneration consists of the combined generation of mechanical energy and useful heat by recovering thermal energy from the exhaust gases. The mechanical energy can be used to drive equipment or to generate power, while the heat can be directly applied into a process (e.g. to heat the digesters in WWTPs) or indirectly used to produce steam, hot water or chilled water.

Cogeneration is already widely used in the industrial sector. For the tertiary sector, however, the implementation is not always feasible due to the comparably small capacities. In this output range, gas turbines demonstrate various advantages in comparison to other engine technologies, such as relatively small size and weight, less moving parts and noise as well as the opportunity to use alternative fuels (PILAVACHI, 2002). Thus, MGTs are chosen for this cogeneration system, mainly due to their high temperature exhaust gases, the increased mobility and the decreased maintenance costs. According to the manufacturer Capstone, the C200 can be fuelled by natural gas, biogas and others. To optimise their efficiency, every combined heat and power (CHP) plant requires a precise calibration of electrical and thermal load to ensure that the generated heat will be used by the consumer – electricity can usually be fed into the grid easily, if connected. Thereby, the highest overall efficiency is usually achieved, if the plant operates in thermal match mode, meaning that it follows the thermal load requirements.

The most common technologies to recover heat from the exhaust gases of a thermal power engine are the absorption refrigeration system to produce chilled water and the heat recovery steam generator (HRSG). The second-mentioned basically consists of a non-firing, convection heat exchanger system (economiser, evaporator and superheater) generating steam. There are two main types of HRSG – with or without supplementary heating. The simpler one without supplementary heating can recover up to 95% of the exhaust gas heat to generate steam (ANTUNES, 1999). The models including supplementary heating are mainly applied to generate a larger amount of steam, or to generate superheated steam. Moreover, it

allows a better controlling and managing of the produced useful heat flow. This may or may not be desired.

In their paper, Somehsaraei et al. (2014) investigated the fuel flexibility of MGT and analysed their performance using biogas. For biogas application, the exhaust gas flow and the pressure ratio decreased in comparison to NG use. Furthermore, the paper states that the electrical efficiency of micro gas turbine (MGT) systems declines with decreasing methane content and therewith decreasing LHV of the fuel. However, biogas use is encouraged, as the reduction in energy efficiency is only about 0.7% when comparing operation using NG (ca. 90% methane) and biogas (45% methane).

According to Gillette (2010), another advantage of MGTs in comparison to other power generating engines is the considerably cleaner exhaust gases. This can lead to a major investment advantage if a costly active exhaust clean-up is not necessary to meet given pollution restrictions. Furthermore, various MGTs can be combined to create a micro-grid with a higher power output but yet simple controlling and managing. For example, five Capstone C200 MGTs can be connected for a 1 MW power output. This provides a higher flexibility regarding the system's load, as the modules can separately be turned on and off to meet the instantaneous load. Thus, the running sub-systems still operate at full-load with maximum efficiency. Figure 3 demonstrates the efficiency difference in partial load between five connected C200 MGTs in comparison to a single larger turbine. The area in-between the two curves equates to the potential fuel savings.

Figure 3 - Comparison of partial load of a MGT micro-grid

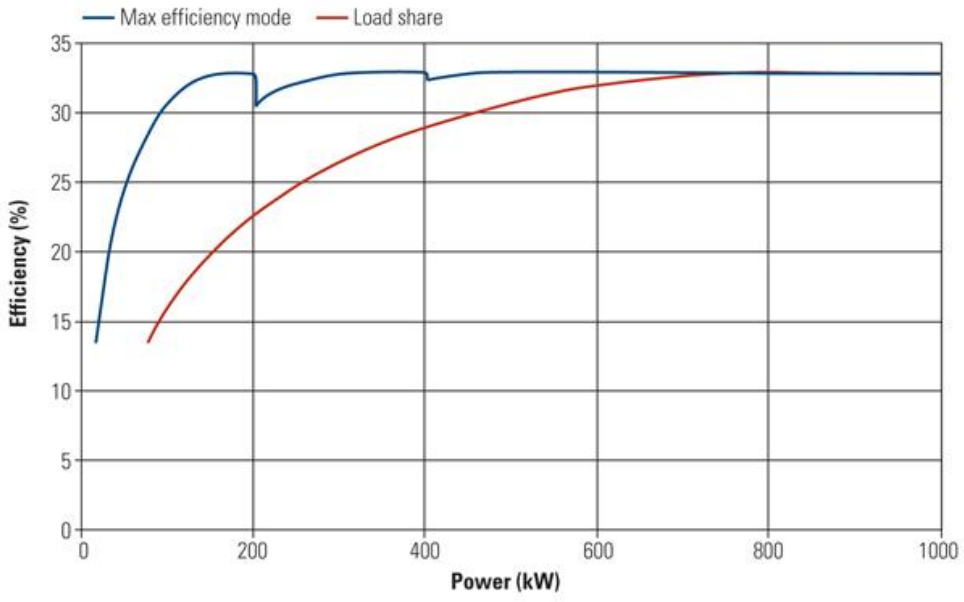

Source: (GILLETTE, 2010).

2.2 NATURAL GAS

Natural gas is the least polluting among all fossil fuels. The exact composition of NG can vary significantly, but usually about 90 vol% of it is methane. Other components are ethane, propane, butane and carbon dioxide. Furthermore, it can contain water and contaminants such as nitrogen. As NG itself is odourless, sulphur compounds have to be added for safety reasons. In accordance to the main provider of NG in São Paulo, COMGÁS (2015a), Table 1 shows the typical composition of NG in São Paulo.

Table 1 – Typical natural gas composition in São Paulo

COMPONENT	VOLUME (%)	MOLAR MASS (g/mol)	MASS (%)	LHV (kJ/kg)
CH_4	88.68	16.04	77.09	50,023*
C_2H_6	5.84	30.07	9.52	47,508*
C_3H_8	2.34	44.10	5.59	46,330*
C_4H_{10}	0.77	58.12	2.43	45,348*
C_5H_{12}	0.13	72.15	0.50	44,974*
C_6H_{14}	0.03	86.16	0.12	44,742*
CO_2	1.62	44.01	3.85	–
N_2	0.59	28.01	0.90	–
Total	100.00	18.45	100.00	47,053

Source: (COMGÁS, 2015a). *from EES

An ideal complete combustion would emit only CO_2 and water vapour, but a real process is much more complex. The principal components of the exhaust gases produced by gas turbines running on NG are carbon oxides (CO_2 and traces of CO), sulphur oxides (SO_2 and SO_3) and nitrous oxide (NO and NO_2, usually termed NO_x). While the carbon and nitrous oxides have a direct influence on global warming, the most commonly known effect of sulphur oxides is acid rain (VILLELA, 2007).

2.3 BIOMASS

The term biomass describes all organic matter (biological material from living or dead organisms), the largest part of it being vegetable plants, and is the only renewable carbon-containing energy source. All these biological materials contain chemical energy – plants store this energy by withdrawing CO_2 from the atmosphere during photosynthesis. Therefore, biomass is considered to have a CO_2-neutral lifecycle, as the same amount of CO_2 is released back into the atmosphere through e.g. burning of biomass (BOERRIGTER; RAUCH, 2005). Biomass can be converted into varies forms of biofuels through biological, chemical and thermochemical processes – making it usable for different applications. Only a very small part of all the biomass on earth is available for human use, and an even smaller fraction is used to produce fuel. In the context of fuels and energy production, the vegetable biomass can be divided into three groups: lignocellulosic biomass composed of carbohydrate polymers (e.g. wood and straw), biomass with a high sugar content (e.g. sugar cane, wheat and maize) and oleaginous biomass (e.g. sunflower, soya and rapeseed). Furthermore, other common sources to produce biofuels are industrial, animal and municipal wastes and residues including the sludge produced in wastewater treatment plants (WWTP). The production of biofuels from wastes is especially environmentally friendly, as this potential was previously not taken advantage of and would otherwise simply be lost. According to Silva et al. (2013), besides the mentioned environmental advantages, the use of biofuels can also offer major economical advantages, as their lower cost can reduce the operational costs despite their small LHV.

The largest percentage of energy obtained from biomass is still the traditional combustion of wood or other plants for heating and cooking purposes. This especially takes place in developing countries. In industries, on the other hand, biomass is converted into varies forms of biofuels through processes such as anaerobic digestion (biogas), gasification (syngas), fermentation (ethanol), transesterification (biodiesel) and others. Figure 4 gives an overview of the biomass to bio-fuel conversion processes.

In Figure 4, the conversion steps are marked with coloured box-filling. The colour light blue represents biological processes, yellow filling indicates chemical processes and purple shows thermochemical processes. Furthermore, in accordance to Gerssen-Gondelach et al. (2014), commercially well-established technologies are highlighted with red arrows and frames, and early commercial technologies are distinguished with green arrows and frames. The black technologies are still in the development, prototype and demonstration phases.

Figure 4 - Schematic overview of biomass to bio-fuel conversion chains

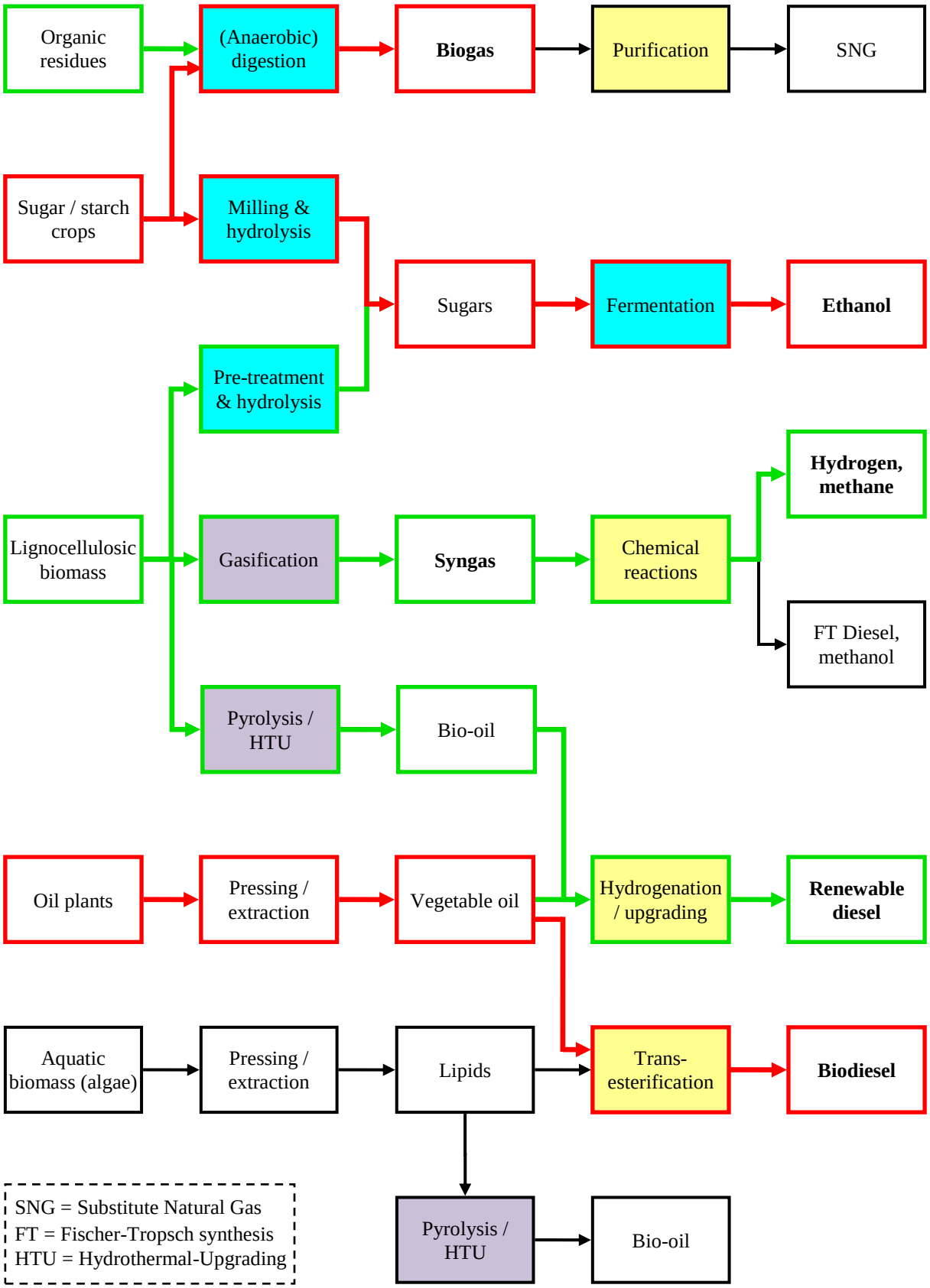

Source: (based on GERSSEN-GONDELACH et al., 2014).

2.4 BIOGAS

Biogas is obtained by anaerobic digestion (without the presence of air) of organic matter (biomass) and consists mainly of methane and carbon dioxide. There are many studies regarding its obtainment and there are various types of digesters around the world that use human or animal residues as well as sugar or starch crops for the production of the gas. Most of the time, the digesters are installed along with WWTP, which makes this a source of renewable energy (CORONADO, 2007). Other plant types are co-digestion plants, farm plants and landfills. The main sources of biomass are the sludge from WWTP, sugar and starch crops, industrial and agricultural wastes and residues as well as aquatic and marine based organisms such as kelps and algae. Theoretically, other sources could be food wastes and wastes from parks and gardens – but these are currently technically and economically not feasible.

The biogas composition varies dramatically depending on the organic matter used as feedstock. In accordance to Mkoma and Mabiki (2011) and Basu et al. (2010), the main components are methane with 50-70 vol% and carbon dioxide with 20-45 vol%. Further components can be smaller amounts of hydrogen and nitrogen, as well as traces of hydrogen sulphide and oxygen. The most common composition is approximately 65 vol% methane and 35 vol% carbon dioxide. Due to the corrosive nature of the acid and incombustible gases like CO_2 and H_2S, biogas is very limited in terms of compressing and transporting it over longer distances. Therefore, its use is mostly limited to the location of the digesters. Furthermore, H_2O in particular needs to be filtered out of the biogas, before it can be effectively used in turbines or other engines.

There is a wide range of technologies to produce biofuels from many different types of biomass. In general, during the biogas production process, organic matter is decomposed in several different steps, using different metabolic groups of microorganisms. The process has to be anaerobic, as these microorganisms cannot survive in the presence of oxygen. Furthermore, in an aerobic process, most energy is lost as heat and new organic matter. Process efficiency depends mainly on the microorganisms and how well the suitable conditions (pH, temperature, content of secondary gases) are controlled. Besides the desired biogas, there are also by-products such as peat, manure or sludge. Figure 5 illustrates the different steps, phases and reactions of the biogas decomposition process. It can be broadly divided into hydrolysis, acidogenesis, acetogenesis and methanogenesis. The complex reactions involve microbes using multi-enzyme systems such as cellulases and amylases

(hydrolysis) as well as lipases (acidogenesis) and others. Figure 6 illustrated an anaerobic digester from a technical point of view.

Figure 5 - Anaerobic biogas digestion process

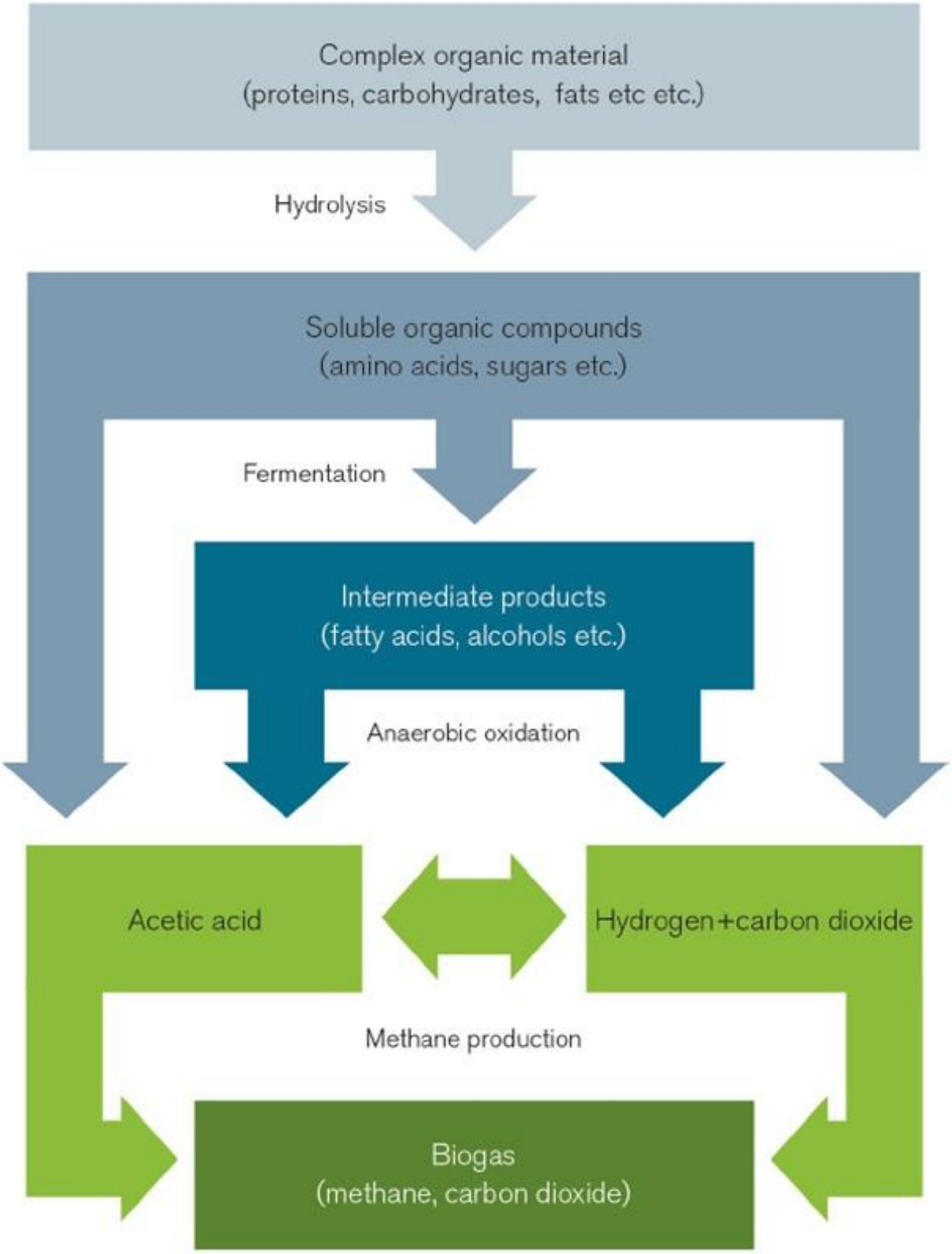

Source: (SWEDISH GAS TECHNOLOGY CENTER, 2012).

Figure 6 - Anaerobic biodigester

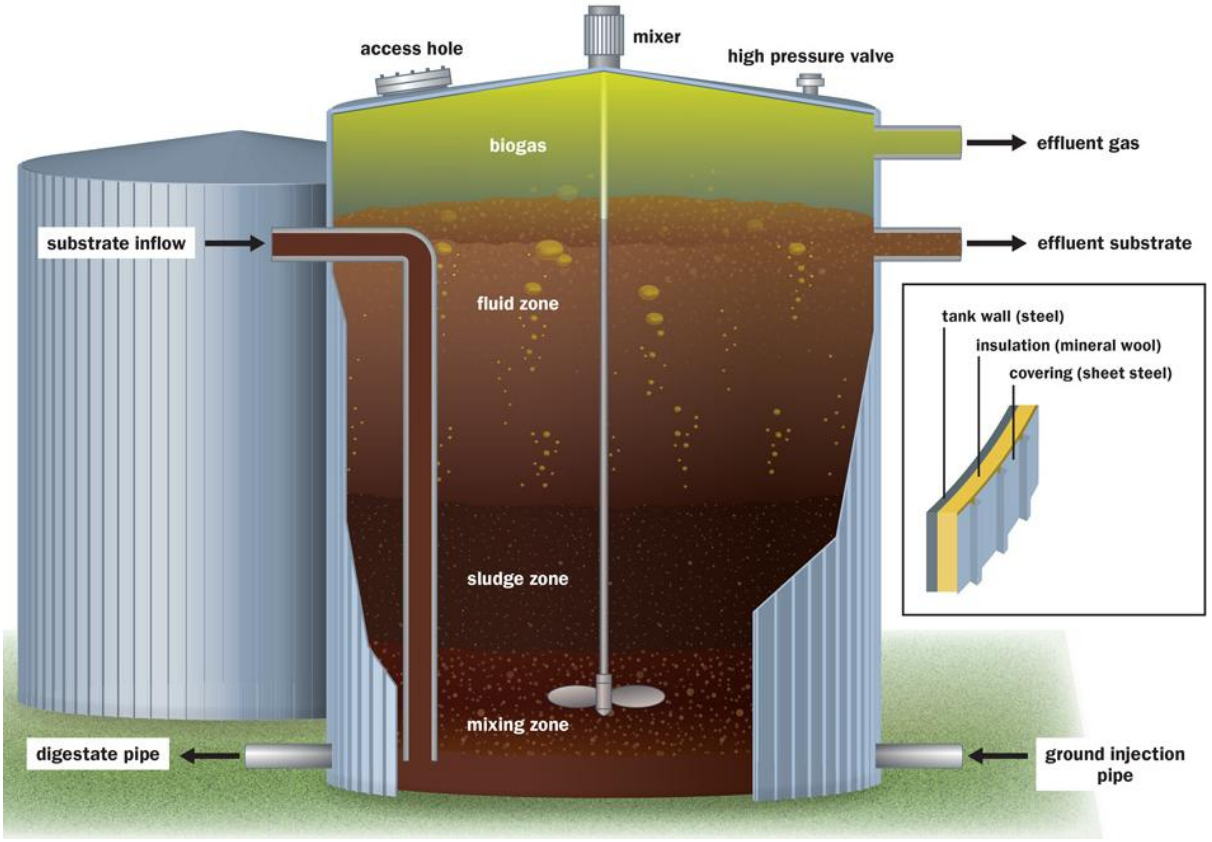

Source: (DAHL, 2015).

Table 2 gives an overview of different biogas compositions found in the literature (BRIZI et al., 2014; BASU et al., 2010; MKOMA; MABIKI, 2011; CAMERETTI; TUCCILLO; PIAZZESI, 2013; KANG et al., 2014).

Table 2 - Literature comparison of biogas compositions

REFERENCE:	Brizi et al.	Basu et al.	Mkoma and Mabiki	Cameretti et al. & Kang et al.
CH_4 (vol.%)	62.7	55-60	50-75	65
CO_2 (vol.%)	2.4	38-40	25-50	35
H_2S (vol.%)	14.1	smaller amounts	50-6000 ppmv	–
N_2 (vol.%)	13.4	traces	0-5	–
CO (vol.%)	5.0	–	–	–
H_2O (vol.%)	2.4	–	0-1	–

Source: based on mentioned authors.

After the production process, the biogas needs to be filtered and cleaned to remove the highly corrosive hydrogen sulphides and siloxanes. The desulphurisation can be achieved through biological or chemical methods. Because the MGT Capstone C200 requires the fuels to be dry and hydrogen-sulphide-free, the biogas composition is adopted in accordance with Table 2 and is shown in Table 3.

Table 3 - Adopted biogas composition (anaerobic digestion of lignocellulosic biomass)

COMPONENT	VOLUME (%)	MOLAR MASS (g/mol)	MASS (%)	LHV (kJ/kg)
CH_4	65.00	16.04	40.36	50,023
CO_2	35.00	44.01	59.64	–
Total	100.00	25.38	100.00	20,192

Source: Author himself.

2.5 SYNGAS

Synthetic fuels are produced by thermochemical processes creating a petroleum-like fuel. Therefore, synthetic fuels, unlike biofuels, can often times be fed into traditional fuel distribution systems and used in machines like gas turbines without the necessity of any machine modifications. Generally speaking, synthetic fuels are produced by breaking down complex molecules into simple ones, like carbon monoxide, methane and hydrogen, and then rebuilding them into the desired fuel. The three main methods to produce synthetic biofuels are gasification, pyrolysis and liquefaction. Both pyrolysis and liquefaction produce a bio-oil that can be further processed into renewable diesel or other fuel products. Gasification, meaning partial oxidation of biomass or other solid fuels, produces gaseous (bio-) fuels. Usually, lignocellulosic biomass (e.g. wood or bagasse) is the feedstock chosen for gasification (DILTZ; PULLAMMANAPPALLIL, 2013).

The gasification process consists of two main steps: pyrolysis and char gasification. During pyrolysis, several complex reactions vaporise the volatile components of the feedstock. According to Pirc, Sekavčnik and Mori (2012), pyrolysis at rather low temperatures (below 450°C) produces mainly char, and at higher temperatures (above 800°C), pyrolysis results in mainly gases (hydrocarbon gases, hydrogen, carbon monoxide and carbon dioxide). Other by-products of pyrolysis are tar, ash and water vapour. Gasification itself

consists of water reduction reactions (including oxygen, steam, carbon monoxide and hydrogen) and burning of the fuel at high temperature and under sub-stoichiometric conditions. According to Woolcock and Broer (2012), oxygen supply needs to be limited to about 25% of the amount required to fully combust the feedstock. As gasification is an endothermic (i.e. heat absorbing) process, part of the fuel, char or gases, depending on the reactor technology, need to be burned (fully oxidised) to maintain the desired gasification temperature (BOERRIGTER; RAUCH, 2005). The most common feedstocks for gasification are coal and carbonaceous biomass. Still according to Boerrigter and Rauch (2005), pyrolysis has a higher significance in biomass gasification, because biomass usually consists of more volatile components than coal.

According to Gerssen-Gondelach et al. (2014), if the gasification temperature is 900-1000°C, the obtained gas is called product gas. This is a mixture of hydrogen, carbon monoxide, carbon dioxide, water vapour, methane and tars. Furthermore, the product gas is diluted with large amounts of nitrogen, if the gasification is performed using air instead of pure oxygen. The application range of product gas can be increased by converting it into syngas, also known as synthesis gas, by catalytic or thermal cracking. Syngas contains mainly hydrogen, carbon monoxide, carbon dioxide and water vapour. It can also be produced directly from biomass, by gasification using almost pure oxygen at higher than 1500°C. Generally, the process including product gas and ensuing conversion into syngas is economically more feasible, due to the necessity of much higher temperatures and pure oxygen for direct syngas gasification (GERSSEN-GONDELACH et al., 2014).

Before being effectively usable in most applications, product gas as well as syngas must pass through cleaning and filtering processes. This is due to impurities in the feedstock such as sulphur, alkalis and chlorine which are also gasified and need to be removed. Furthermore, some products of the gasification process itself, like tar, ash and char need to be filtered out to obtain clean syngas. Syngas gasification and cleaning processes are illustrated in Figure 7.

Just like biogas, syngas has great importance in researches and in the search of renewable energy sources. Although its obtaining techniques were already well known, it ceased to matter after World War II and only returned to relevance in the late 20th and early 21st century due to the oil crisis, environmental problems and the imminent depletion of fossil fuels (SIEDLECKI; DE JONG; VERKOOIJEN, 2011). In Brazil, the use of synthesis gas is very attractive due to the large production of biomass in the form of bagasse from sugarcane mills. In this sense, the gasification of biomass presents an important alternative to power MGTs to generate power and useful heat.

Figure 7 - Syngas gasification and cleaning processes

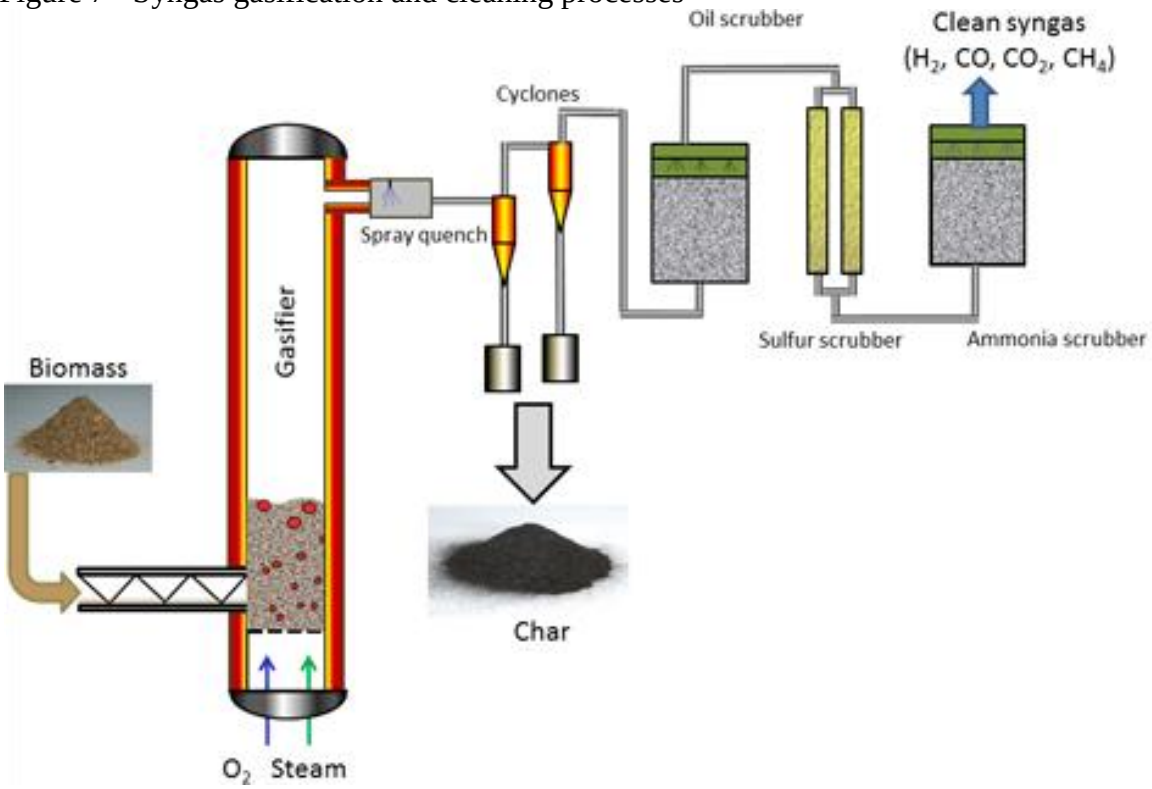

Source: (WOOLCOCK; BROER, 2012).

The mainly industrially used gasification reactors are fixed bed, fluidized bed and moving bed. According to Gerssen-Gondelach et al. (2014), the most commonly used is atmospheric circulating fluidized bed (CFB) gasification. Table 4 gives an overview of different syngas compositions achieved through lignocellulosic biomass gasification at 850°C and various conditions.

Table 4 - Typical syngas compositions of CFB gasification of lignocellulosic biomass

Pressure:	1 bar	1 bar	20 bar
Gasification Medium:	air	O_2 / Steam	O_2 / Steam
H_2 (vol.%)	14	32	19
CO (vol.%)	21	27	20
CO_2 (vol.%)	14	29	40
CH_4 (vol.%)	7	12	21
N_2 (vol.%)	44	0	0
LHV (kJ/kg)	5,801	10,928	10,057

Source: (based on BOERRIGTER; RAUCH, 2005).

Table 5 shows the syngas composition selected for this study in accordance to Boerrigter and Rauch (2005): CFB gasification of lignocellulosic biomass at 1 bar using oxygen and steam. This production process was selected, because it offers a good compromise between low production cost and high LHV of the syngas. According to Kang et al. (2012), a LHV smaller than 10,000 kJ/kg can reduce the surge margin of the gas turbine's compressor so significantly, that the compressor operation becomes highly unstable.

Table 5 - Selected syngas composition (CFB gasification of lignocellulosic biomass)

COMPONENT	VOLUME (%)	MOLAR MASS (g/mol)	MASS (%)	LHV (kJ/kg)
H_2	32	2.02	2.82	119,946*
CO	27	28.01	33.03	10,102*
CO_2	29	44.01	55.74	–
CH_4	12	16.04	8.41	50,023*
Total	100	22.98	100.00	10,928

Source: Author himself. *from EES

2.6 ADJUSTMENT OF GAS TURBINE DATA TO LOCAL CONDITIONS

To conduct an energetic analysis, the standard ISO condition gas turbine data (determined at sea level, 15°C, and 60% relative humidity) obtained from its manufacturer need to be adjusted to the local climatic conditions. If these adjustments cannot be performed using information and statistics given by the manufacturer, universal coefficients can be determined to give an estimate.

Local ambient temperature, i.e. the temperature of the MGT inlet air, has a direct impact on the gas turbine performance. Universal coefficients for the ambient temperatures influence on the turbine shaft power, the heat rate and the exhaust gas flow are introduced in accordance to Antunes (1999) and shown in Figure 8. The coefficients are determined using the illustrated performance curves.

Figure 8 - Correctional coefficients for the local temperature

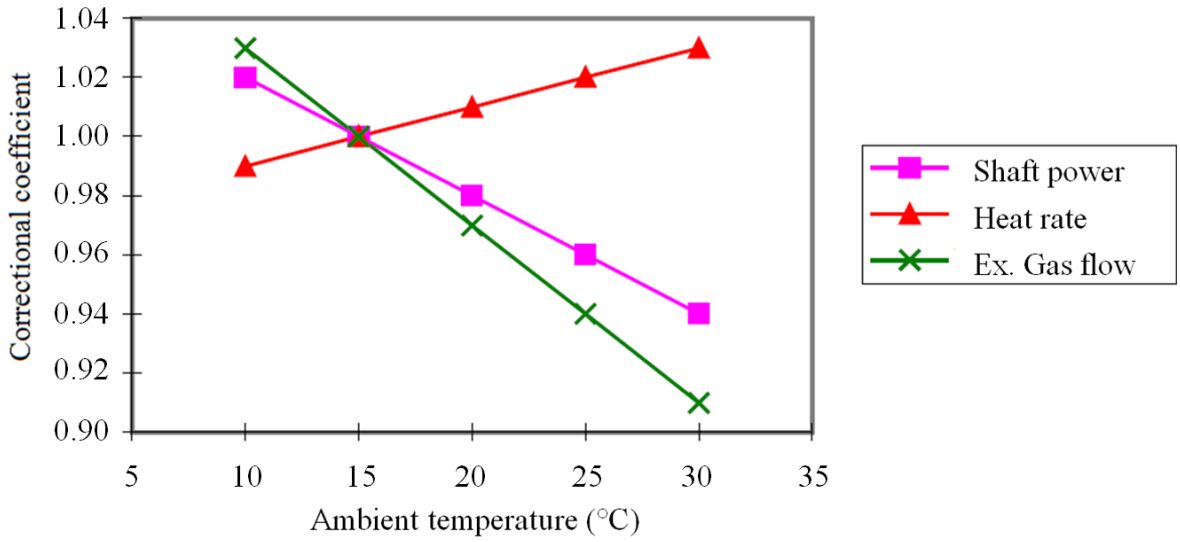

Source: (based on ANTUNES, 1999).

The local altitude also affects the performance of the micro gas turbine. Figure 9 shows the effect on the shaft power and exhaust gas flow, for altitudes between 200 and 2800 m above sea level:

Figure 9 - Correctional coefficient for the local altitude

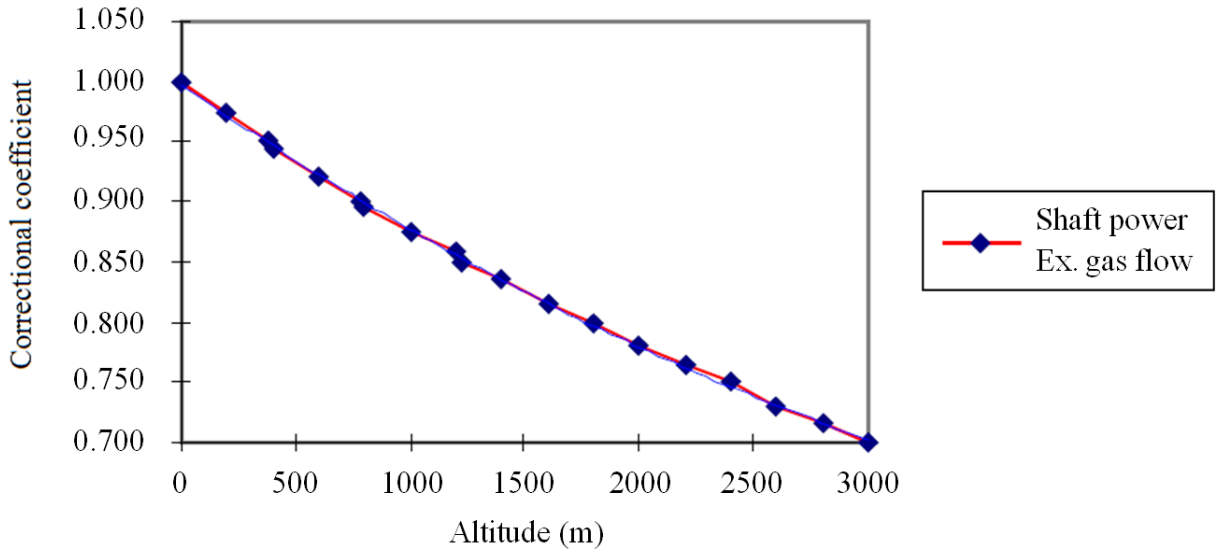

Source: (based on ANTUNES, 1999).

Furthermore, the specific humidity influences the shaft power and the heat rate, as shown in Figures 10 and 11, respectively.

Figure 10 - Correctional coefficient for the local humidity on the heat rate

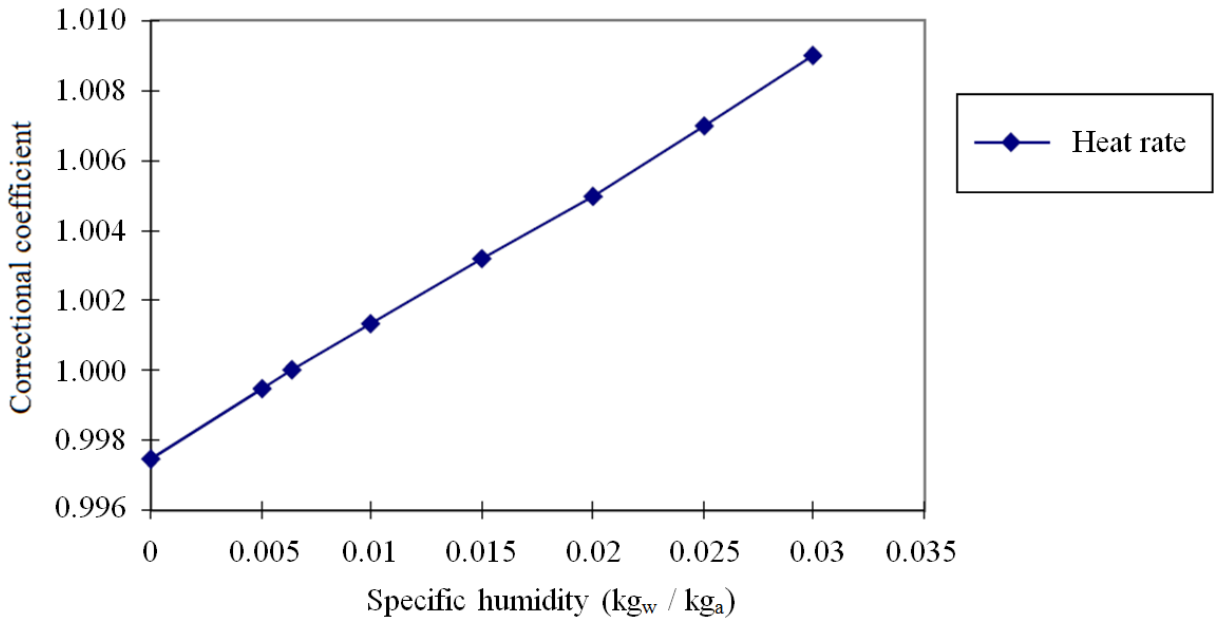

Source: (based on ANTUNES, 1999).

Figure 11 - Correctional coefficient for the local humidity on the shaft power

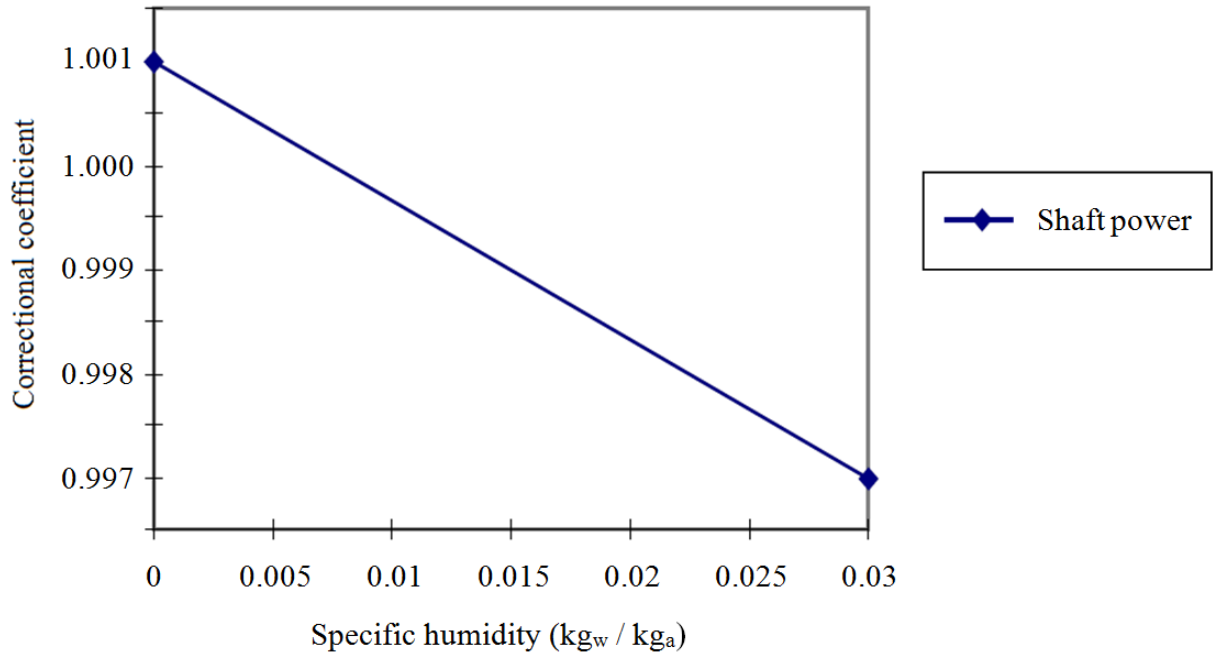

Source: (based on ANTUNES, 1999).

The universal coefficients' functions are mathematically described in accordance to the respective performance curves illustrated above (Figures 8, 9, 10 and 11).

a.) Correction of the power in the turbine shaft using universal coefficients

$$W_{shaft} = W_{shaft,ISO} \cdot f_{cT} \cdot f_{cAlt} \cdot f_{cUe} \quad (1)$$

$$W_{shaft,ISO} = \frac{W_{elGT}}{\eta_{\text{ger}}} \quad (2)$$

$$f_{cT} = -0.004 \cdot T_0 + 1.06 \quad (3)$$

$$f_{cAlt} = -0.0001 \cdot a + 0.9816 \quad (4)$$

$$f_{cUe} = -0.1333 \cdot U_e + 1.001 \quad (5)$$

$$U_e = \frac{0.622 \cdot p_g \cdot U_{rel}}{p_a \cdot 100\%} \quad (6)$$

$$p_g = 6 \cdot 10^{-5} \cdot T_0^{\,3} + 5 \cdot 10^{-4} \cdot T_0^{\,2} + 0.0523 \cdot T_0 + 0.0628 \quad (7)$$

$$p_a = p_0 - \frac{\rho_{air} \cdot g \cdot a}{1000} \quad (8)$$

b.) Correction of the heat rate using universal coefficients

$$HR = HR_{ISO} \cdot f_{cT} \cdot f_{cUe} \quad (9)$$

$$f_{cT} = 0.002 \cdot T_0 + 0.97 \quad (10)$$

$$f_{cUe} = 0.3795 \cdot U_e + 0.9975 \quad (11)$$

c.) Correction of the exhaust gas flow using universal coefficients

$$\dot{m}_{cg} = \dot{m}_{cg,ISO} \cdot f_{cT} \cdot f_{cAlt} \quad (12)$$

$$f_{cT} = -0.006 \cdot T_0 + 1.07 \quad (13)$$

$$f_{cAlt} = -0.0001 \cdot a + 0.9816 \quad (14)$$

3 MATERIAL AND METHOD

The analyses in this dissertation are conducted using the principles of ideal gases for the air and the combustion gases and assuming steady state system operation. Additionally, all processes are considered adiabatic and it is assumed that the MGT is available in specific versions (modified fuel injection system) for the combustion of NG, biogas and syngas, and that all three versions have the same price and operational data.

Moreover, it is assumed that the plant operates in thermal match mode, which is more efficient than power match mode. The points T_i with i = 1 ... 10 refer to Figure 12. Operation mode of the proposed MGT cogeneration system is described using Figure 12:

Figure 12 - Schematic overview of the cogeneration plant using a Capstone C200

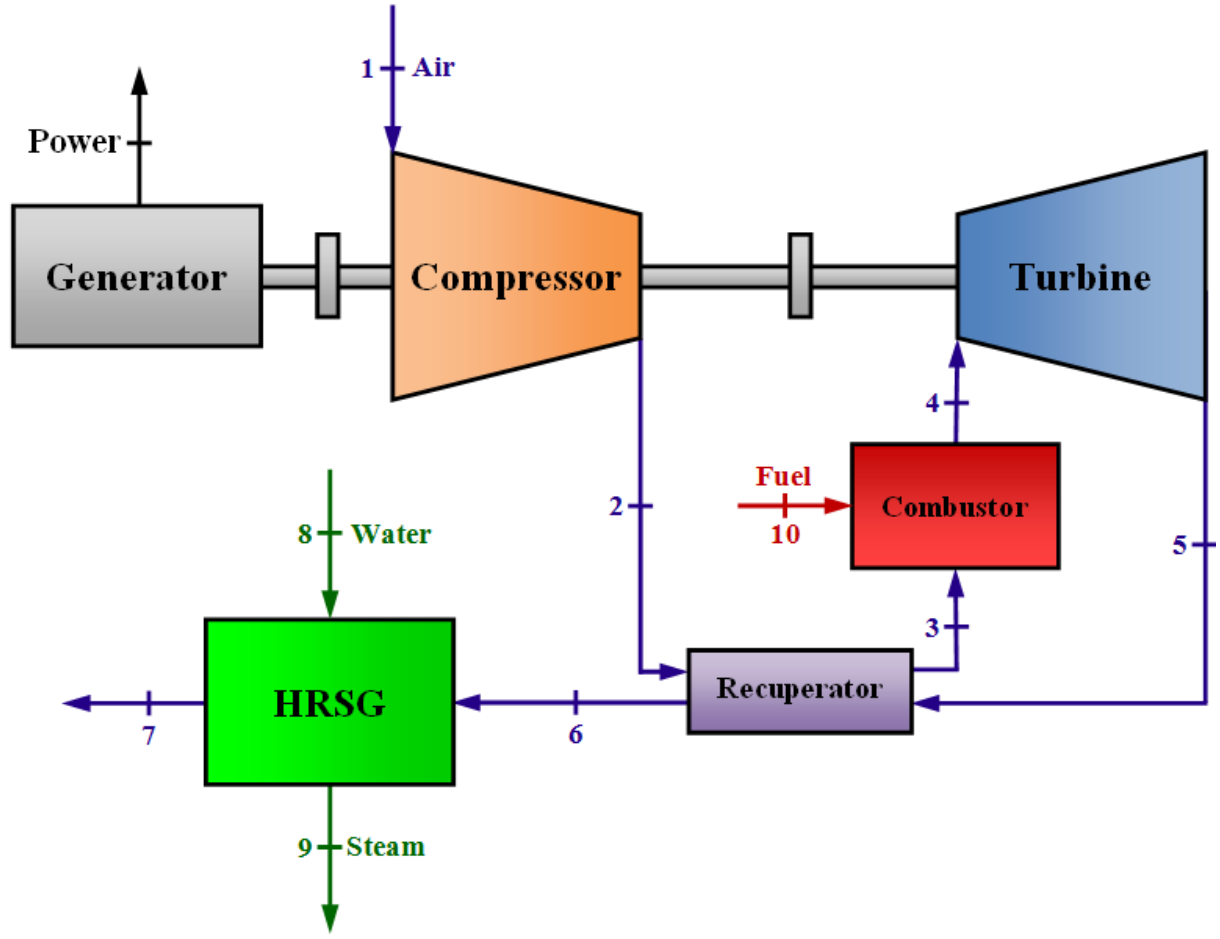

Source: Author himself.

Incoming air (point 1) is compressed (point 2) and directed through the recuperator where it is pre-heated and then (point 3) mixed with the high-pressure fuel (point 10) in the combustor. After combustion, the high-temperature and -pressure gases (point 4) are expanded through the gas turbine, transferring part of their energy onto the turbine shaft. Typically, compressor, turbine and power generator are all mounted on the same shaft – part of the energy is used to drive the compressor, the rest is transformed by the generator into high-frequency AC and must be conditioned through power electronics to provide a usable DC power output. The exhaust gases exiting the turbine (point 5) pass through the recuperator to pre-heat the compressed air and therewith reduce the fuel consumption, hence improving the electrical efficiency of the turbine. Leaving the recuperator, the exhaust gases (point 6) are fed into the HRSG along with water (point 8) to generate steam (point 9). To avoid condensation and acid formation, the temperature of the exhaust gases leaving the HRSG (point 7) must not be too low and the pinch point has to be considered. In this study, a HRSG without supplementary heating is chosen.

For the analyses relevant, nominal data of the MGT C200 is shown in Table 6:

Table 6 - Nominal data of the Capstone C200 Micro Gas Turbine

MODEL	POWER OUTPUT (kW)	PRESSURE RATIO	EX. GAS FLOW (kg/s)	EXHAUST TEMP. (°C)	HEAT RATE (MJ/kWh)	TURBINE PRICE (USD)
C200	200	4.0	1.32	279.4	10.9	220,000

Source: (based on GAS TURBINE WORLD, 2011).

All the adopted and estimated values are listed in Table 7.

Table 7 - Important adopted and estimated values

SYMBOL	DEFINITION	VALUE	REFERENCE
C_{bio}	Biogas price	0.019 USD/kWh	Brizi et al. (2014)
$C_{M,cb}$	Main. & op. cost conv. boiler sys.	0.008 USD/kWh	Antunes (1999)
$C_{M,HRSG}$	Main. and op. cost of HRSG	0.006 USD/kWh	Kang et al. (2014)
$C_{M,gts}$	Main. and op. cost of MGT sys.	0.012 USD/kWh	Barigozzi et al. (2015)
C_{NG}	NG price	0.063 USD/kWh	COMGÁS (2015b)
C_{syn}	Syngas price	0.070 USD/kWh	Parajuli et al. (2014)
H	Hours of operation per year	7000 h/year	–
k_{civ}	Factor for civil engineering cost	1.3	Kang et al. (2014)
k_{import}	Factor for import and tax cost	1.4	–
P_{el}	Electric energy price	0.19 USD/kWh	Bandeirante Energia
P_{oil}	Fuel oil price	0.093 USD/kWh	Sun et al. (2015)
p_s	Process steam pressure	1.5 MPa	–
R_{air}	Gas constant of air	0.287 kJ/kg K	–
T_{7ai}	Initially adopted exh. gas temp.	150°C	–
T_8	Steam temp. entering the HRSG	95°C	–
T_9	Steam temp. leaving the HRSG	250°C	–
Δp_{cc}	Pressure losses in comb. chamber	0.05	Silveira et al. (2004)
Δp_{HRSG}	Pressure losses in HRSG	0.02	Capstone (2009)
Δp_{inlet}	Inlet pressure drop	0.5 kPa	Capstone (2009)
Δp_{rec}	Pressure losses in recuperator	0.03	Silveira et al. (2004)
ΔT_{pp}	Pinch point temp. difference	10°C	Nadir et al. (2015)
η_{cb}	Eff. of conv. boiler for st. gen.	0.85	Antunes (1999)
η_{cc}	Energetic eff. of comb. chamber	0.99	Silveira et al. (2003)
η_{ger}	Energetic eff. of power generator	0.99	Silveira et al. (2003)
η_{HRSG}	Energetic efficiency of HRSG	0.75	Balestieri (2002)
$\eta_{isoComp}$	Isentropic eff. of compressor	0.82	Silveira et al. (2003)
η_{isoGT}	Isentropic eff. of gas turbine	0.87	Silveira et al. (2003)

Source: Author himself.

3.1 FIRST LAW OF THERMODYNAMICS ANALYSIS

This analysis is based on the First Law of Thermodynamics, the law of conservation of energy. This equation basically establishes an energetic balance for each process. Considering steady state and neglecting kinetic and potential energy variation, it is expressed as shown in equation (1.1):

$$\dot{Q} - \dot{W} = \sum_{out} \dot{m}_{out} \cdot h_{out} - \sum_{in} \dot{m}_{in} \cdot h_{in} \qquad (1.1)$$

with:

$\dot{Q}$ is the heat flow transferred through the analysed control volume, in kW.

Ẇ is the work per unit time transferred through the analysed control volume, in kW.

ṁ is the mass flow of energy steams (steam, gases, etc.), in kg/s.

h is the enthalpy of the energy streams, in kJ/kg.

The First Law analysis is performed by applying equation (1.1) to control volumes for each component depicted in Figure 12. To conduct an energetic analysis, the standard ISO condition data (determined at sea level, 15°C, and 60% relative humidity) of the gas turbine C200 obtained from its manufacturer need to be adjusted to the local climatic conditions, in this case Guaratinguetá, Brazil. Thereafter, the important energetic data can be calculated for all the points of the system to obtain the energetic efficiencies of the single components as well as the system as a whole.

3.1.1 Adjustment of Capstone C200 data to local conditions

The performance data of the MGT are provided by the manufacturer for standard ISO conditions (sea level, 15°C and 60% relative humidity) and have to be adjusted to the local conditions. In case of this study, the conditions in Guaratinguetá are: ambient temperature T_0 is 25°C, relative humidity U_{rel} is 70% and altitude a is 620m.

These adjustments are realised in accordance to Capstone Turbine Corporation (2009). Local ambient temperature, i.e. the temperature of the MGT inlet air, has a direct impact on the gas turbine performance. The values of efficiency, exhaust temperature and exhaust mass flow are adjusted using Table 8. Capstone Turbine Corporation (2009) presents a table for ambient temperature at sea level from -20 °C to 50 °C. Table 8 is an extract.

Table 8 - Influence of ambient temperature on data of MGT C200

Ambient Temperature (°C)	Net Power (kW)	Net Efficiency (%)	Exhaust Temperature (°C)	Exh. Mass Flow Rate (kg/s)	Net Heat Rate (BTU/kWh)
-15	200.0	34.3	229.8	1.36	10,501
0	200.0	33.8	252.8	1.33	10,655
15	200.0	32.8	279.5	1.33	10,967
20	200.0	32.5	287.7	1.33	11,075
25	196.4	32.1	294.7	1.32	11,208
30	186.9	31.7	299.0	1.30	11,372

Source: (based on CAPSTONE TURBINE CORPORATION, 2009).

The data determined using Table 8 is:

Net Power E'_{el} is 196.4 kW. Net Efficiency η'_{GT} is 32.1 %. Exhaust Temperature T'_{6} is 294.7 °C. Exhaust Mass Flow Rate $\dot{m}'_{cg}$ is 1.32 kg/s.

Next, the net power output has to be adjusted to the ambient temperature as well as the local altitude. This is done using Figure 13:

Figure 13 - Influence of ambient temp. and pressure on power output of Capstone C200

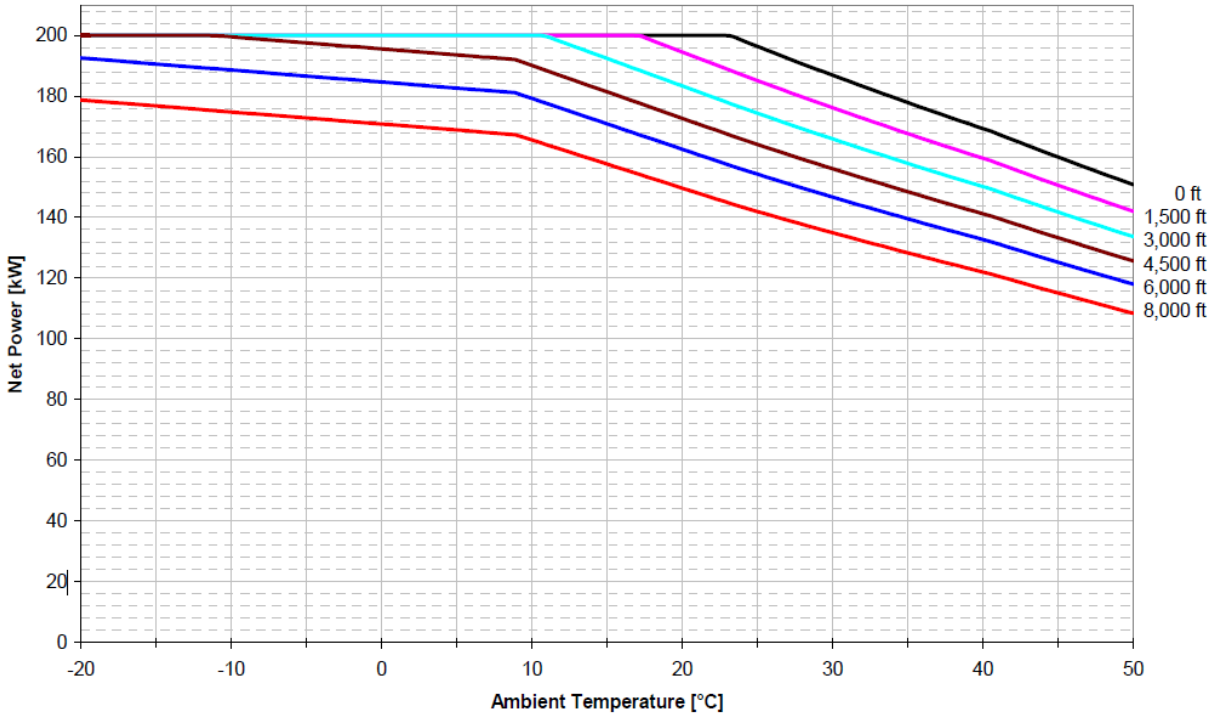

Source: (CAPSTONE TURBINE CORPORATION, 2009).

The local altitude in Guaratinguetá is 2034 ft (620 m).

From Figure 13: E''_{el} (T = 25°C; a = 1500 ft) ≈ 185 kW

E''_{el} (T = 25°C; a = 3000 ft) ≈ 174 kW

Interpolation: E''_{el} (T = 25°C; a = 2034 ft) ≈ 181 kW

The reason why the net power output of the C200 MGT is constant at low temperatures and small altitudes is that, in these cases, power output is not limited by the ambient conditions, but regulated by power electronics. This is illustrated in Figure 14:

Figure 14 - Net power output of Capstone C200 limited by power electronics

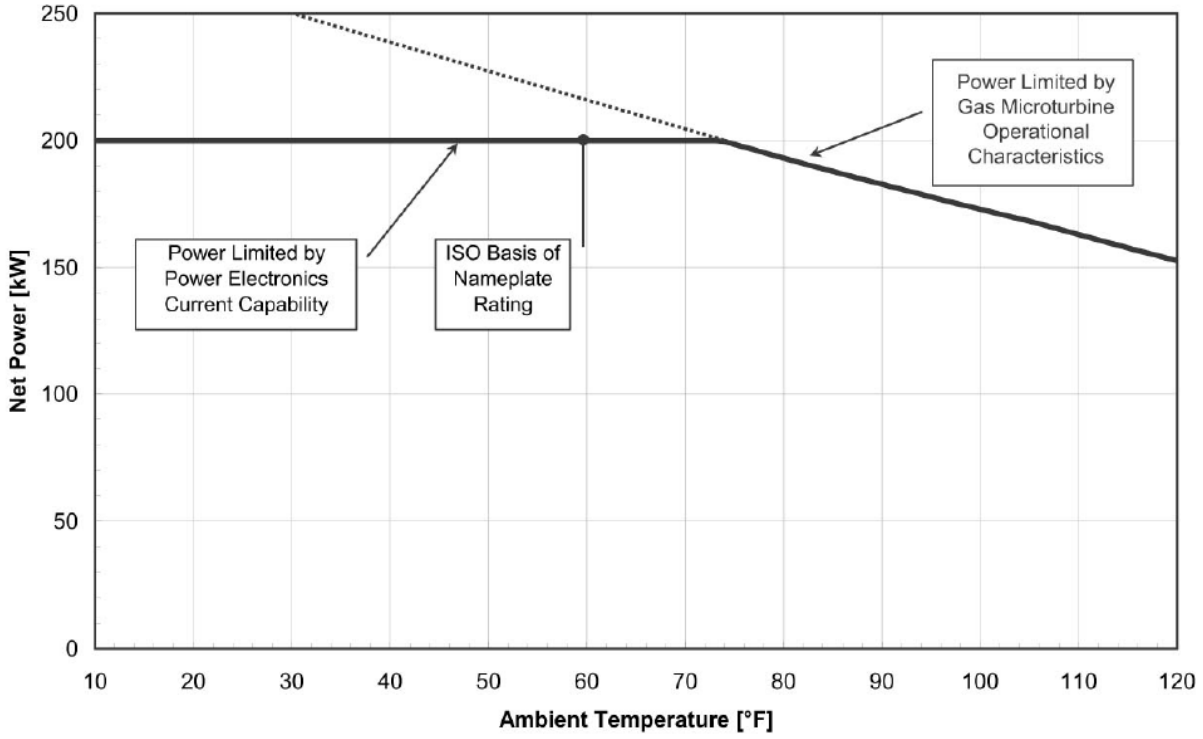

Source: (CAPSTONE TURBINE CORPORATION, 2009).

Furthermore, net power output and net efficiency of the turbine have to be adjusted depending on inlet pressure drop and exhaust back pressure. Inlet pressure drop depends mainly on the air filtering systems and, for this study, is adopted as 0.5 kPa (2 inches of water). The influence of inlet pressure drop is shown in Table 9:

Table 9 - Influence of inlet pressure drop on power output and efficiency of MGT C200

Inlet Pressure Drop (Inches of Water)	Correction Factor for Power ($CF_{inlet,P}$)	Correction Factor for Efficiency ($CF_{inlet,Eff}$)
0.0	1.000	1.000
1.0	0.994	0.998
2.0	0.987	0.995
3.0	0.981	0.993
4.0	0.974	0.990
5.0	0.968	0.988
6.0	0.961	0.986
7.0	0.955	0.983
8.0	0.949	0.981
9.0	0.942	0.978
10.0	0.936	0.976

Source: (CAPSTONE TURBINE CORPORATION, 2009).

In accordance to Table 9 the correction factors for an inlet pressure drop of 0.5 kPa are determined as follows:

$CF_{inlet,P}$ is 0.987 and $CF_{inlet,Eff}$ is 0.995.

According to Capstone Turbine Corporation (2009), the maximum allowable exhaust back pressure for a Capstone C200 MGT is 8 inches of water (2 kPa). This limits the HRSG to pressure losses of no more than 2%. The influence of back pressure is shown in Table 10. In accordance to Table 10 the correction factors for a back pressure of 2 kPa (8 inches of water) are determined as follows:

$CF_{back,P}$ is 0.969 and $CF_{back,Eff}$ is 0.981.

Table 10 - Influence of back pressure on power output and efficiency of MGT C200

Back Pressure (Inches of Water)	Correction Factor for Power ($CF_{back,P}$)	Correction Factor for Efficiency ($CF_{back,Eff}$)
0.0	1.000	1.000
1.0	0.996	0.998
2.0	0.992	0.995
3.0	0.988	0.993
4.0	0.985	0.990
5.0	0.981	0.988
6.0	0.977	0.985
7.0	0.973	0.983
8.0	0.969	0.981

Source: (CAPSTONE TURBINE CORPORATION, 2009).

The net power output and the net efficiency can now be adjusted to the inlet pressure drop and the back pressure:

$$E_{el,NG} = E'_{el}\left(\mathrm{T} = 25°\mathrm{C}; \mathrm{a} = 2034\mathrm{ft}\right) \cdot CF_{inlet,P} \cdot CF_{back,P} \tag{1.2}$$

$$\eta_{GT,NG} = \eta'_{GT}\left(\mathrm{T} = 25°\mathrm{C}; \mathrm{a} = 2034\mathrm{ft}\right) \cdot CF_{inlet,Eff} \cdot CF_{back,Eff} \tag{1.3}$$

$E_{el,NG}$ = 173.1 kW

$\eta_{GT,NG}$ = 31,3 %

The adjusted heat rate is calculated using the adjusted net efficiency:

$$HR = \frac{3600}{\eta_{GT}} \tag{1.4}$$

HR_{NG} = 11501

Finally, in accordance to Capstone Turbine Corporation (2009), the exhaust mass flow rate is adjusted to the altitude and the adjusted power output:

$$\dot{m}_{cg} = \dot{m}'_{cg}\left(\mathrm{T} = 25°\mathrm{C}; \mathrm{a} = 0\ \mathrm{ft}\right) \cdot \frac{E''_{el}[elevation]}{E'_{el}[sea.level]} \cdot \left(1 - \frac{0.005 \cdot \mathrm{a}\,[\,ft]}{1000}\right) \quad (1.5)$$

$\dot{m}_{cg}$ = 1.25 kg/s

In accordance to Capstone Turbine Corporation (2009), the impacts of specific humidity on heat rate and power output are not considered.

3.1.2 Adjustment of gas turbine performance for biogas and syngas operation

According to the South America sales manager of Capstone Turbine Corporation, Vescovo (2015), the adjusted values of exhaust temperature, exhaust mass flow rate and power output are not impacted by the fuel and are therefore adopted as valid for all three fuels and turbine versions. Furthermore, in accordance to Somehsaraei et al. (2014), while the power output is constant, electric efficiency of a 100 kW MGT declines with decreasing methane content in the biogas. In other words, the electric efficiency of MGTs declines with decreasing LHV of the fuel. This behaviour is shown in Figure 15:

Figure 15 - Influence of the LHV on electric efficiency of a 100 kW MGT

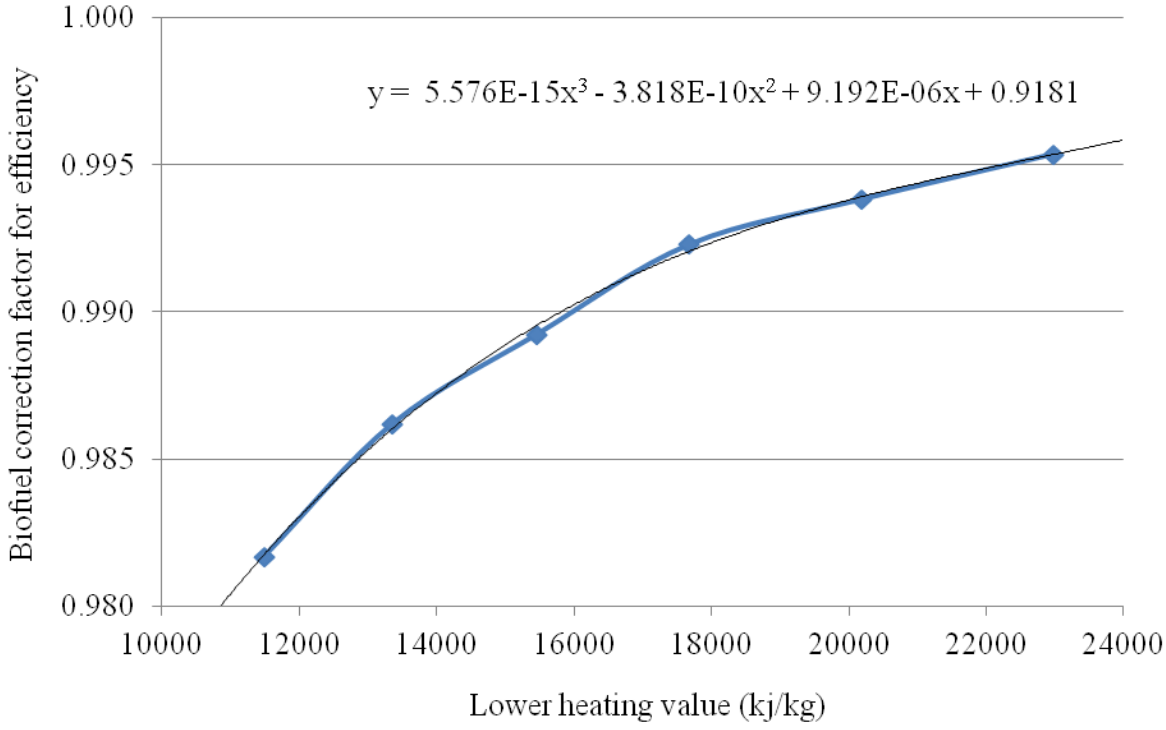

Source: (based on SOMEHSARAEI et al., 2014).

For the purpose of this study, it is adopted that the efficiency factors depending on the LHV shown in Figure 15 can be applied to the MGT Capstone C200 operating on biogas as well as syngas. The correction factors for the proposed biogas composition (CF_{BIO}) and the proposed syngas composition (CF_{SYN}) are determined to be 0.994 and 0.980, respectively.

Moreover, in case of low pressure fuels (biogas and syngas), a gas booster (compressor) is necessary to generate the pressure to inject the fuel into the combustion chamber. The gas booster recommended for the C200 MGT is the COMPEX MT11, with a maximum absorbed power of 11 kW (CAPSTONE TURBINE CORPORATION, 2009). The gas booster further reduces the plant's electric efficiency. Therefore, the electric efficiency and the power output for biogas and syngas operation can be expressed as follows:

$$E_{el,BIO} = E_{el,NG} - W_{GB} \tag{1.6a}$$

$$E_{el,SYN} = E_{el,NG} - W_{GB} \tag{1.6b}$$

$$\eta_{GT,BIO} = \eta_{GT,NG} \cdot CF_{BIO} \cdot \frac{E_{el,BIO}}{E_{el,NG}} \tag{1.7a}$$

$$\eta_{GT,SYN} = \eta_{GT,NG} \cdot CF_{SYN} \cdot \frac{E_{el,SYN}}{E_{el,NG}} \tag{1.7b}$$

3.1.3 Calculation of the percentage of excess air

The amount of excess air used in the combustion process is calculated as follows:

$$\%EA = 100 \cdot \left(\frac{m_a}{m_{as}} - 1 \right) \tag{1.8}$$

with:

%EA is the amount of excess air, in percent.

m_a is the mass of the combustion air per mass of fuel, in kg_{AIR}/kg_{FUEL}.

m_{as} is the mass of the stoichiometric combustion air per mass of fuel, in kg_{AIR}/kg_{FUEL}.

The air and fuel flows in the MGT are determined by the efficiency of the turbine:

$$m_a = \frac{\dot{m}_{air}}{\dot{m}_{fuel}} \tag{1.9}$$

$$\dot{m}_{air} = \dot{m}_{cg} - \dot{m}_{fuel} \tag{1.10}$$

$$\dot{m}_{fuel} = \frac{E_{fuel}}{LHV} \tag{1.11}$$

$$E_{fuel} = \frac{E_{el}}{\eta_{GT}} \tag{1.12}$$

The LHVs of NG, biogas and syngas can be taken from Tables 1, 3 and 5, respectively.

The stoichiometric combustion air, also known as theoretical air, is determined using stoichiometric combustion equations for each fuel considering zero excess of air (complete combustion). As all fuels are mixtures of different gases, the stoichiometric relations are developed for each gas component (e.g. methane) and then weighted by their mole fractions to obtain the multi-component equation. Air is assumed to consist of 21% oxygen and 79% nitrogen and dissociation in the combustion process is not considered. Therefore, a general stoichiometric combustion equation for a hydrocarbon fuel ($C_\alpha H_\beta O_\gamma$) with air is:

$$C_\alpha H_\beta O_\gamma + \left(\alpha + \frac{\beta}{4} - \frac{\gamma}{2}\right) \cdot \left(O_2 + \frac{79}{21} N_2\right) \rightarrow \alpha \cdot CO_2 + \frac{\beta}{2} \cdot H_2O + \frac{79}{21}\left(\alpha + \frac{\beta}{4} - \frac{\gamma}{2}\right) \cdot N_2 \tag{1.13}$$

For methane:

$$CH_4 + 2 \cdot \left(O_2 + \frac{79}{21} N_2\right) \rightarrow CO_2 + 2 \cdot H_2O + \left(7 + \frac{11}{21}\right) \cdot N_2 \tag{1.13a}$$

For ethane:

$$C_2H_6 + 3.5 \cdot \left(O_2 + \frac{79}{21} N_2\right) \rightarrow 2 \cdot CO_2 + 3 \cdot H_2O + \left(13 + \frac{1}{6}\right) \cdot N_2 \tag{1.13b}$$

For propane:

$$C_3H_8 + 5 \cdot \left(O_2 + \frac{79}{21} N_2\right) \rightarrow 3 \cdot CO_2 + 4 \cdot H_2O + \left(18 + \frac{17}{21}\right) \cdot N_2 \tag{1.13c}$$

For butane:

$$C_4H_{10} + 6.5 \cdot \left(O_2 + \frac{79}{21} N_2\right) \rightarrow 4 \cdot CO_2 + 5 \cdot H_2O + \left(24 + \frac{19}{42}\right) \cdot N_2 \tag{1.13d}$$

For pentane:

$$C_5H_{12} + 8 \cdot \left(O_2 + \frac{79}{21} N_2 \right) \rightarrow 5 \cdot CO_2 + 6 \cdot H_2O + \left(30 + \frac{2}{21} \right) \cdot N_2 \qquad (1.13e)$$

For hexane:

$$C_6H_{14} + 9.5 \cdot \left(O_2 + \frac{79}{21} N_2 \right) \rightarrow 6 \cdot CO_2 + 7 \cdot H_2O + \left(35 + \frac{31}{42} \right) \cdot N_2 \qquad (1.13f)$$

For hydrogen:

$$H_2 + 0.5 \cdot \left(O_2 + \frac{79}{21} N_2 \right) \rightarrow H_2O + \left(\frac{79}{42} \right) \cdot N_2 \qquad (1.13g)$$

For carbon oxide:

$$CO + 0.5 \cdot \left(O_2 + \frac{79}{21} N_2 \right) \rightarrow CO_2 + \left(\frac{79}{42} \right) \cdot N_2 \qquad (1.13h)$$

a.) Stoichiometric combustion equation for one mol of the proposed NG composition (see Table 1):

$$\begin{aligned} &0.8868 \cdot CH_4 + 0.0584 \cdot C_2H_6 + 0.0234 \cdot C_3H_8 + 0.0077 \cdot C_4H_{10} + \\ &0.0013 \cdot C_5H_{12} + 0.0003 \cdot C_6H_{14} + 0.0162 \cdot CO_2 + 0.0059 \cdot N_2 + \\ &2.1579 \cdot (O_2 + 79/21 \cdot N_2) \rightarrow 1.1288 \cdot CO_2 + 2.0905 \cdot H_2O + 8.1237 \cdot N_2 \end{aligned} \qquad (1.14a)$$

Equation (1.14a) shows that, in case of stoichiometric combustion, one mol of NG reacts with 10.28 mol of air (2.16 mol of oxygen and 8.12 mol of nitrogen). This equals a stoichiometric combustion air mass of 0.2964 kg_{AIR} per mol of NG. Considering the NG molar mass of 18.45 g/mol, **m_{as} is 16.06 kg_{AIR}/kg_{NG}**. This lies in the expected range for hydrocarbon fuels of 14 to 20 kg of air per kg of fuel (MCALLISTER; CHEN; FERNANDEZ-PELLO, 2011). Equations (1.8), (1.9) and (1.10) result in: m_a is 101.1 kg_{AIR}/kg_{NG} and $\%EA_{NG}$ is 529.3 %.

b.) Stoichiometric combustion equation for one mol of the proposed biogas composition (see Table 3):

$$0.65 \cdot CH_4 + 0.35 \cdot CO_2 + 1.3 \cdot \left(O_2 + \frac{79}{21} N_2 \right) \rightarrow 1.0 \cdot CO_2 + 1.3 \cdot H_2O + 4.8905 \cdot N_2 \quad (1.14b)$$

Equation (1.14b) shows that, in case of stoichiometric combustion, one mol of biogas reacts with 6.19 mol of air (1.3 mol of oxygen and 4.89 mol of nitrogen). This equals a stoichiometric combustion air mass of 0.1786 kg_{AIR} per mol of biogas. Considering the biogas molar mass of 25.83 g/mol, **m_{as} is 6.91 kg_{AIR}/kg_{BIO}**. Equations (1.8), (1.9) and (1.10) result in: m_a is 42.6 kg_{AIR}/kg_{BIO} and $\%EA_{BIO}$ is 515.4 %.

c.) Stoichiometric combustion equation for one mol of the proposed syngas composition (see Table 5):

$$0.12 \cdot CH_4 + 0.27 \cdot CO + 0.32 \cdot H_2 + 0.29 \cdot CO_2 + 0.535 \cdot \left(O_2 + \frac{79}{21} N_2 \right) \longrightarrow 0.68 \cdot CO_2 + 0.56 \cdot H_2O + 2.0126 \cdot N_2 \quad (1.14c)$$

Equation (1.14c) shows that, in case of stoichiometric combustion, one mol of syngas reacts with 2.55 mol of air (0.54 mol of oxygen and 2.01 mol of nitrogen). This equals a stoichiometric combustion air mass of 0.0735 kg_{AIR} per mol of biogas. Considering the syngas molar mass of 22.90 g/mol, **m_{as} is 3.21 kg_{AIR}/kg_{SYN}**. Equations (1.8), (1.9) and (1.10) result in: m_a is 22.2 kg_{AIR}/kg_{SYN} and $\%EA_{SYN}$ is 592.8 %.

3.1.4 Calculation of the turbine inlet temperature

The turbine inlet temperature, considering the efficiency of the combustion chamber, is calculated using the principle of conservation of energy, comparing the enthalpy of the product mixture with the enthalpy of the reactant mixture (MCALLISTER, CHEN, FERNANDEZ-PELLO, 2011).

$$H_P(T_P) = H_R(T_R) \cdot \eta_{cc} \tag{1.15}$$

with:

H_p is the enthalpy of the product mixture at product temperature (at turbine inlet), in kJ.

H_R is the enthalpy of the reactants at reactant temperature (before combustion), in kJ.

The efficiency of the combustion chamber is adopted as 0.99, referring to Silveira and Tuna (2003).

$$H_P(T_P) = \sum_i N_{i,P} \cdot \left[\Delta h^0_{i,P} + h_{si,p}(T_P)\right] \tag{1.16}$$

$$H_R(T_R) = \sum_i N_{i,R} \cdot \left[\Delta h^0_{i,R} + h_{si,R}(T_R)\right] \tag{1.17}$$

with:

N is the number of moles, in mol.

Δh^0 is the enthalpy of formation, in kJ/mol.

$h_s(T)$ is the sensible enthalpy difference between T and T_0, in kJ/mol.

The determination of the adiabatic flame temperature is graphically shown in Figure 16:

Figure 16 - Graphical interpretation of adiabatic flame temperature

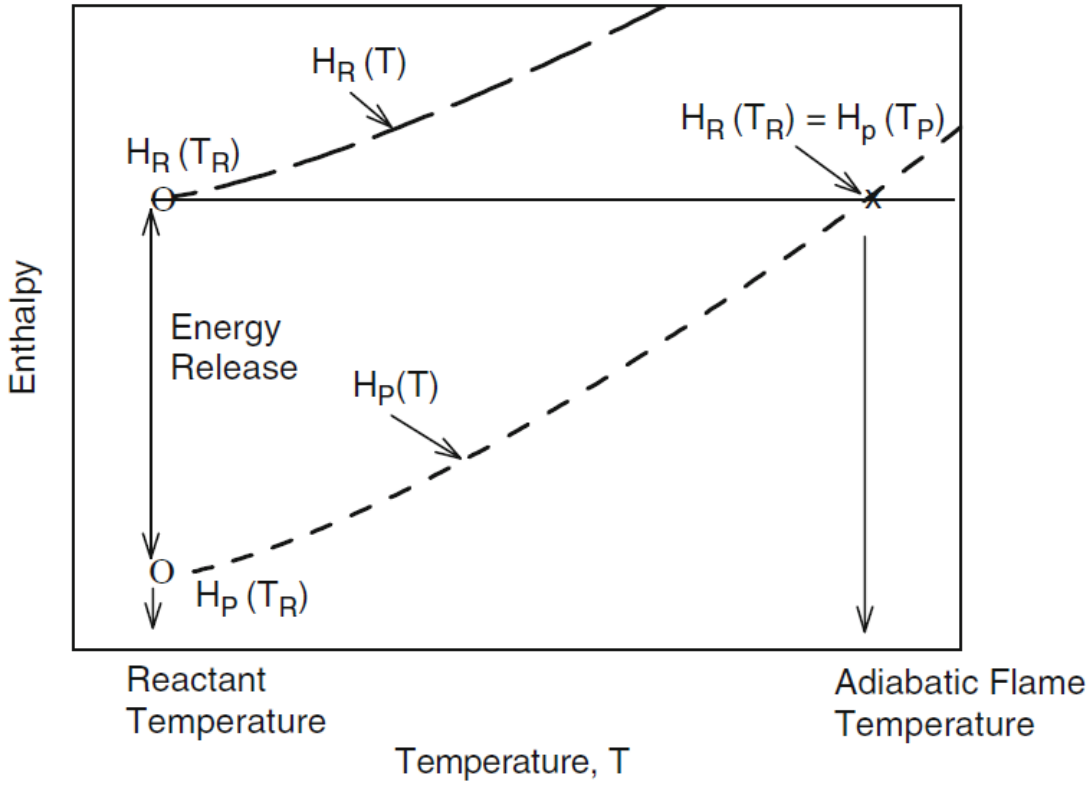

Source: (MCALLISTER, CHEN, FERNANDEZ-PELLO, 2011).

At the reactant temperature before combustion, the enthalpy of the product mixture is smaller than the enthalpy of the reactant mixture. The energy released by the combustion reaction heats the product mixture, until equation (1.15) is fulfilled. Therefore, to determine the turbine inlet temperature, the mole fraction compositions of reactant mixture and product mixture need to be determined. This is achieved by considering the percentage of excess air in the combustion equations. A general combustion equation for a hydrocarbon fuel ($C_\alpha H_\beta O_\gamma$) with an excess of air is:

$$C_\alpha H_\beta O_\gamma + \left(\frac{\%EA}{100}+1\right)\cdot\left(\alpha+\frac{\beta}{4}-\frac{\gamma}{2}\right)\cdot\left(O_2+\frac{79}{21}N_2\right)\longrightarrow$$
$$\alpha\cdot CO_2+\frac{\beta}{2}\cdot H_2O+\frac{79}{21}\cdot\left(\frac{\%EA}{100}+1\right)\cdot\left(\alpha+\frac{\beta}{4}-\frac{\gamma}{2}\right)\cdot N_2+\left(\alpha+\frac{\beta}{4}-\frac{\gamma}{2}\right)\cdot\frac{\%EA}{100}\cdot O_2 \tag{1.18}$$

a.) Combustion equation for one mol of the proposed NG and 529.3 %EA:

$$0.8868\cdot CH_6+0.0584\cdot C_2H_6+0.0234\cdot C_3H_8+0.0077\cdot C_4H_{10}+0.0013\cdot C_5H_{12}$$
$$+0.0003\cdot C_6H_{14}+0.0162\cdot CO_2+0.0059\cdot N_2+13.5795\cdot\left(O_2+\frac{79}{21}N_2\right)$$
$$\longrightarrow 1.1288\cdot CO_2+2.0905\cdot H_2O+51.0909\cdot N_2+11.4217\cdot O_2 \tag{1.18a}$$

b.) Combustion equation for one mol of the proposed biogas and 515.4 %EA:

$$0.65\cdot CH_4+0.35\cdot CO_2+8.0002\cdot\left(O_2+\frac{79}{21}N_2\right)\longrightarrow$$
$$1.0\cdot CO_2+1.3\cdot H_2O+30.0960\cdot N_2+6.7002\cdot O_2 \tag{1.18b}$$

c.) Combustion equation for one mol of the proposed syngas and 592.8 %EA:

$$0.12\cdot CH_4+0.27\cdot CO+0.32\cdot H_2+0.29\cdot CO_2+3.7065\cdot\left(O_2+\frac{79}{21}N_2\right)$$
$$\longrightarrow 0.68\cdot CO_2+0.56\cdot H_2O+13.9434\cdot N_2+3.1715\cdot O_2 \tag{1.18c}$$

As an alternative to calculating the adiabatic flame temperature as demonstrated above, T_4 can also be defined using an energy balance of the combustion chamber:

$$h_4 = \frac{\dot{m}_{fuel} \cdot LHV \cdot \eta_{cc} + \dot{m}_{air} \cdot h_3}{\dot{m}_{cg}} \tag{1.19}$$

$$h_i = c_{p,cg}(T_i) \cdot (T_i - T_0) \tag{1.20}$$

3.1.5 Determination of the combustion gas compositions

The compositions of the combustion gases (CG), depending on the fuel and the amount of excess air, are calculated using the combustion equations for each component.

a.) Natural gas firing:

Considering the determined 529.3 % excess air, the NG composition of Table 1 and the fuel and air flow rates, the composition of the NG combustion gases is calculated using combustion equations for each component (see equation 1.18a) and is shown in Table 11:

Table 11 - Composition of the NG combustion gases considering 529.3 %EA

COMPONENT	VOLUME (%)	MOLAR MASS (g/mol)	MASS (%)
CO_2	1.72	44.01	2.64
H_2O	3.18	18.02	2.00
N_2	77.73	28.01	75.96
O_2	17.38	32.00	19.40
Total	100.00	28.66	100.00

Source: Author himself.

b.) Biogas firing:

The composition of the biogas combustion gases, considering 515.4 % excess air and the biogas composition of Table 3, is calculated using stoichiometric combustion equations for each component (see equation 1.18b) and is shown in Table 12:

Table 12 - Composition of the biogas combustion gases considering 515.4 %EA

COMPONENT	VOLUME (%)	MOLAR MASS (g/mol)	MASS (%)
CO_2	2.56	44.01	3.91
H_2O	3.33	3.73	2.08
N_2	76.98	28.01	74.94
O_2	17.14	32.00	19.06
Total	100.00	28.77	100.00

Source: Author himself.

c.) Syngas firing:

The composition of the syngas combustion gases, considering 592.8 % excess air and the syngas composition of Table 5, is calculated using stoichiometric combustion equations for each component (see equation 1.18c) and is shown in Table 13:

Table 13 - Composition of the syngas combustion gases considering 592.8 %EA

COMPONENT	VOLUME (%)	MOLAR MASS (g/mol)	MASS (%)
CO_2	3.70	44.01	5.62
H_2O	3.05	18.02	1.90
N_2	75.97	28.01	73.40
O_2	17.28	32.00	19.07
Total	100.00	28.98	100.00

Source: Author himself.

The calculated percentages of O_2 in the combustion gases for all three fuels correspond to the “approximately 18% O_2” informed by the manufacturer (CAPSTONE TURBINE CORPORATION, 2009).

3.1.6 Calculation of the pressures

The pressures are not affected by the fuel.

$$p_a = p_0 - \frac{\rho_{air} \cdot g \cdot a}{1000} \tag{1.21}$$

$$p_7 = p_a \tag{1.22}$$

$$p_1 = p_a - \Delta p_{inlet} \tag{1.23}$$

$$PR = \frac{p_2}{p_1} \tag{1.24}$$

$$p_2 = \frac{p_3}{1 - \Delta p_{rec}} \tag{1.25}$$

$$p_3 = \frac{p_4}{1 - \Delta p_{cc}} \tag{1.26}$$

$$p_6 = \frac{p_7}{1 - \Delta p_{HRSG}} \tag{1.27}$$

$$p_5 = \frac{p_6}{1 - \Delta p_{rec}} \tag{1.28}$$

In accordance to Silveira and Tuna (2004), pressure losses in the combustion chamber (Δp_{cc}) and the recuperator (Δp_{rec}) are 5% and 3%, respectively. In accordance to Capstone Turbine Corporation (2009), the inlet pressure drop (Δp_{inlet}) is adopted at 0.5 kPa and pressure losses in the HRSG (Δp_{HRSG}) are 2%. Furthermore, the average atmospheric pressure at sea level is 101.325 kPa and the density of the air is set at a constant value of 1.2 kg/m³.

3.1.7 Calculation of the MGT system

a.) Temperatures T_2, T_3, T_4 and T_5

T_1 is the inlet air temperature and is equivalent to the ambient temperature. T_6 is the exhaust gas temperature given by the turbine manufacturer. T_2 is calculated with an energy balance for the compressor:

$$T_2 = T_1 \cdot \left\{ 1 + \frac{1}{\eta_{isoComp}} \cdot \left[\left(\frac{P_2}{P_1} \right)^{\frac{\delta_{air}-1}{\delta_{air}}} - 1 \right] \right\} \tag{1.29}$$

with:

δ_{air} is the polytropic index, also known as specific heat ratio (c_p / c_v) of air.

$$\delta_{air}(T_1) = \frac{1}{1 - \frac{R_{air}}{c_{p,air}(T_1)}} \tag{1.30}$$

$$c_{p,air}(T) = 1.04841 - 0.000383719 \cdot T + \frac{9.45378 \cdot T^2}{10^7} - \frac{5.49031 \cdot T^3}{10^{10}} + \frac{7.92981 \cdot T^4}{10^{14}} \tag{1.31}$$

In accordance to Silveira and Tuna (2003), the isentropic efficiency of the compressor ($\eta_{isoComp}$) and the isentropic efficiency of the MGT (η_{isoGT}) are set at 0.82 and 0.87, respectively. The gas constant of air (R_{air}) is 0.287 kJ/(kg K). T_5 is determined using an energy balance of the gas turbine:

$$T_5 = T_4 \cdot \left[1 - \eta_{isoGT} \cdot \left(1 - \frac{P_4}{P_5}^{\frac{1-\delta_{cg}}{\delta_{cg}}} \right) \right] \tag{1.32}$$

with:

δ_{cg} is the polytropic index, also known as specific heat ratio (c_p / c_v) of the combustion gases.

$$\delta_{cg}(T_4) = \frac{1}{1 - \frac{R_{cg}}{c_{p,cg}(T_4)}} \tag{1.33}$$

$$R_{cg} = \frac{R_u}{M_{cg}} \tag{1.34}$$

with:

R_u is the universal gas constant (8.3143 kJ/kg K).

M_{cg} is the molar mass of the combustion gas, in g/mol.

The molar masses of the NG, biogas and syngas combustion gases can be taken from Tables 2, 4 and 7, respectively. The specific heat capacities of the combustion gases are calculated by weighing the specific heat equations of the gas components (CO_2, H_2O, N_2 and O_2) according to the mass fractions of the combustion gases (Tables 11, 12 and 13):

$$c_{p,NG}(T) = 0.98738 + \frac{8.75193 \cdot T}{10^5} + \frac{1.66504 \cdot T^2}{10^7} - \frac{0.69474 \cdot T^3}{10^{10}} \tag{1.35a}$$

$$c_{p,BIO}(T) = 0.98210 + \frac{10.39016 \cdot T}{10^5} + \frac{1.54662 \cdot T^2}{10^7} - \frac{0.66569 \cdot T^3}{10^{10}} \tag{1.35b}$$

$$c_{p,SYN}(T) = 0.97166 + \frac{12.78966 \cdot T}{10^5} + \frac{1.35483 \cdot T^2}{10^7} - \frac{0.61708 \cdot T^3}{10^{10}} \tag{1.35c}$$

The specific heats can be determined more precisely using software, e.g. the Engineering Equation Solver (EES).

T_3 is determined using equation (1.20) and an energy balance for the recuperator, with the assumption that no heat is lost, as the heat exchangers outside area is negligible in comparison to the heat transfer area:

$$h_3 = h_2 + \frac{\dot{m}_{cg}\left(h_5 - h_6\right)}{\dot{m}_{air}} \tag{1.36a}$$

$$T_3 = T_1 + \frac{1}{c_p(T_3)} \cdot \left(h_2 + \frac{\dot{m}_{cg}\left(h_5 - h_6\right)}{\dot{m}_{air}} \right) \tag{1.36b}$$

The recuperator effectiveness is defined as:

$$Effec_{rec} = \frac{\left(T_3 - T_2\right)}{\left(T_5 - T_2\right)} \tag{1.37}$$

b.) Shaft power according to power output

$$W_{shaft} = \frac{E_{el}}{\eta_{ger}} \tag{1.38}$$

In accordance to Silveira and Tuna (2003), the efficiency of the power generator is adopted as 0.99.

c.) Power of the compressor (W_c)

$$W_c = \dot{m}_{air} \cdot (h_2 - h_1) \tag{1.39}$$

c.) Power of the MGT (W_{GT})

$$W_{GT} = W_c + W_{shaft} \tag{1.40}$$

3.1.8 Calculation of the HRSG

The exhaust gas temperature at the exit of the HRSG T_{7ai} is adopted as an initial value of 150°C and will be adjusted according to pinch point. T_8 and T_9 are adopted as 95°C (368.2 K) and 250°C (523.2 K), respectively. Furthermore, h_8 is the enthalpy of the compressed water at T_8. In accordance to Balestieri (2002), the efficiency of the HRSG (η_{HRSG}) is adopted at 0.80 and steam process pressure is adopted at 1.5 MPa.

a.) Steam flow in HRSG calculated using initial exhaust temp. T_{7ai} ($\dot{m}_{st,ai}$)

$$\dot{m}_{st,ai} = \dot{m}_{cg} \cdot \eta_{HRSG} \frac{h_6 - h_{7ai}}{h_9 - h_8} \tag{1.41}$$

h_8 (T = 368.2 K; P = 1500 kPa) = 399 kJ / kg *

h_9 (T = 523.2 K; P = 1500 kPa) = 2923 kJ / kg *

*Data from EES

b.) Correction of the exhaust gas temperature at point 7, using the *pinch point* (T_7)

According to Nadir and Ghenaiet (2015), the pinch point has to be adjusted to avoid condensation and corrosive sulphuric-acid formation of the exhaust gases and therewith prevent excessive damaging of the HRSG. The process steam pressure p_s is set at 1.5 MPa and the design pinch point temperature difference ΔT_{pp} is set at 10°C, in accordance to Nadir and Ghenaiet (2015). T_s is the saturation temperature corresponding to p_S. Furthermore, h_p is the specific enthalpy of the saturated liquid, considering the saturation pressure. The pinch point is illustrated in Figure 17.

Figure 17 – Graphical analysis of pinch point

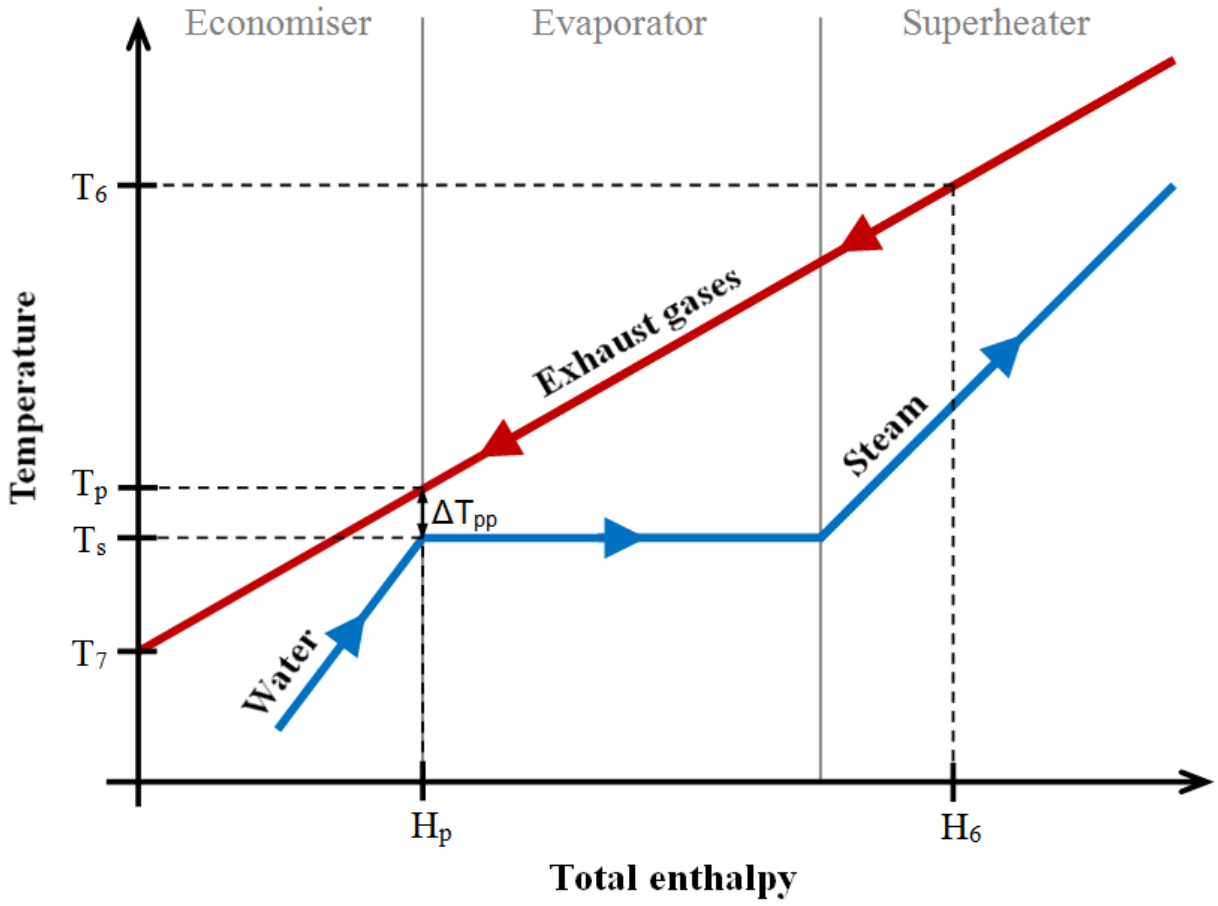

Source: Author himself.

Considering Figure 17, the intersect theorem results in the following equation:

$$\frac{T_6 - T_7}{T_6 - T_p} = \frac{H_6}{H_6 - H_p} \tag{1.42a}$$

$$T_7 = T_6 - \frac{T_6 - T_p}{H_6 - H_p} \cdot H_6 \tag{1.42b}$$

with:

T_7 is the pinch point adjusted exhaust temperature T_{7ai}, in K.

T_s (p_s = 1.5 MPa) = 198.3 °C

h_p = 844.9 kJ / kg

$$T_p = T_s + \Delta T_{pp} \tag{1.43}$$

$$H_p = \dot{m}_{st,ai} \cdot h_p \tag{1.44}$$

$$H_6 = \dot{m}_{cg} \cdot h_6 \tag{1.45}$$

c.) Heat flow recovered from the exhaust gases (E_R)

$$E_R = \dot{m}_{cg} \cdot (h_6 - h_7) \tag{1.46}$$

d.) Heat flow effectively transferred into the water / steam (E_{st})

$$E_{st} = \eta_{HRSG} \cdot E_R \tag{1.47}$$

e.) Steam flow in the HRSG adjusted to the *pinch point* ($\dot{m}_{st}$)

$$\dot{m}_{st} = \frac{E_{st}}{h_9 - h_8} \tag{1.48}$$

3.1.9 Calculation of the cogeneration plant's overall efficiency (η_{plant})

$$\eta_{plant} = \frac{E_{el} + E_{st}}{E_{fuel}} \tag{1.49}$$

note: a pump for the process steam / water is not considered in the analyses.

3.2 EXERGY ANALYSIS

The exergy analysis, based on the Second Law of Thermodynamics, allows a high quality assessment of the cogeneration system considering the exergy losses and destruction to determine the exergetic efficiencies. Exergy describes the potential of e.g. fluids inside a control volume to perform work. This potential is calculated comparing the state (e.g. temperature, pressure and velocity) inside the control volume with the conditions of the reference state, i.e. the environment.

The total exergy of a system consist of physical, chemical, kinetic and potential exergy and is defined as:

$$Ex = Ex^{PH} + Ex^{CH} + Ex^{KIN} + Ex^{PT} \tag{2.1}$$

For this study, the specific exergy is defined as the physical exergy:

$$ex = h - h_0 - T_0(s - s_0) \tag{2.2}$$

This excludes the influences of chemical reactions as well as kinetic and potential exergies. It means that in the equilibrium state with the environment, the fluid has zero work potential. For an ideal gas, the specific exergy is defined as follows:

$$ex = c_p \cdot (T - T_0) - T_0 \left[c_p \cdot \ln\left(\frac{T}{T_0}\right) - R \cdot \ln\left(\frac{p}{p_0}\right) \right] \tag{2.3}$$

The exergy flow rate is defined as:

$$\dot{E}x = ex \cdot \dot{m} \tag{2.4}$$

For ideal gases, specific entropy is expressed as:

$$s = c_p \cdot \ln\left(\frac{T}{T_0}\right) - R \cdot \ln\left(\frac{p}{p_0}\right) \tag{2.5}$$

In accordance to Tsatsaronis (2007), the exergetic efficiency, also known as second-law efficiency, is defined as the ratio between the product exergy leaving and the fuel exergy entering the control volume of the considered system:

$$\varepsilon = \frac{Ex_{product}}{Ex_{fuel}} \tag{2.6}$$

with:

$Ex_{product}$ is the desired (exergetic) result produced by the system, in kW.

Ex_{fuel} is the (exergetic) resource consumed by the system to obtain the product exergy, in kW.

The rational efficiency of Bonsjakovic describes the exergy destruction and exergy losses inside the system, and is defined as the ratio between total output of exergy and total input of exergy over a control volume:

$$\psi = \frac{\sum Ex_{out}}{\sum Ex_{in}} \tag{2.7}$$

in which $\sum Ex_{out}$ is the sum of all exergy transferred at the exit and $\sum Ex_{in}$ is the sum of all exergy transferred at the entrance of the system.

The irreversibility (entropy production) of a system, limited by a control volume, can be described in two different aspects. On the one hand, there are the external irreversibilities, meaning exergy losses to the environment and on the other hand, there are the internal irreversibilities, also well known as exergy destruction. The irreversibility as a combination of both aspects is defined as follows:

$$I = \sum \dot{E}x_{in} - \sum \dot{E}x_{out} \tag{2.8}$$

3.2.1 Determination of the specific exergies and specific entropies

The specific exergy at points 2 through 7 is determined using equation (2.3), while the specific entropy of the gases is calculated using equation (2.4). The specific exergy at checkpoints 8 and 9 is not affected by the fuel and is calculated with equation (2.2). Point 1 is air at atmospheric conditions; therefore the exergy and entropy at this point are both 0 kJ/kg. The fuel enters the combustion chamber at ambient temperature and the specific exergy of the fuel is determined as follows:

$$\mathrm{ex}_{10} = ex_{fuel}^{CH} \tag{2.9}$$

$$ex_{fuel}^{CH} = LHV \cdot \varphi \tag{2.10}$$

with:

φ is the estimated ratio of chemical exergy to LHV of fuel.

For complex fuels such as natural gas or biogas, the ratio φ can be estimated using the following empirical equation, in accordance to Szargut (2005):

$$\varphi = 1.0407 + 0.0154 \cdot \frac{H}{C} + 0.5904 \cdot \frac{S}{C} \cdot \left(1 - 0.175 \cdot \frac{H}{C}\right) \quad (2.11)$$

with:

H, C and S are the mass fractions of the elements hydrogen, carbon and sulphur, respectively.

In accordance to equation (2.11), the ratio φ for NG, biogas and syngas are estimated at 1.045, 1.044 and 1.043, respectively.

3.2.2 Calculation of the exergetic efficiencies

The exergetic efficiencies are calculated using a control volume and equation (2.6) for each of the components and the cogeneration system as a whole.

a.) Compressor

$$\varepsilon_c = \frac{\dot{E}x_2 - \dot{E}x_1}{W_c} \quad (2.12)$$

b.) Combustion chamber

$$\varepsilon_{cc} = \frac{\dot{E}x_4 - \dot{E}x_3}{\dot{E}x_{10}} \quad (2.13)$$

c.) Gas turbine

$$\varepsilon_{gt} = \frac{W_{GT}}{\dot{E}x_4 - \dot{E}x_5} \quad (2.14)$$

d.) Recuperator

$$\varepsilon_{rec} = \frac{\dot{E}x_3 - \dot{E}x_2}{\dot{E}x_5 - \dot{E}x_6} \quad (2.15)$$

e.) HRSG

$$\varepsilon_{HRSG} = \frac{\dot{E}x_9 - \dot{E}x_8}{\dot{E}x_6 - \dot{E}x_7} \quad (2.16)$$

f.) Power generator

$$\varepsilon_{ger} = \eta_{ger} \tag{2.17}$$

g.) Overall exergetic efficiency of the cogeneration plant

$$\varepsilon_{plant} = \frac{\dot{E}x_9 + E_{el}}{\dot{E}x_8 + \dot{E}x_{10}} \tag{2.18}$$

3.2.3 Calculation of the rational efficiencies

The rational efficiencies are calculated by applying a control volume and equation (2.7) to each of the components and the cogeneration system as a whole.

a.) Compressor

$$\psi_c = \frac{\dot{E}x_2}{\dot{E}x_1 + W_c} \tag{2.19}$$

b.) Combustion chamber

$$\psi_{cc} = \frac{\dot{E}x_4}{\dot{E}x_3 + \dot{E}x_{10}} \tag{2.20}$$

c.) Gas turbine

$$\psi_{gt} = \frac{W_{GT} + \dot{E}x_5}{\dot{E}x_4} \tag{2.21}$$

d.) Recuperator

$$\psi_{rec} = \frac{\dot{E}x_6 + \dot{E}x_3}{\dot{E}x_5 + \dot{E}x_2} \tag{2.22}$$

e.) HRSG

$$\psi_{HRSG} = \frac{\dot{E}x_7 + \dot{E}x_9}{\dot{E}x_6 + \dot{E}x_8} \tag{2.23}$$

f.) Power generator

$$\psi_{ger} = \eta_{ger} \tag{2.24}$$

g.) Overall rational efficiency of the cogeneration plant

$$\psi_{plant} = \frac{\dot{E}x_7 + \dot{E}x_9 + E_{el}}{\dot{E}x_8 + \dot{E}x_{10}} \tag{2.25}$$

3.2.4 Calculation of the irreversibilities of each component

The irreversibilities are calculated by applying a control volume and equation (2.8) to each of the components and the system as a whole.

a.) Compressor

$$I_c = \dot{E}x_1 + W_c - \dot{E}x_2 \tag{2.26}$$

b.) Combustion chamber

$$I_{cc} = \dot{E}x_3 + \dot{E}x_{10} - \dot{E}x_4 \tag{2.27}$$

c.) Gas turbine

$$I_{gt} = \dot{E}x_4 - \dot{E}x_5 - W_{GT} \tag{2.28}$$

d.) Recuperator

$$I_{rec} = \dot{E}x_2 + \dot{E}x_5 - \dot{E}x_3 - \dot{E}x_6 \tag{2.29}$$

e.) HRSG

$$I_{HRSG} = \dot{E}x_6 + \dot{E}x_8 - \dot{E}x_7 - \dot{E}x_9 \tag{2.30}$$

f.) Power generator

$$I_{ger} = E_{el} \cdot \left(\frac{1}{\eta_{ger}} - 1 \right) \tag{2.31}$$

g.) Total irreversibility

$$I_{plant} = I_c + I_{cc} + I_{gt} + I_{rec} + I_{HRSG} + I_{ger} \tag{2.32}$$

3.3 EMISSIONS ANALYSIS

According to Cârdu and Baica (1999a), the principal pollutant emissions of thermoelectric power plants are gaseous carbon dioxide, sulphur dioxide and nitrogen oxides (NO_x – mainly NO and NO_2). While CO_2 emissions are the major contributor to the greenhouse effect, SO_2 can reduce lung function and contributes to acid rain – damaging forests and ecosystems in rivers and lakes. NO_x contributes to global warming as well as acid rain, and can also affect human and animal health directly.

The emissions analysis evaluates the environmental impact of the cogeneration plant for each fuel. Environmental impacts are effects on humans and the environment. The emissions analysis is based on the assumption of a complete combustion of the fuel with the percentage of excess air determined in chapter 3.1.2. Therewith, the chemical reactions in the combustion chamber are simulated and a mass balance provides the combustion gas composition. Finally, the CO_2-equivalent is calculated, based on CO_2, SO_2 and NO_x emissions, to assess the pollution indicator and the ecologic efficiency.

a.) Calculation of the CO_2-equivilent of the emissions

The CO_2-equivalent, in kg per kg of fuel, scales the effects of the principal pollutant exhaust gas emissions (CO_2, SO_2, and NO_x), comparing the environmental effect of each gas to the environmental effect of CO_2. The factors are determined by dividing the maximum accepted concentration of CO_2 by the maximum concentrations of CO_2, SO_2 and NO_x, respectively. The maximum accepted concentrations for one hour, according to international air pollution standards, are shown in Table 14.

Table 14 - Pollution limits considering international air quality standards

Gas	Max. accepted concentration for one hour ($\mu g/m^3$)
CO_2	10,000
SO_2	125
NO_x	200

Source: (VILLELA; SILVEIRA, 2007; VILLELA, 2007).

In words, the CO_2-equivalent defined by equation (3.1) expresses, that the environmental effects of SO_2 and NO_x are, respectively, 80 and 50 times more harming than the effects of CO_2.

$$(CO_2)_e = (CO_2) + 80 \cdot (SO_2) + 50 \cdot (NO_x) \tag{3.1}$$

with:

(CO_2) is the mass of CO_2 in the exhaust gases per mass of fuel, in kgCO2/kgFUEL.

(SO_2) is the mass of SO_2 in the exhaust gases per mass of fuel, in kgSO2/kgFUEL.

(NO_x) is the mass of NO_x in the exhaust gases per mass of fuel, in kgNOx/kgFUEL.

b.) Calculation of the pollution indicator

The pollution indicator, in kg per MJ, relates the CO_2-equivalent to the LHV of the fuel. The unit kg refers to $(CO_2)_e$ mass (CÂRDU; BAICA, 1999a).

$$\Pi g = \frac{(CO_2)_e}{LHV_{fuel}} \tag{3.2}$$

with:

LHV_{fuel} is the LHV of the fuel, in MJ/kg.

c.) Calculation of the ecologic efficiency

The ecologic efficiency compares the pollution indicator (and therewith the CO_2-equivilent of the exhaust emissions) to air quality standards, also considering the energetic efficiency of the power plant. In accordance to Cârdu and Baica (1999b), the ecologic efficiency is described as follows:

$$\varepsilon_{eco} = \left[\frac{0.204 \cdot \eta_{plant}}{\eta_{plant} + \Pi g} \cdot \ln(135 - \Pi g) \right]^{0,5} \quad (3.3)$$

The ecologic efficiency is directly proportional to the energetic power plant efficiency and inversely proportional to the pollution indicator. As already expressed in equation (3.1), pure sulphur as fuel (SO_2 emissions) has the most severe environmental impact and thus has an ecologic efficiency of 0. The combustion of pure hydrogen, not considering the hydrogen production, has an ecologic efficiency of 1 (VILLELA; SILVEIRA, 2007). Some key ecologic efficiency values are presented in Table 15:

Table 15 - Ecologic efficiency values

Fuels	Πg (kg/MJ)	ε
Hydrogen	0	1
Sulphur	134	0
Others	1-134	0-1

Source: (VILLELA; SILVEIRA, 2007).

To calculate the CO_2-equivilent, and therewith the pollution indicator and the ecologic efficiency, the CO_2, SO_2, NO_x and PM emissions have to be determined for each fuel.

d.) Calculation of the ratio of CO_2-mass in the exhaust gases per mass of fuel

$$(CO_2) = \frac{w_{CO2} \cdot M_{CO2}}{M_{fuel}} \quad (3.4)$$

with:

M_{fuel} is the molar mass of the fuel, in g/mol.

M_{CO2} is the molar mass of CO_2, 44.01 g/mol.

w_{CO2} is the mol of CO_2 in the exhaust gases per mol of fuel, in mol/mol [equation (1.18)].

For biogas and syngas, the lifecycle of the fuel is considered: During plant (biomass) growth, CO_2 is absorbed by photosynthesis, neutralizing some or even all of the CO_2 combustion emissions of biofuels. In case of biogas and syngas operation, the biofuel is adopted to be produced on site. Therefore CO_2 emissions that could for example be caused by

transportation are small. As a result, in accordance to Huttunen, Manninen and Leskinen (2014), the CO_2-lifecycles of biogas is adopted to be 90% closed and hence, only 10% of its CO_2-emissions are considered in the CO_2-equivalent-calculation. In case of syngas, according to Machin (2015), 25.8% of its CO_2-emissions are considered in the calculation.

e.) Calculation of the ratio of SO_2-mass in the exhaust gases per mass of fuel

$$(SO_2) = n_{H2S} \cdot \frac{M_{SO2}}{M_{H2S}} \tag{3.5}$$

with:

n_{H2S} is the mass of H_2S in the fuel per mass of fuel, in kgH2S/kgFUEL.

M_{SO2} is the molar mass of SO_2, 64.07 g/mol.

M_{H2S} is the molar mass of H_2S, 34.08 g/mol.

3.3.1 Emissions analysis of natural gas firing

a.) Estimation of the amount of NO_x in the exhaust gases (NG)

According to Capstone Turbine Corporation (2008), the NO_x emissions of the Capstone C200 MGT are 0.181 kg/MWh_e when operating on NG. Considering the electric efficiency of the gas turbine system (31.3%) and the LHV of NG (47,053 kJ/kg) results in NO_x emissions of $7.4 \cdot 10^{-4}$ kgNOx/kgNG.

b.) Estimation of the amount of SO_2 in the exhaust gases (NG)

According to the main provider of NG in São Paulo, COMGÁS (2015a), the maximum amount of H_2S in local NG is 10 mg per Nm^3 of NG. Considering NG density of 0.77 kg/m^3 results in $1.3 \cdot 10^{-5}$ kgH2S/kgNG. Equation (3.5) is formulated assuming that all the sulphur from H_2S is transformed into SO_2, by reaction with oxygen. Further calculation of (SO_2) is conducted using equation (3.5).

3.3.2 Emissions analysis of biogas firing

a.) Estimation of the amount of NO_x in the exhaust gases (biogas)

According to Capstone Turbine Corporation (2008), the NO_x emissions of the Capstone C200 MGT are also 0.181 kg/MWh_e when operating on biogas. Considering the electric efficiency of the gas turbine system (31.3%) and the LHV of biogas (20,192 kJ/kg) results in NO_x emissions of $3.2 \cdot 10^{-4}$ kgNOx/kgBIO.

b.) Estimation of the amount of SO_2 in the exhaust gases (biogas)

In accordance to Swedish Gas Technology Center (2012) and Mkoma and Mabiki (2011), the amount of H_2S in the unfiltered biogas is estimated at 500 ppmV. The filtering process is adopted to remove 99% of the H_2S. Considering the molar masses of H_2S (34.08 g/mol) and biogas (25.38 g/mol) results in $6.7 \cdot 10^{-6}$ kgH2S/kgBIO. Further calculation of (SO_2) is conducted using equation (3.5).

3.3.3 Emissions analysis of syngas firing

a.) Estimation of the amount of NO_x in the exhaust gases (syngas)

As the selected syngas composition contains 32 %vol of H_2 (LHV of 119,946 kJ/kg), leading to significantly higher flame temperatures, the NO_x emissions of the Capstone C200 MGT are estimated at 0.4 kg/MWh_e when operating on syngas. Considering the electric efficiency of the gas turbine system (31.3%) and the LHV of syngas (10,928 kJ/kg) results in NO_x emissions of $3.8 \cdot 10^{-4}$ kgNOx/kgSYN.

b.) Estimation of the amount of SO_2 in the exhaust gases (syngas)

In accordance to Boerrigter and Rauch (2005) the sum um all sulphur compounds in the filtered syngas is adopted at 1 ppmV. Considering the molar masses of H_2S (34.08 g/mol) and syngas (22.98 g/mol) results in $1.5 \cdot 10^{-6}$ kgH2S/kgSYN. Further calculation of (SO_2) is conducted using equation (3.5).

3.4 ECONOMIC ANALYSIS

In the economic analysis, annualised production costs of all products are calculated based on investment, fuel cost and maintenance cost. Thereafter, the expected annual saving is determined by comparing the power and steam production costs of the proposed

cogeneration plant with the products' costs on the market. For the analysis, it is adopted that the process consumes all generated power and steam.

3.4.1 Annualised production cost per kWh

The annualized production cost depends on the following aspects:

$$C = C_{INV} + C_{FPO} + C_M \tag{4.1}$$

with:

C_{INV} is the cost related to the initial investment in the plant, in USD/kWh.

C_{FPO} is the cost related to the fuel per plant output, in USD/kWh.

C_M is the maintenance and operation cost, in USD/kWh.

a.) Annualised power production cost in accordance to Silveira et al. (2012):

$$C_{el} = \frac{I_{gts} \cdot f}{H \cdot \left(E_{el} - W_{GB}\right)} + C_{fuel} \cdot \frac{E_{fuel} - E_R - \frac{E_{los}}{2}}{E_{el} - W_{GB}} + C_{M,gts} \tag{4.2}$$

with:

I_{gts} is the investment in the gas turbine system, in USD.

f is the annuity factor, in year $^{-1}$.

H is the hours of operation per year, in h/year.

$$I_{gts} = I_{MGT} \cdot k_{civ} \cdot k_{import} + I_{GB} \tag{4.2}$$

note: I_{GB} is only added in case of low pressure biofuel operation (biogas and syngas)

The annual operation load (H) is set as 7000 h/year. In accordance to Kang et al. (2014), the factor for civil engineering and transportation cost (k_{civ}) is adopted as 1.3. The factor for import and tax cost for Brazil (k_{import}) is estimated at 1.4. The total investment in the gas booster (I_{GB}) is estimated at 10,000 USD. The annuity factor (f) and the interest rate quotient are defined according to Silveira et al. (2012).

$$f = q^k \frac{q-1}{q^k - 1} \tag{4.3}$$

with:

q is the interest rate quotient.

k is the payback, the amortisation period of the investment, in years.

$$q = 1 + \frac{r}{100} \tag{4.4}$$

with:

r is the annual interest rate, in percent.

The energy losses per unit of time are described as follows:

$$E_{los} = E_{fuel} - E_{el} - E_R \tag{4.5}$$

In accordance to Kang et al. (2014) and Barigozzi et al. (2015), the maintenance and operation cost of the MGT system ($C_{M,gts}$) is estimated at 0.012 USD/kWh. The cost of NG (C_{NG}) is determined in accordance to the main provider of NG in São Paulo, COMGÁS (2015b); see Table 16:

Table 16 - Price rates of NG for commercial use (November 2015)

Consumption (m³/month)	Fixed price (BRL/month)	Variable price (BRL/m³)
0.01 – 50.00	32.70	4.408561
50.01 – 150.00	53.14	3.999775
150.01 – 500.00	94.01	3.728959
500.01 – 2,000.00	214.60	3.487708
2,000.01 – 3,500.00	989.25	3.100441
3,500.01 – 50,000.00	3,709.76	2.323742
> 50,000.00	9,841.57	2.201106

Source: (COMGÁS, 2015b).

Table 17 shows the NG price rates, considering an exchange rate of 0.26 USD/BRL (November 2015) and a NG density of 0.77 kg/m³.

Table 17 - Price rates of NG for commercial use (in USD and kg)

Consumption (kg/month)	Fixed price (USD/month)	Variable price (USD/kg)
0.01 – 38.50	8.50	1.488605
38.51 – 115.50	13.82	1.350573
115.51 – 385.00	24.44	1.259129
385.01 – 1,540.00	55.80	1.177668
1,540.01 – 2,695.00	257.21	1.046902
2,695.01 – 38,500.00	964.54	0.784640
> 38,500.00	2558.81	0.743231

Source: (based on COMGÁS, 2015b).

The price of NG in USD/kg depending on monthly consumption is shown in Figure 18:

Figure 18 - Price of NG depending on monthly consumption

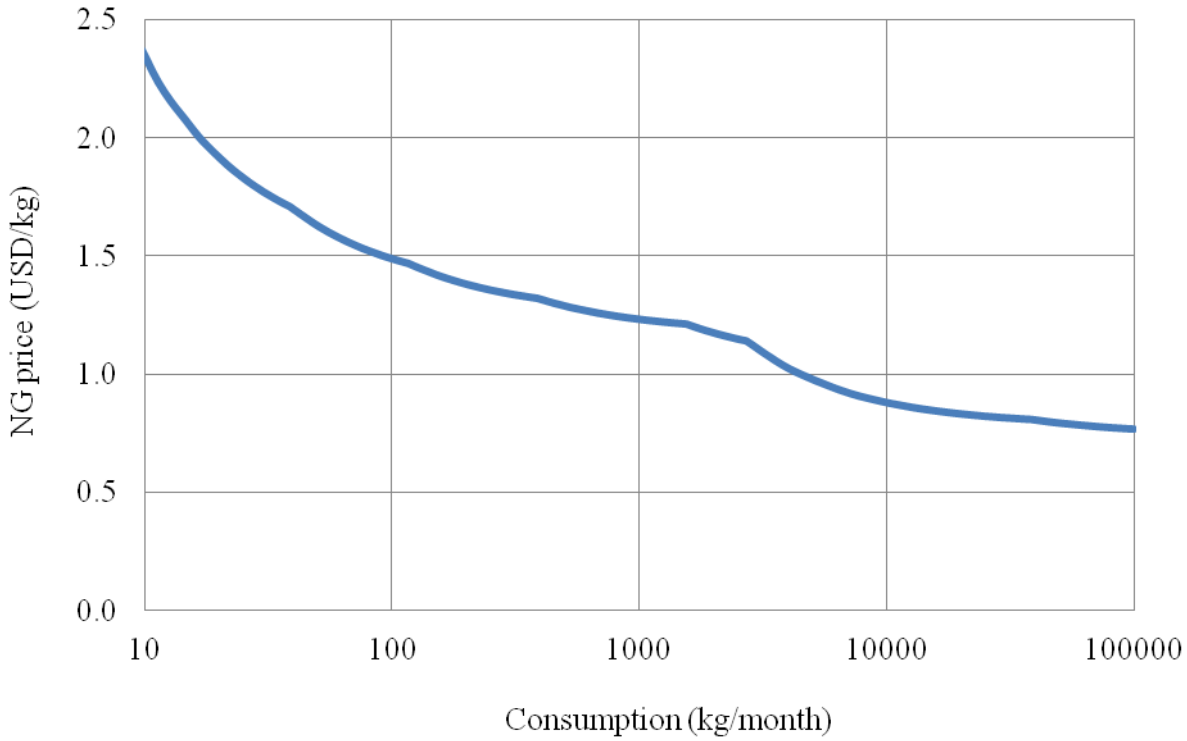

Source: Author himself.

The NG consumption calculated in chapter 3.1 is 0.01175 kg/s. Considering the adopted 7000 hours of operation per year, results in a consumption of 24,675 kg/month and a price of

0.8237 USD/kg. Further considering the LHV of NG (47,053 kJ/kg or 13.07 kWh/kg) results in a NG price of 0.063 USD/kWh.

The price ratio of NG to biogas is estimated at 3.25, in accordance to Brizi et al. (2014). Herewith, price of filtered biogas (C_{bio}) is adopted at 0.019 USD/kWh. The production of syngas by biomass gasification is a much more complex process. Considering the syngas consumption of 0.05 kg/s determined in chapter 3.1, syngas density of 0.95 kg/m³ and a syngas LHV of 10,928 kJ/kg (3.04 kWh/kg), price of filtered syngas (C_{syn}) is estimated at 0.070 USD/kWh, in accordance to Parajuli et al. (2014) and Deng and Parajuli (2011).

b.) Annualised steam production cost in accordance to Silveira et al. (2012):

$$C_{st} = \frac{I_{HRSG} \cdot f}{H \cdot E_{st}} + C_{fuel} \cdot \frac{E_R + \frac{E_{los}}{2}}{E_{st}} + C_{M,HRSG} \tag{4.6}$$

The maintenance cost and operation of HRSG ($C_{M,HRSG}$) are adopted as 0.006 USD/kWh and the investment in the HRSG is estimated as follows (KANG et al., 2014; BARIGOZZI et al., 2015):

$$I_{HRSG} = 0.3 \cdot I_{MGT} \cdot k_{import} \tag{4.7}$$

3.4.2 Expected annual saving

The expected annual saving determines the annual cash flow that can be economised by implementing the proposed power plant, instead of purchasing power and producing steam with conventional boilers.

$$\mathrm{Re} = \mathrm{Re}_{el} + \mathrm{Re}_{st} \tag{4.8}$$

$$\mathrm{Re}_{el} = E_{el} \cdot H \cdot \left(P_{el} - C_{el}\right) \tag{4.9}$$

$$\mathrm{Re}_{st} = E_{st} \cdot H \cdot \left(C_{spc} - C_{st}\right) \tag{4.10}$$

with:

C_{spc} is the steam production cost using conventional boilers (already amortised) burning fuel oil, in USD/kWh.

The electric energy price (P_{el}) in Guaratinguetá, including 20% taxes, is adopted at 0.19 USD/kWh, in accordance with ANEEL (Agência Nacional de Energia Elétrica) and Bandeirante Energia S.A. (local electricity provider), November 2015. The steam production cost using conventional boilers (already amortised) burning fuel oil is determined in accordance to Antunes (1999):

$$C_{spc} = \frac{P_{oil}}{\eta_{cb}} + C_{M,cb} \tag{4.11}$$

In accordance to Antunes (1999), the efficiency of the conventional boiler (η_{cb}) is 0.85 and the maintenance and operation cost of the conventional boiler system ($C_{M,cb}$) is adjusted in comparison to other maintenance costs and estimated at 0.008 USD/kWh. According to Sun, Doyle and Smith (2015), the price relation of fuel oil to NG is 1.47. Using this ratio and the NG price of November 2015, the fuel oil price (P_{oil}) is estimated at 0.093 USD/kWh.

4 RESULTS & DISCUSSION

The analyses presented in chapter 3 are conducted using the software EES. Diagrams are created using Microsoft Excel. First, the universal coefficients to adjust the gas turbine ISO-condition-data to the local conditions, introduced in chapter 2.6, are compared to the adjustment method for the Capstone C200 MGT recommended by its manufacturer, demonstrated in chapter 3.1.1. Table 18 presents a numeric overview of the adjustment coefficients for both methods.

Table 18 - Comparison of turbine data adjustment methods

PARAMETER (ISO-Value)	ADJUSTMENT METHOD	ADJUSTMENT COEFFICIENTS					ADJUSTED VALUE
		T_0	a	U	ipd*	ebp*	
E_{el} (200 kW)	Capstone C200	0.982	0.922	-	0.987	0.969	173.1 kW
	Universal	0.960	0.920	0.999	-	-	176.4 kW
HR (10.9 MJ/kWh)	Capstone C200	1.026	-	-	1.005	1.019	11.5 MJ/kWh
	Universal	1.020	-	1.003	-	-	11.1 MJ/kWh
$\dot{m}_{cg}$ (1.32 kg/s)	Capstone C200	1.000	0.909	-	-	-	1.20 kg/s
	Universal	0.920	0.920	-	-	-	1.12 kg/s
T_6 (279.4°C)	Capstone C200	1.055	-	-	-	-	294.7°C
	Universal	-	-	-	-	-	279.4°C

Source: Author himself. *ipd is inlet pressure drop and ebp is exhaust back pressure

The most significant difference between the two methods is that Capstone adjusts the exhaust gas temperature (T_6) depending on the ambient temperature (T_0), whereas the presented universal method does not adjust T_6. As the exhaust gas temperature has a significant influence on the steam production in the HRSG, the Capstone method promises more correctness in this regard. Furthermore, Capstone does not consider the local humidity, while the universal method neither considers the inlet pressure drop nor the exhaust back pressure. Whereas the humidity has a negligible influence (ISO relative humidity is 60% and local relative humidity is 70%), the pressure coefficients decrease the turbine performance significantly (E_{el} and HR). Another noticeable disparity is the temperature coefficient for the

exhaust mass flow rate ($\dot{m}_{cg}$). In the universal model, the mass flow rate is already significantly influenced at 25°C (0.920), whereas Capstone suggests a much smaller impact, even at 30°C (0.985). This results in a significant difference in gaseous mass flow rate and plant performance. The two methods offer a high congruence regarding the other ambient temperature and altitude (pressure) coefficients. Overall, the Capstone C200 method presents a higher overall accuracy – as to be expected from a turbine-specific adjustment method.

4.1 RESULTS AND DISCUSSION OF FIRST LAW ANALYSIS

The state variables at points 1 through 10 for NG, biogas and syngas operation are presented in Tables 19, 20 and 21, respectively.

Table 19 - State variables for NG operation

POINT	Fluid	$\dot{m}$ (kg/s)	T (°C)	p (kPa)	c_p (kJ/kg K)	h (kJ / kg)	H (kW)
1	Air	1.188	25.0	93.5	1.004	0.0	0.0
2	Air	1.188	201.8	374.1	1.025	181.1	215.2
3	Air	1.188	544.8	362.9	1.102	572.8	680.6
4	CG	1.200	876.2	344.7	1.202	1023.5	1228.1
5	CG	1.200	616.1	98.9	1.148	678.6	814.3
6	CG	1.200	294.7	96.0	1.078	290.7	348.9
7	CG	1.200	193.4	94.0	1.057	178.1	213.7
8	Steam	0.043	95.0	1500.0	-	399.3	17.1
9	Steam	0.043	250.0	1500.0	-	2923.0	125.3
10	NG	0.012	25.0	550.0	-	0.0	0.0

Source: Author himself.

Table 20 - State variables for biogas operation

POINT	Fluid	ṁ (kg/s)	T (°C)	p (kPa)	c_p (kJ/kg K)	h (kJ / kg)	H (kW)
1	Air	1.172	25.0	93.5	1.004	0.0	0.0
2	Air	1.172	201.8	374.1	1.025	181.1	212.4
3	Air	1.172	553.9	362.9	1.104	584.0	684.7
4	CG	1.200	879.2	344.7	1.205	1029.6	1235.5
5	CG	1.200	619.8	98.9	1.151	684.5	821.4
6	CG	1.200	294.7	96.0	1.079	290.9	349.1
7	CG	1.200	193.4	94.0	1.057	178.0	213.7
8	Steam	0.043	95.0	1500.0	-	399.3	17.1
9	Steam	0.043	250.0	1500.0	-	2923.0	125.5
10	Biogas	0.028	25.0	550.0	-	0.0	0.0

Source: Author himself.

Table 21 - State variables for syngas operation

POINT	Fluid	ṁ (kg/s)	T (°C)	p (kPa)	c_p (kJ/kg K)	h (kJ / kg)	H (kW)
1	Air	1.148	25.0	93.5	1.004	0.0	0.0
2	Air	1.148	201.8	374.1	1.025	181.1	208.2
3	Air	1.148	577.4	362.9	1.110	612.9	703.8
4	CG	1.200	896.1	344.7	1.208	1052.1	1262.5
5	CG	1.200	635.0	98.9	1.153	703.6	844.3
6	CG	1.200	294.7	96.0	1.076	290.3	348.3
7	CG	1.200	193.4	94.0	1.054	177.5	213.0
8	Steam	0.043	95.0	1500.0	-	399.3	17.1
9	Steam	0.043	250.0	1500.0	-	2923.0	125.4
10	Syngas	0.052	25.0	550.0	-	0.0	0.0

Source: Author himself.

The pressures in the cogeneration system are not influenced by the fuel and hence are the same for NG, biogas and syngas operation. Besides the fuel flow rates, the most characterising values from Tables 19, 20 and 21 are the respective turbine inlet temperatures (T_4) of 876.2°C for NG, 879.2°C for biogas and 896.1°C for syngas operation. Because the efficiency of the gas turbine decreases for biogas and especially syngas, the biofuels need to insert more fuel energy into the combustor to maintain the power output of the generator, resulting in higher turbine inlet temperatures.

Table 22 gives an overview of important energetic data of the cogeneration system and how they behave, depending on the fuel:

Table 22 - Overview of important energetic data of the cogeneration system

	NG operation	Biogas operation	Syngas operation
E_{el} (kW)	173.1	162.1	162.1
E_{fuel} (kW)	553.0	556.4	564.3
η_{GT} (%)	31.3	29.1	28.7
E_{st} (kW)	108.2	108.4	108.3
$\dot{m}_{fuel}$ (kg/s)	0.012	0.028	0.052
W_c (kW)	215.2	212.4	208.0
%EA (%)	529.3	515.4	592.8
$Effec_{rec}$ (%)	82.8	84.2	86.7
η_{plant} (%)	50.9	48.6	47.9

Source: Author himself.

In accordance to Vescovo (2015), the power output of the electric generator is a design value that is not influenced by the fuel. The lower plant power output for biogas and syngas operation is only due to the power consume of the gas booster, necessary to compress the low pressure biofuels. The power output of the electric generator can be kept constant, because the MGT Capstone C200 is available in specific versions for different fuels. Each version has a fuel-specific fuel injection system, allowing the fuel flow rate to be increased with decreasing fuel heating value. The fuel flow rate has to be programmed manually depending on the LHV of the fuel, to ensure that the required fuel energy is inserted into the system. Furthermore, the Capstone C200 always operates with a very large excess of air (more than 500 %EA), independent of the chosen fuel. Therefore, the combustion chamber allows complete

combustion of NG, biogas and syngas, without the need for chamber modifications. This is also the reason, why the combustion gas mass flow ($\dot{m}_{cg}$) is not influenced by the fuel (the pressures are also independent of the fuel) – the combustion gas mass flow is defined by the turbine, combustion chamber and compressor design. Consequently, increase of fuel flow leads to a slight decrease of air flow rate and decrease of power absorbed by the compressor (W_c). Due to the great amount of excess air, the compositions and specific heats (c_p) of the exhaust gases are very similar for all fuels. This combined with the constant exhaust gas temperature (T_6) and the constant combustion gas flow rate, results in basically identical steam output (E_{st}). The electric efficiency of the gas turbine (η_{GT}) is the highest for NG operation, as the MGT is designed for this fuel. According to Somehsaraei et al. (2014), the electric efficiency declines with decreasing LHV of the fuel, because the fuel and gas properties change. Therefore, all the components of the system no longer operate at the design point, but in off-design mode (similar to partial load mode). But the major efficiency drop from NG to biofuels is caused in large part by the energy consumed by the gas booster. The energetic plant efficiencies for natural gas, biogas and syngas operation are in the expected range for micro gas turbines of this capacity.

The specific heat curves of the combustion gases, depending on the temperature, are shown in Figure 19 for NG, biogas and syngas operation. Due to the large amount of excess air, resulting in predominant amounts of nitrogen and oxygen in the combustion gases, the specific heats are very similar.

Figure 19 - Specific heat curves of combustion gases of each fuel

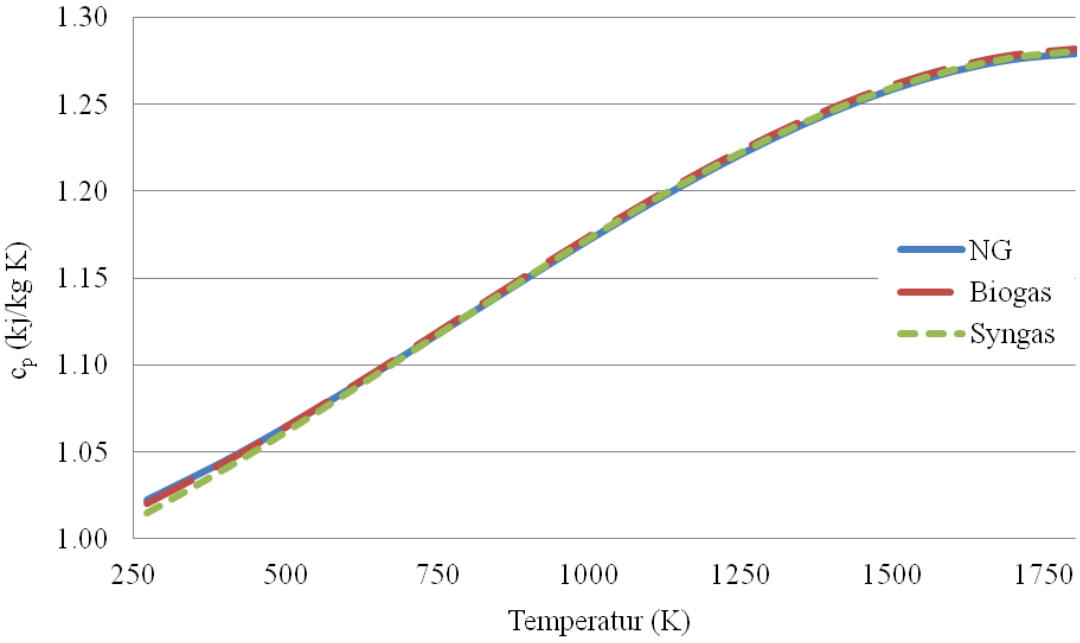

Source: Author himself.

Figure 20 shows the temperature and enthalpy profiles of the air and the combustion gases in the MGT system for NG, biogas and syngas operation. Both temperature and enthalpy increase in the compressor, the air side of the recuperator and the combustion chamber. Thereupon, they decrease in the gas turbine, the combustion gas side of the recuperator and in the HRSG.

Figure 20 - Temperature and enthalpy profiles for NG, biogas and syngas operation

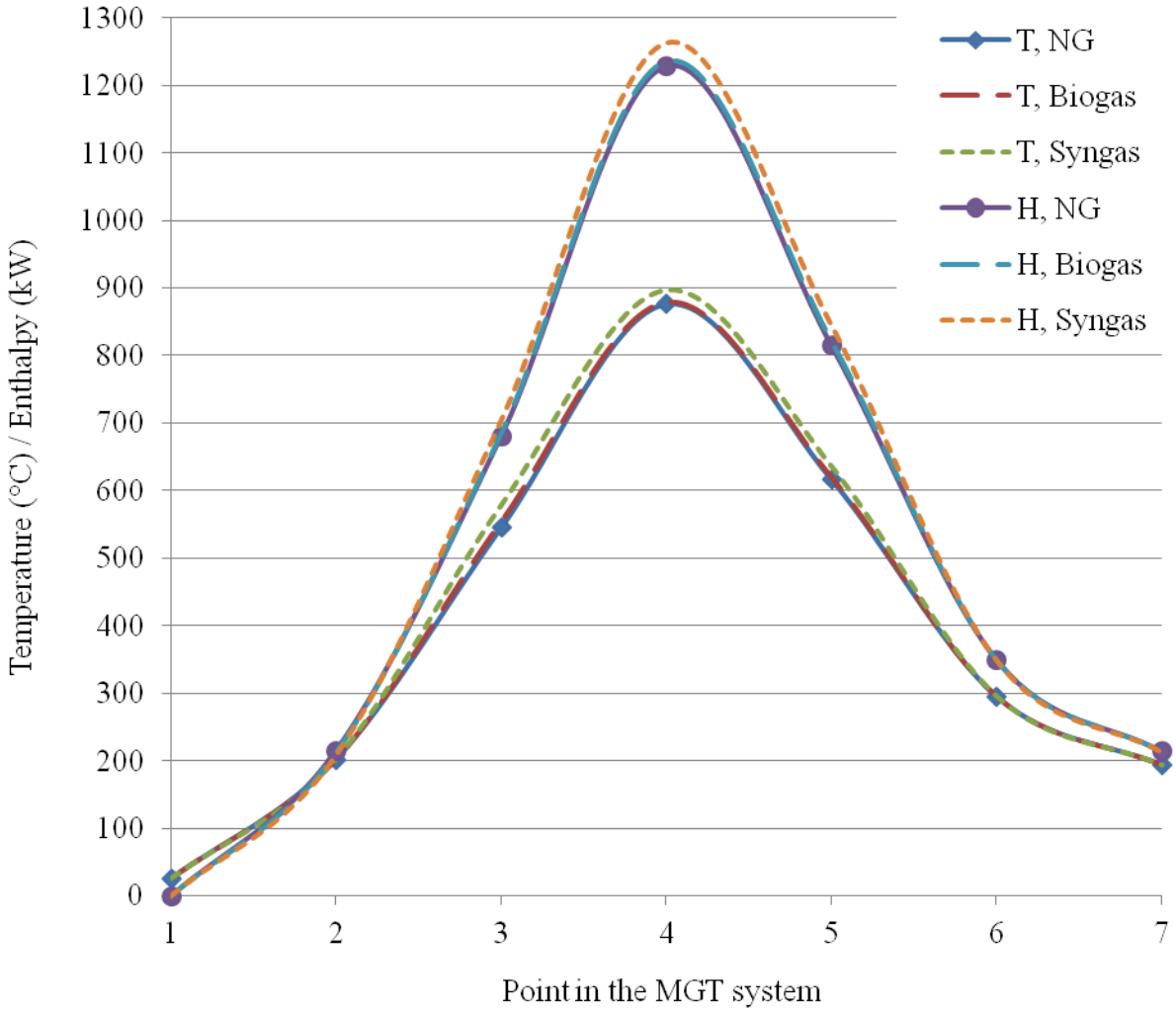

Source: Author himself.

The energetic efficiencies of each component of the CHP plant are presented as part of the energy and exergy analysis comparison in Table 26.

4.2 RESULTS AND DISCUSSION OF EXERGY ANALYSIS

The principle exergetic data at points 1 through 10 for NG, biogas and syngas operation are presented in Tables 23, 24 and 25, respectively.

Table 23 - Exergetic data at points 1 through 10 for NG operation

POINT	Fluid	T (°C)	s (kJ/kg K)	ex (kJ / kg)	Ėx (kW)
1	Air	25.0	0.0000	0.0	0.0
2	Air	201.8	0.0792	157.5	187.2
3	Air	544.8	0.7230	357.2	424.5
4	CG	876.2	1.2440	652.6	783.1
5	CG	616.1	1.2383	309.4	371.3
6	CG	294.7	0.6871	85.9	103.1
7	CG	193.4	0.4719	37.4	44.8
8	Steam	95.0	1.2520	30.6	1.3
9	Steam	250.0	8.0240	534.8	23.9
10	NG	25.0	-	49170.4	577.9

Source: Author himself.

Table 24 - Exergetic data at points 1 through 10 for biogas operation

POINT	Fluid	T (°C)	s (kJ/kg K)	ex (kJ / kg)	Ėx (kW)
1	Air	25.0	0.000	0.0	0.0
2	Air	201.8	0.0792	157.5	184.7
3	Air	553.9	0.7374	364.1	426.9
4	CG	879.2	1.2525	656.1	787.3
5	CG	619.8	1.2462	313.0	375.6
6	CG	294.7	0.6876	85.9	103.1
7	CG	193.4	0.4719	37.4	44.8
8	Steam	95.0	1.2520	30.6	1.3
9	Steam	250.0	8.0240	534.8	23.0
10	Biogas	25.0	-	21080.0	577.4

Source: Author himself.

Table 25 - Exergetic data at points 1 through 10 for syngas operation

POINT	Fluid	T (°C)	s (kJ/kg K)	ex (kJ / kg)	Ėx (kW)
1	Air	25.0	0.0000	0.0	0.0
2	Air	201.8	0.0792	157.5	181.1
3	Air	577.4	0.7740	382.1	438.8
4	CG	896.1	1.2762	671.6	805.9
5	CG	635.0	1.2686	325.3	390.4
6	CG	294.7	0.6861	85.7	102.9
7	CG	193.4	0.4705	37.2	44.7
8	Steam	95.0	1.2520	30.6	1.3
9	Steam	250.0	8.0240	534.8	22.9
10	Syngas	25.0	-	11397.9	576.8

Source: Author himself.

As already mentioned and explained in chapter 4.1, the by far most significant difference between the three fuel scenarios are the LHVs, and therewith also the specific exergies of the fuels. Because the Capstone C200 is available in different, fuel-optimised versions, the fuel flow can be adjusted without a significant effect on the system's efficiencies. This observation is also reflected in the efficiency overview demonstrated in Table 26. The principle differences between energetic and exergetic efficiencies are identified for the combustion chamber and the HRSG. At 62% and 37%, respectively, they also present the lowest exergetic efficiencies of all components. This is also underlined by **Fehler! Verweisquelle konnte nicht gefunden werden.**, presenting the irreversibilities, which include exergy destruction.

Table 26 - Overview of all component efficiencies

COMPONENT	FUEL	ENERGETIC EFFICIENCY η (%)	EXERGETIC EFFICIENCY ε (%)	RATIONAL EFFICIENCY Ψ (%)
Compressor	NG	82.0*	87.0	87.0
	Biogas	82.0*	87.0	87.0
	Syngas	82.0*	87.0	87.0
Recuperator	NG	82.8**	88.5	94.5
	Biogas	84.5**	88.9	94.6
	Syngas	86.7**	89.7	94.8
Combustion Chamber	NG	99.0*	62.1	78.1
	Biogas	99.0*	62.1	78.1
	Syngas	99.0*	62.4	78.4
Gas Turbine	NG	0.87*	94.7	97.2
	Biogas	0.87*	91.3	95.5
	Syngas	0.87*	89.5	94.6
Power Generator	NG	99.0*	99.0	99.0
	Biogas	99.0*	99.0	99.0
	Syngas	99.0*	99.0	99.0
HRSG	NG	80.0*	37.1	64.9
	Biogas	80.0*	37.2	64.9
	Syngas	80.0*	37.2	64.9
Overall	NG	50.9	33.8	41.6
	Biogas	48.6	31.8	39.5
	Syngas	47.9	31.4	39.0

Source: Author himself. *adopted value **determined effectiveness

Figure 21 - Irreversibility of each component

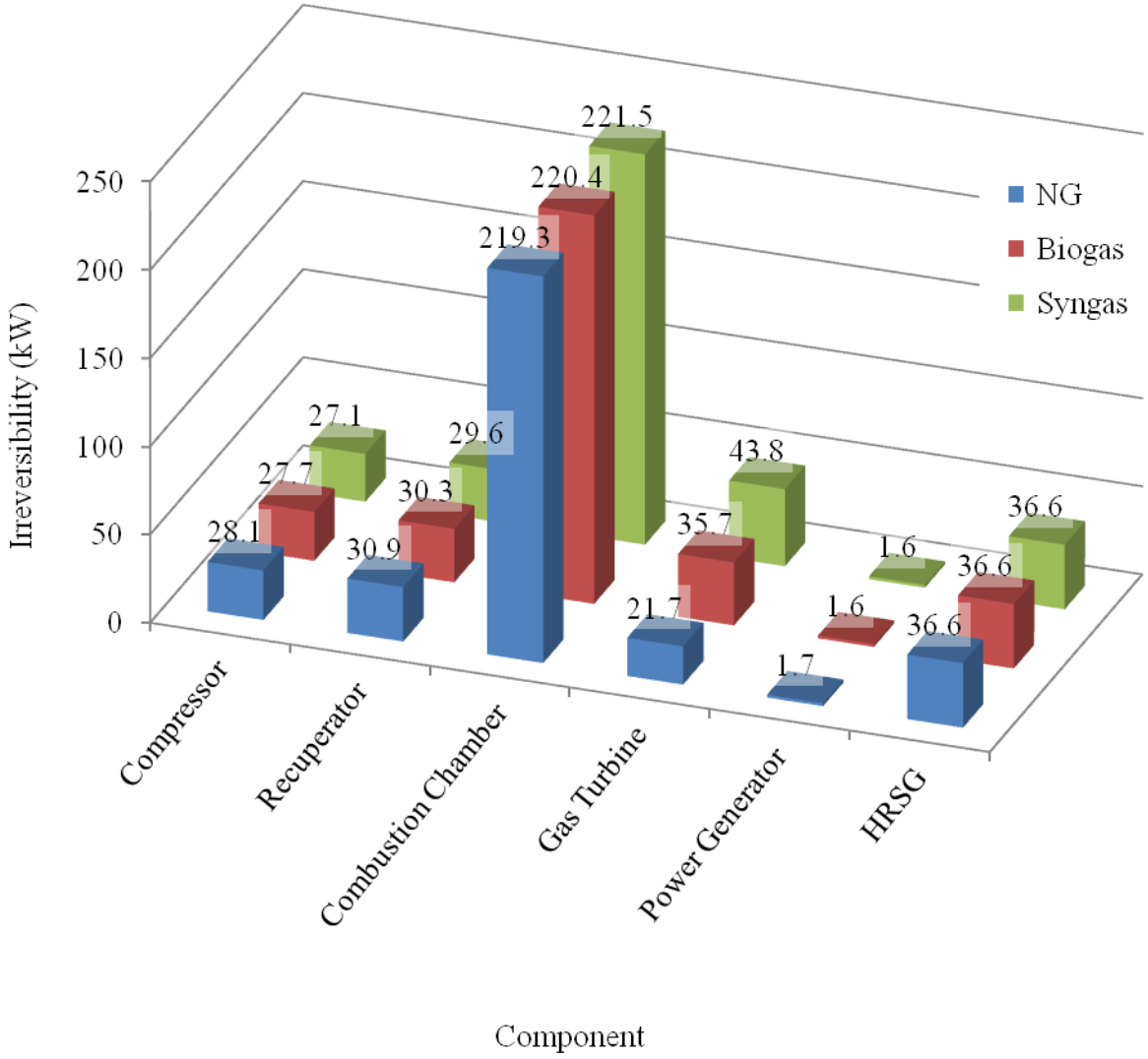

Source: Author himself.

Figures 20 and 21 show that the greatest amount of irreversibility takes place in the combustion chamber (approximately 220 kW – 63% of total plant irreversibility). The high irreversibility is caused mainly by the chemical combustion reactions which cannot be reversed – it is impossible to produce fuel out of combustion gases and heat – and conforms to the literature (ANVARI, SARAY and BAHLOULI, 2015). The irreversibilities in the HRSG and the recuperator are caused mostly by the temperature differences between the involved fluids and the irreversibilities in the compressor, gas turbine and power generator result primarily from the respective energetic component efficiencies. Just like the energetic efficiency, also the exergetic efficiency of the gas turbine declines with decreasing LHV of the fuel – consequently, the irreversibility increases. The total plant irreversibilities for NG, biogas and syngas operation are 338.4 kW, 352.3 kW and 360.1 kW, respectively.

Figure 22 - Mean percentage distribution of irreversibilities in the components

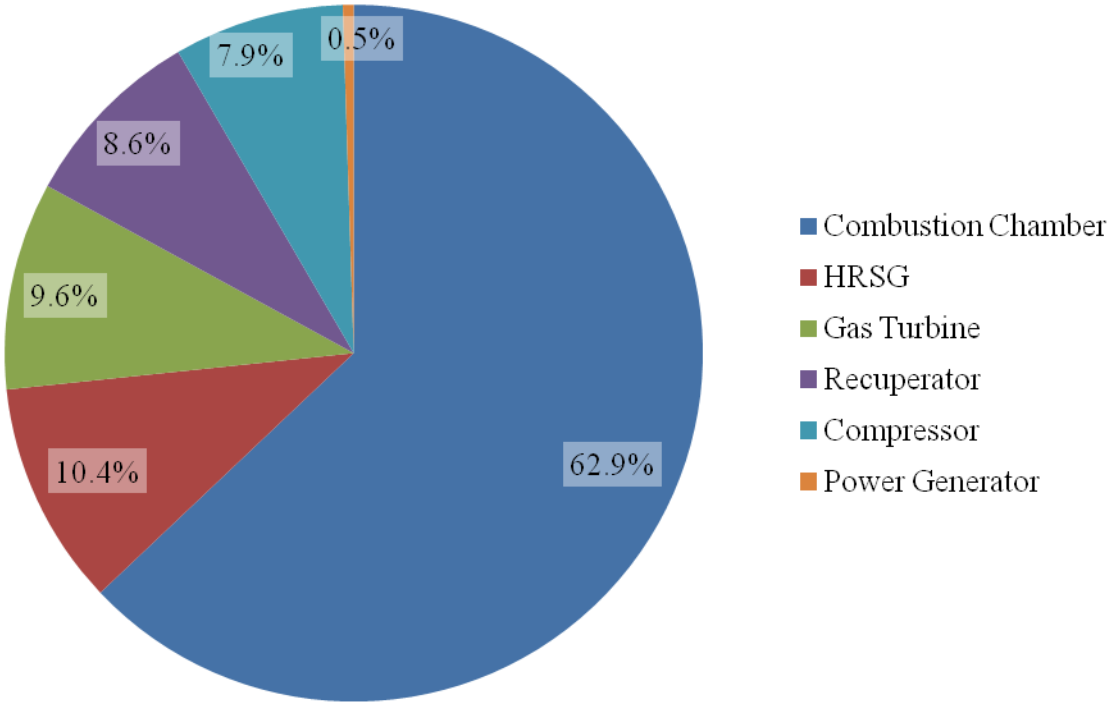

Source: Author himself.

4.3 RESULTS AND DISCUSSION OF EMISSIONS ANALYSIS

The pollutant emissions (CO_2, SO_2 and NO_x) and the CO_2-equivalent for NG, biogas and syngas operation are shown in Table 27, in kg emissions per kg of fuel and in tonnes of emissions per year (considering 7000 hours of operation per year). For the interpretation of Table 27, it is important to remember, that due to the LHV of the fuels, the fuel-flow of NG is the smallest (0.012 kg/s), biogas presents a medium fuel-flow (0.028 kg/s) and syngas the largest fuel flow (0.052 kg/s). As a result, due to its greater heating value, i.e. NG has the highest NO_x emissions per kg of fuel, but the lowest NO_x emissions per year. The more important statistics are the emissions per year. The CO_2 emissions of the biofuels biogas and syngas are adjusted to the lifecycle (see chapter 3.3). Therefore, their CO_2 emissions are much lower than the ones of NG. This is also directly reflected in the CO_2-equivalent used to calculate the pollution indicator and the ecologic efficiency. Besides the CO_2 emissions, the most significant difference between the three fuels is the greater amount of NO_x emissions per year for syngas operation – approximately twice as higher than for NG and biogas operation. All in all, the CO_2-equivalent of biogas per year is the smallest, while NG accounts for the by far greatest emissions.

Table 27 - Pollutant emissions per kg of fuel and per year

EMISSION	NG (kg/kg)	BIOGAS (kg/kg)	SYNGAS (kg/kg)	NG (t/year)	BIOGAS (t/year)	SYNGAS (t/year)
(CO_2)	2.693	0.173*	0.336*	797.3	119.7*	428.5*
(SO_2)	$24 \cdot 10^{-6}$	$13 \cdot 10^{-6}$	$3 \cdot 10^{-6}$	$7 \cdot 10^{-3}$	$9 \cdot 10^{-3}$	$4 \cdot 10^{-3}$
(NO_x)	$740 \cdot 10^{-6}$	$320 \cdot 10^{-6}$	$380 \cdot 10^{-6}$	$219 \cdot 10^{-3}$	$221 \cdot 10^{-3}$	$485 \cdot 10^{-3}$
$(CO_2)_e$	2.732	0.190	0.355	808.8	131.4	453.0

Source: Author himself. *Lifecycle adjusted

An overview of the pollution indicators and ecologic efficiencies of the three cases are presented in Table 28. To help understand and classify the values, the ecologically cleanest fuel (hydrogen) and the most polluting fuel (sulphur) are included in the table. Of the three studied fuels, Biogas offers the highest ecologic efficiency (99.1%). Syngas has a lower ecologic efficiency due to its higher CO_2 and NO_x. NG has the lowest ecologic efficiency, as the CO_2 lifecycle cannot be considered for fossil fuels.

Table 28 - Pollution indicator and ecologic efficiency

FUEL	Πg (kg/MJ)	ε
Hydrogen	0.000	1.000
Biogas	0.009	0.991
Syngas	0.033	0.968
NG	0.058	0.948
Sulphur	134.000	0.000

Source: Author himself.

4.4 RESULTS AND DISCUSSION OF ECONOMIC ANALYSIS

When it comes to economic analyses, it is important to stress, that the prices of both purchased and sold products greatly influence the results. Moreover, the prices of electricity and fuels succumb to strong fluctuations and uncertainties – even more so, when converting local Brazilian prices from BRL to USD. It is therefore difficult to pinpoint particular prices.

Keeping this in mind, Table 29 presents an overview of prices and costs thoughtfully determined and adopted in chapter 3.3. The applied currency exchange rate is 0.26 USD/BRL, from November 2015.

Table 29 - Overview of prices and costs

SYMBOL	DEFINITION	VALUE (USD/kWh)
C_{bio}	Biogas price	0.019
$C_{M,cb}$	Maintenance and op. cost of the conv. boiler system	0.008
$C_{M,HRSG}$	Maintenance and operation cost of HRSG	0.006
$C_{M,gts}$	Maintenance and operation cost of MGT system	0.012
C_{NG}	NG price	0.063
C_{syn}	Syngas price	0.070
P_{el}	Electric energy price	0.190
P_{oil}	Fuel oil price	0.093

Source: Author himself.

The determined production costs of electric power and steam are illustrated for all fuels in Figures 23 and 24, respectively, with variation of the annual interest rate between 4%, 8% and 12%. Because the system presents very similar efficiencies, power outputs and steam outputs for all fuels, the production costs are mainly influenced by the fuel costs and the annual interest rate. Furthermore, in case of biogas and syngas operation, 11 kW of the produced electric power are absorbed by the gas booster (compressor), necessary to generate the pressure to inject the fuel into the combustion chamber. NG is already supplied in high-pressure, and does not require further pressurisation.

Figure 23 - Electric power production costs with variation of the annual interest rate

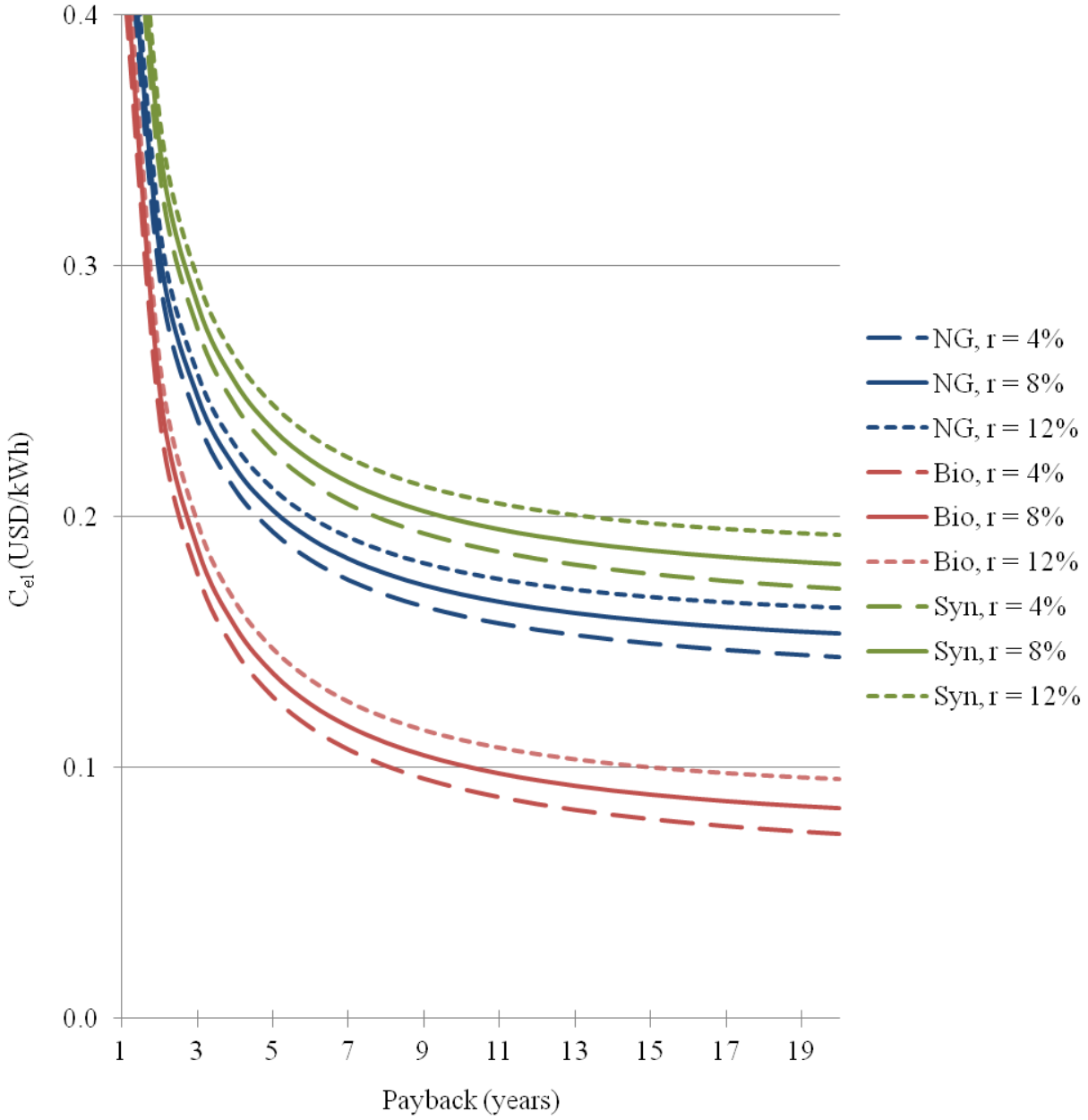

Source: Author himself.

The production costs decrease over the years, even though the fuel costs are adopted as constant values, because the cost related to the initial investment in the plant (C_{INV}) reduces as the plant is amortised with time – see equations (4.2) and (4.6). This behaviour is described by the annuity factor, depending on the annual interest rate, and is depicted in Figure 25. Another factor that can influence C_{INV} is the hours of operation per year (H). But for this study, H is a fixed value of 7000 h/year and its impact is therefore not discussed.

Figure 24 - Steam production costs with variation of the annual interest rate

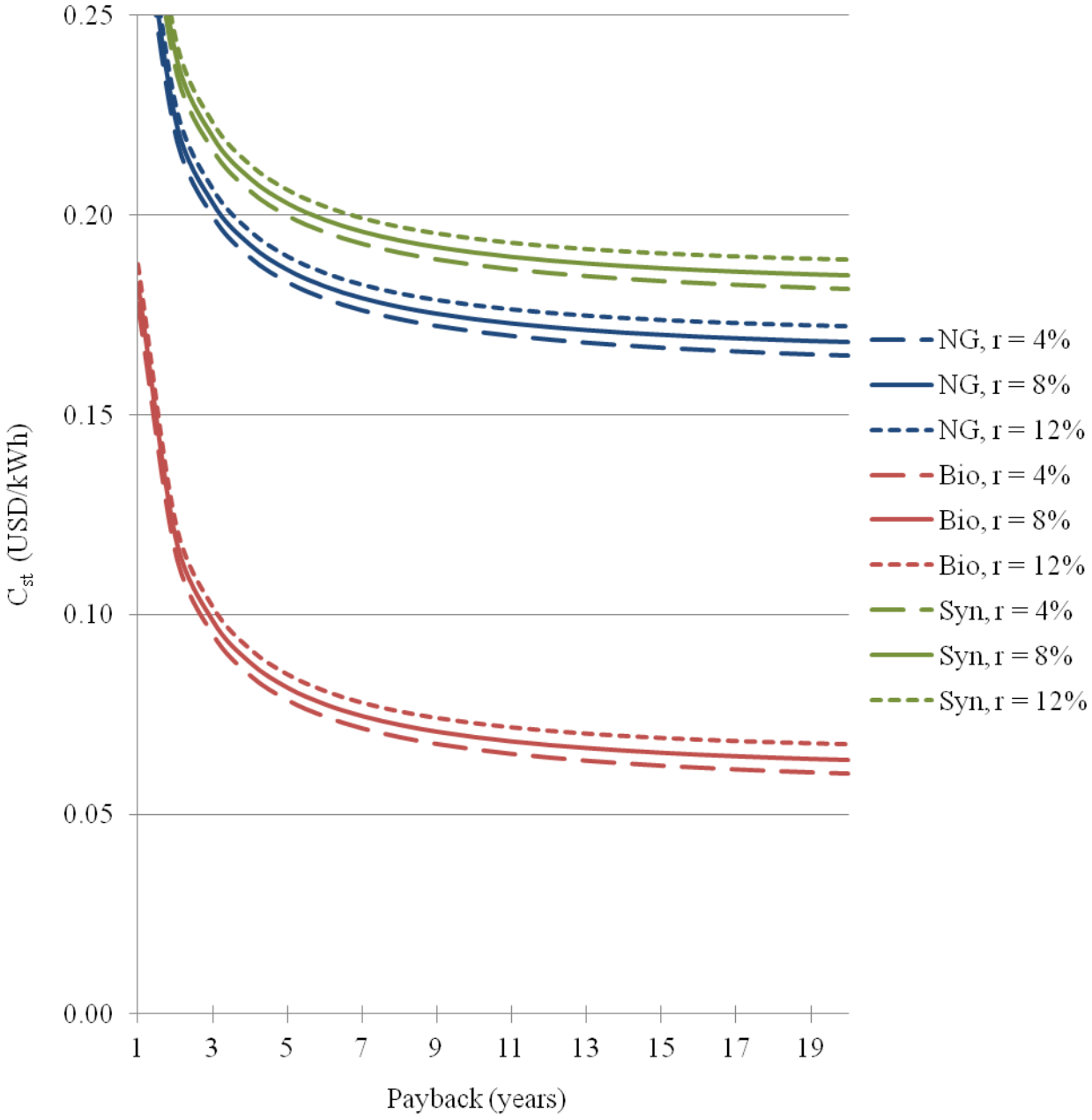

Source: Author himself.

An interesting development when comparing power (C_{el}) and steam (C_{st}) production costs is that for NG operation (e.g. r = 8%), C_{el} is higher than C_{st} in the first seven years and afterwards C_{st} is higher. In case of syngas operation (e.g. r = 8%), this change occurs only after 15 years. For biogas operation, C_{el} is always higher than C_{st}.

Figure 25 - Development of annuity factor over time, depending on annual interest rate

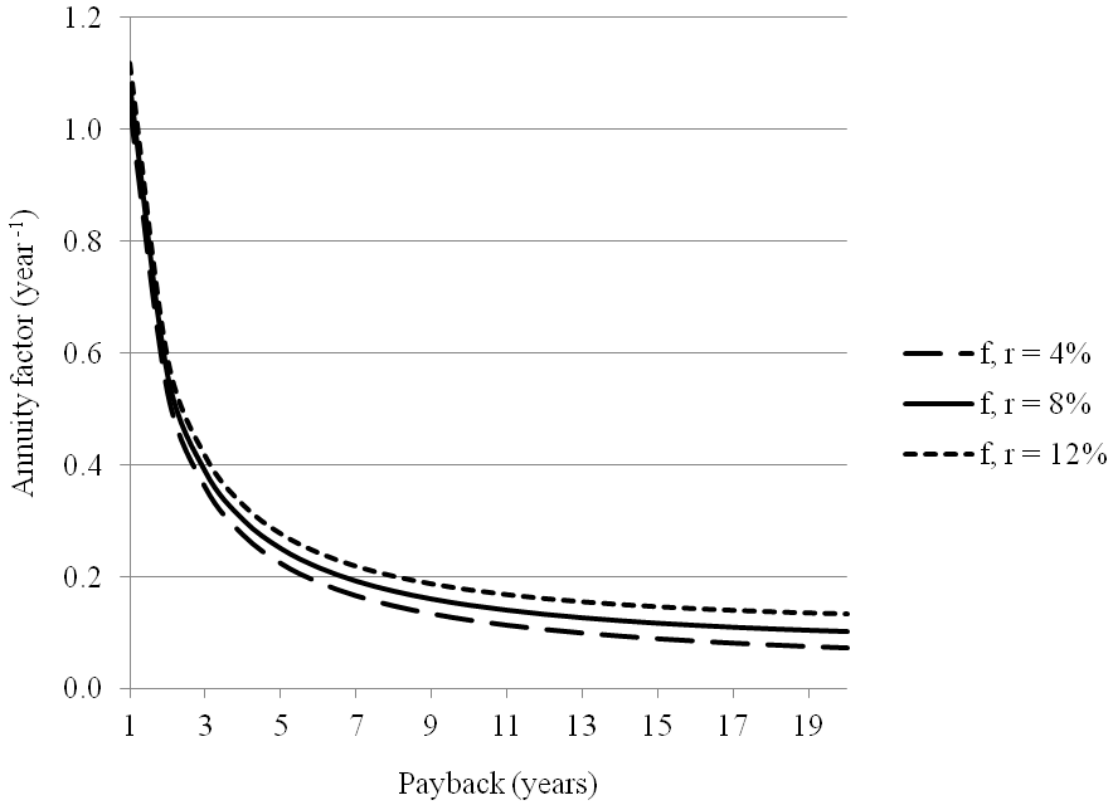

Source: Author himself.

The total expected annual saving, including electric power and steam savings, for all three fuel cases is presented in Figure 26, with variation of the annual interest rate. In case of NG operation, the shortest determined payback period is 11 years, when assuming a low annual interest rate of 4%. Considering a more realistic annual interest rate of 8% increases the payback period to 16 years. Therefore, with the current cost situation, NG operation of the Capstone C200 cannot be considered feasible and is not recommended for investment in Brazil. This is because electricity prices in Brazil have not increased significantly in the last several years, even though NG prices have risen dramatically.

Due to the estimated low cost of biogas (approximately 30% of NG price), the biogas scenario offers the highest expected annual saving and fastest payback. The payback periods for biogas operation and annual interest rates of 4%, 8% and 12% are 2.5, 2.8 and 3.0 years, respectively. This combined with the large expected annual saving, shows that biogas operation of the Capstone C200 in cogeneration mode is economically highly feasible and recommendable for investment independent of the annual interest rate. The implementation of the proposed cogeneration plant is hence mainly limited by biogas production and availability.

The syngas production process by biomass gasification is much more complex than anaerobic digestion to produce biogas. Moreover, according to Gerssen-Gondelach et al.

(2014), it is still an early commercial technology and not as well established as anaerobic digestion. As a result, syngas cost is much higher than biogas cost and for the required small consumption, even higher than NG cost. Due to this, syngas operation is found to be economically unfeasible for this MGT.

NG operation would become economically feasible (for this scenario defined by payback periods of six years considering an annual interest rate of 8%) if NG prices would drop to 0.05 USD/kWh or less, or alternatively, if electricity prices would rise to 0.23 USD/kWh or more. Accordingly for syngas operation, economically feasible syngas prices would be 0.45 USD/kWh or less, or alternatively electricity prices of 0.27 USD/kWh or more.

Figure 26 - Expected annual saving with variation of the annual interest rate

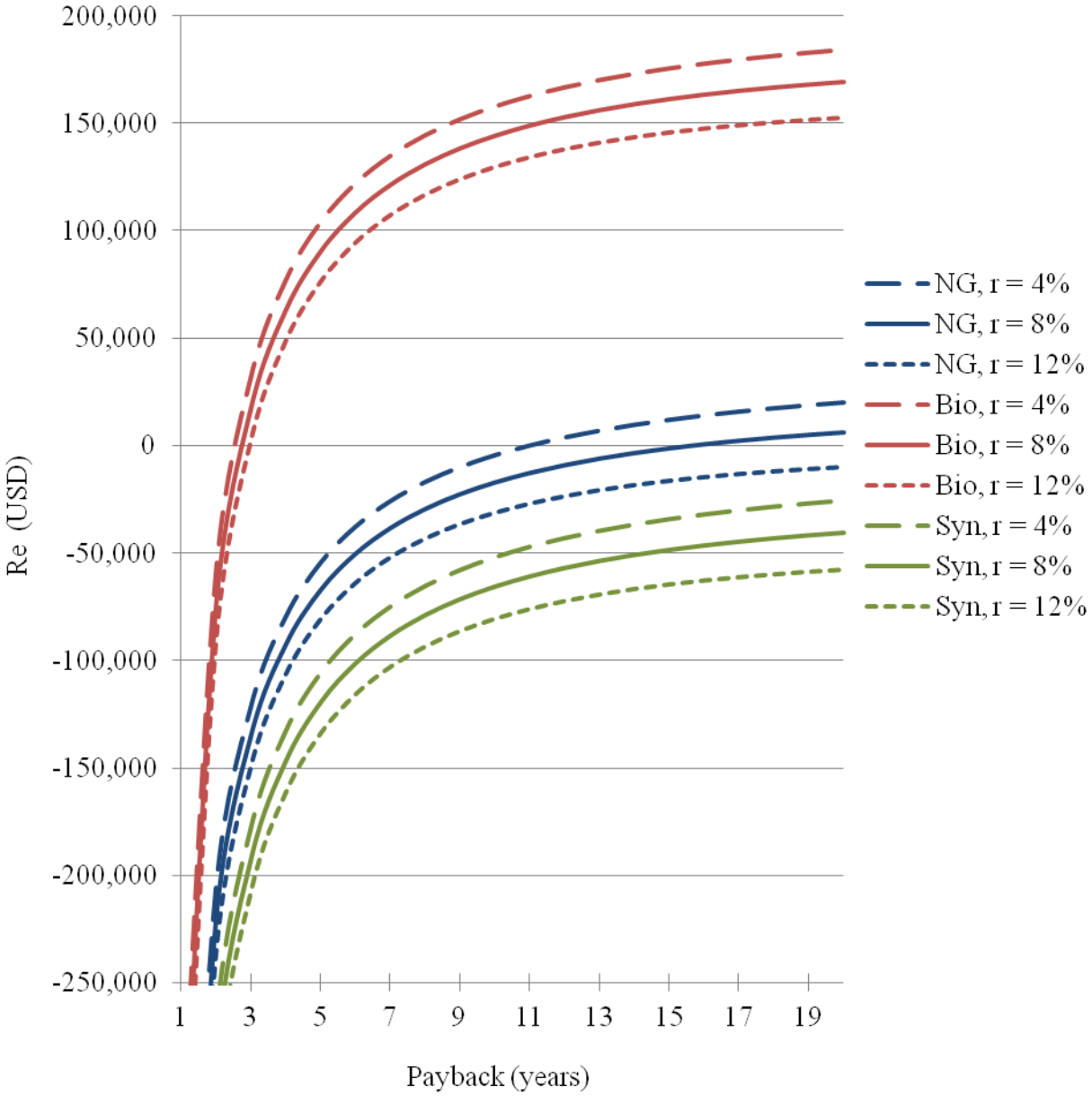

Source: Author himself.

5 CONCLUSION

The successfully conducted analyses show that the MGT Capstone C200 with a nominal power output of 200 kW is technically feasible for NG, biogas and syngas operation and can also be implemented for cogeneration. The available fuel-specific versions of the Capstone C200 allow operation at high efficiencies and performance with all three fuels. The determined energetic and exergetic efficiencies correspond with the literature and are in the expected range for micro gas turbines of this capacity. The high irreversibility (exergetic destruction) in the combustion chamber is a mostly unavoidable result of the chemical combustion reactions. Furthermore, the irreversibility in the MGT increases with decreasing LHV of the fuel, as the turbine operates in off-design mode.

Moreover, the two presented methods for the adjustment of ISO-condition gas turbine data to local conditions stand in decent accordance with one another and can hence be considered viable.

Regarding the pollutant exhaust gas emissions considering the CO_2-lifecycle for biofuels, biogas operation was found to have the highest ecologic efficiency, closely followed by syngas. Syngas has a lower ecologic efficiency than biogas, due to its higher CO_2 and NO_x emissions. NG presented the lowest ecologic efficiency, as the CO_2 lifecycle cannot be considered for fossil fuels. Nevertheless, NG can be considered as the cleanest fossil fuel.

On the one hand, oil and therefore NG prices have risen dramatically in the last several years. The Brazilian electricity, on the other hand, is predominantly produced by hydropower and therefore the local electric power prices have not increased significantly – not even nearly proportional to the NG price. As a result, the MGT cogeneration system operating on NG was determined to be economically unfeasible – even when considering very low annual interest rates. The biogas price, however, is estimated much lower than the NG price. Thus, the cogeneration plant operating on biogas proved to be economically highly feasible (for all analysed annual interest rates) with short payback periods and large expected annual saving. All in all, the plant operating on biogas is limited principally by the biogas production and availability. Because biogas is difficult to compress and transport, its use is mostly constricted to the site of anaerobic digestion. The adopted syngas price is even slightly higher than the NG price. In accordance to Parajuli et al. (2014), syngas price depends greatly on production capacity of the facility. Consequently, syngas operation is economically not feasible for a single MGT (small fuel consumption). In accordance to Gerssen-Gondelach et al. (2014), syngas production by gasification is still an early commercial technology. Syngas prices are

hence likely to reduce in the future through further optimisation and commercialisation and could then become economically feasible for use in MGTs.

Summarising all results, the proposed cogeneration plant promises the highest overall feasibility operating on biogas. From a technical standpoint, it is important to consider fuel optimisation of the combustion chamber and especially the fuel injection system. Furthermore, biogas operation offered the lowest values for pollutant emissions and therefore the highest ecologic efficiency. Biogas was found to be a very attractive fuel that promises high annual savings and can simultaneously contribute to the reduction of global warming and counteract against the imminent depletion of fossil fuels.

Finally, experimental tests and studies are suggested to verify whether the exhaust gas temperature (T_6) and the exhaust mass flow ($\dot{m}_{cg}$) of the MGT Capstone C200 really are independent of the fuel, as adopted in accordance to Vescovo (2015).

REFERENCES

ANTUNES, J. S. **Código computacional para análise de sistemas de cogeração com turbinas a gás** *(Computer code for analysis of cogeneration systems with gas turbines)*. 196 p. Thesis (Doctor in Mechanical Engineering) – Faculty of Engineering of Guaratinguetá, São Paulo State University, Guaratinguetá, 1999 (in Portuguese).

ANVARI, S., SARAY, R., K., BAHLOULI, K. Conventional and advanced exergetic and exergoeconomic analyses applied to a tri-generation cycle for heat, cold and power production. **Energy.** v. 91, p. 925-939. 2015.

BALESTIERI, J. A. P. **Cogeração:** geração combinada de eletricidade e calor *(Cogeneration: Combined generation of electricity and heat)*. Florianópolis: Editora da UFSC, 2002. 219 p (in Portuguese).

BARGOZZI, G., PERDICHIZZI, A., GRITTI, C., GUAIATELLI, I. Techno-economic analysis of gas turbine inlet air cooling for combined cycle power plant for different climatic conditions. **Applied Thermal Engineering.** v. 82, p. 57-67. 2015.

BASU, S., KHAN, A. L., CANO-ODENA, A., LIU, C., VANKELECOM, I. F. J. Membrane-based technologies for biogas separations. **Chemical Society Reviews.** v. 39, p. 750-768. 2010.

BOERRIGTER, H., RAUCH, R. Syngas production and utilisation. In: KNOEF, H. A. M. (Ed.). **Handbook Biomass Gasification.** Enschde: Biomass Technology Group (BTG), 2005. cap. 10, p. 211-230.

BRIZI, F., SILVEIRA, J. L., DESIDERI, U., REIS, J. A., TUNA, C. E., LAMAS, W. Q. Energetic and economic analysis of a Brazilian compact cogeneration system: comparison between natural gas and biogas. **Renewable and Sustainable Energy Reviews.** v. 38, p. 193-211. 2014.

CAMERETTI, M. C., TUCCILLO, R., PIAZZESI, R. Study of an exhaust gas recirculation equipped micro gas turbine supplied with bio-fuels. **Applied Thermal Engineering.** v. 59, p. 162-173. 2013.

CAPSTONE TURBINE CORPORATION. **Capstone corporate brochure.** Chatsworth: 2015. 17 p. Available at: <www.ibtgroup.it/download/pdf/en/Capstone%20Overview.pdf> Accessed on 17. Sept. 2015.

CAPSTONE TURBINE CORPORATION. **Capstone C200 microturbine:** technical reference. 410066 Rev C. Chatsworth: 2009. 137 p.

CAPSTONE TURBINE CORPORATION. **Technical reference: capstone MicroTurbine™ systems emissions.** 410065 Rev B. Chatsworth: 2008. 6 p.

CÂRDU, M., BAICA, M. Regarding a global methodology to estimate the energy-ecologic efficiency of thermopower plants. **Energy Conversion & Management.** v. 40, p. 71-87. 1999a.

CÂRDU, M., BAICA, M. Regarding a new variant methodology to estimate globally the ecologic impact of thermopower plants. **Energy Conversion & Management.** v. 40, p. 1569-1575. 1999b.

COMGÁS. **Comgás website:** data of natural gas. 2015a. Available at: <http://www.comgas.com.br/pt/gasNatural/conhecaGasNatural/Paginas/a-composicao.aspx> Accessed on 17. Oct. 2015.

COMGÁS. **Comgás website:** price rates of natural gas. 2015b. Available at: <http://www.comgas.com.br/pt/nossosServicos/Tarifas/Paginas/comercial.aspx> Accessed on 3. Nov. 2015.

CORONADO, C. J. R. **Análise técnica econômica de um gaseificador de biomassa de 100 kg/h para acionamento de um motor de combustão interna** *(Technical and economical analysis of a biomass gasifier of 100 kg/h to drive an internal combustion engine).* 195 p. Dissertation (Master in Mechanical Engineering) – Faculty of Engineering of Guaratinguetá, São Paulo State University, Guaratinguetá, 2007 (in Portuguese).

CORONADO, C. J. R., YOSHIOKA, J. T., SILVEIRA, J. L. Electricity, hot water and cold water production from biomass. Energetic and economic analysis of compact system of cogeneration run with woodgas from a small downdraft gasifier. **Renewable and Sustainable Energy Reviews.** v. 36, p. 1861-1868. 2011.

DAHL, R. A Second life for scraps: making biogas from food waste. **Environmental Health Perspectives.** v. 123, nr. 7, p. 181-183. 2015.

DENG, Y., PARAJULI, P. B. **Evaluation of syngas production unit cost of bio-gasification facility using regression analysis techniques.** In: 2011 ASABE Annual International Meeting. Louisville: 2011. 11 p.

DILTZ, R., PULLAMMANAPPALLIL P. Biofuels from algae. In: FANG, Z. (Ed.). **Liquid, gaseous and solid biofuels:** conversion techniques. InTech, 2013. cap. 14. p. 431-449. Available at: <http://www.intechopen.com/> Accessed on 24. Sept. 2015.

GAS TURBINE WORLD. **2012 gas turbine world handbook.** Fairfield: Pequot Publication Inc., 2011. 212 p.

GERSSEN-GONDELACH, S. J., SAYGIN, D., WICKE, B., PATEL, M. K., FAAJI, A. P. C. Competing uses of biomass: assessment and comparison of the performance of bio-based heat, power, fuels and materials. **Renewable and Sustainable Energy Reviews.** v. 40, p. 964-998. 2014.

GILLETTE, S. **Microturbine technology matures**. Capstone Turbine Corp. 2010. Available at: <http://www.powermag.com/microturbine-technology-matures/?pagenum=1> Accessed on 17. Sept. 2015.

GUPTA, K. K., REHMAN, A., SARVIYA, R. M. Bio-fuels for the gas turbine: a review. **Renewable and Sustainable Energy Reviews.** v. 14, p. 2946-2955. 2010.

HUTTUNEN, S., MANNINEN, K., LESKINEN, P. Combining biogas LCA reviews with stakeholder interviews to analyse life cycle impacts at a practical level. **Journal of Cleaner Production.** v. 80, p. 5-16. 2014.

KANG, D. W., KIM, T. S., HUR, K. B., PARK, J. K. The effect of firing biogas on the performance and operating characteristics of simple and recuperative cycle gas turbine combined heat and power systems. **Applied Energy.** v. 93, p. 215-228. 2012.

KANG J. Y., KANG, D. W., KIM, T. S., HUR, K. B. Comparative economic analysis of gas turbine-based power generation and combined heat and power systems using biogas fuel. **Energy.** v. 67, p. 309-318. 2014.

MACHIN, E. B. **Analise técnica, econômica e ecológica da incorporação de sistemas de gaseificação de bagaço de cana-de-açúcar no setor sucroalcooleiro:** uso de ciclos combinados para o aumento da oferta de eletricidade *(Technical, economic and ecological analysis of incorporating gasification of sugarcane bagasse systems into the sugar and alcohol sector: the use of combined cycles to increase electricity supply)*. 172 p. Thesis (Doctor in Mechanical Engineering) – Faculty of Engineering of Guaratinguetá, São Paulo State University, Guaratinguetá, 2015 (in Portuguese).

MCALLISTER, S., CHEN, J.-Y., FERNANDEZ-PELLO, A. C. Thermodynamics of combustion. In: **Fundamentals of combustion processes.** New York: Springer, 2011. p. 15-47.

MKOMA, S. L., MABIKI F. P. Theoretical and practical evaluation of jatropha as energy source biofuel in Tanzania. In: BERNARDES, M. A. S. (Ed.). **Economic effects of biofuel production**. InTech, 2011. cap. 9. p. 181-200. Available at: <http://www.intechopen.com/> Accessed on 24. Sept. 2015.

NADIR, M., GHENAIET, A. Thermodynamic optimization of several (heat recovery steam generator) HRSG configurations for a range of exhaust gas temperatures. **Energy.** v. 86, p. 685-695. 2015.

NIKPEY, H., ASSADI, M., BREUHAUS, P., MØRKVED, P. T. Experimental evaluation and ANN modeling of a recuperative micro gas turbine burning mixtures of natural gas and biogas. **Applied Energy.** v. 117, p. 30-41. 2014.

PARAJULI, P. B., DENG, Y., KIM, H., Yu, F. Cost analysis model for syngas production cost evaluation using the graphical user interface. **Energy and Power.** v. 2, p. 35-40. 2014.

PILAVACHI, P. A. Mini- and micro-gas turbines for combined heat and power. **Applied Thermal Engineering.** v. 22, p. 2003-2014. 2002.

PIRC, A., SEKAVČNIK, M., MORI, M. Universal model of a biomass gasifier for different syngas compositions. **Journal of Mechanical Engineering**. v. 58, p. 291-299. 2012.

SIEDLECKI, M., DE JONG, W., VERKOOIJEN, A. H. M. Fluidized bed gasification as a mature and reliable technology for the production of bio-syngas and applied in the production of liquid transportation fuels: a review. **Energies.** v. 4, p. 389-434, 2011.

SILVA, E. B., BRINGHENTI, C., ASSATO, M., LIMA, R. C. Gas turbine performance analysis operating with low heating value fuels. **Thermal Engineering.** v. 12, p. 8-15. 2013.

SILVEIRA, J. L. **Cogeração disseminada para pequenos usuários:** estudos de casos para o setor terciário *(Cogeneration disseminated to small users: Case studies for the tertiary sector)*. 192 p. Thesis (Doctor in Mechanical Engineering) – Faculty of Mechanical Engineering, Campinas State University, Campinas, 1994 (in Portuguese).

SILVEIRA, J. L., LAMAS, W. Q., TUNA, C. E, VILLELA, I. A. C., MIRO, L. S. Ecological efficiency and thermoeconomic analysis of a cogeneration system at a hospital. **Renewable and Sustainable Energy Reviews.** v. 16, p. 2894-2906, 2012.

SILVEIRA, J. L., TUNA, C. E. Thermoeconomic analysis method for optimization of combined heat and power systems. Part I. **Progress in Energy and Combustion Science.** v. 29, p. 479–485, 2003.

SILVEIRA, J. L., TUNA, C. E. Thermoeconomic analysis method for optimization of combined heat and power systems. Part II. **Progress in Energy and Combustion Science.** v. 30, p. 673–678, 2004.

SILVEIRA, J. L., WALTER, A. C. S., LUENGO, C. A. A case study of compact cogeneration using various fuels. **Elsevier.** v. 76, p. 447-451. 1997.

SOMEHSARAEI, H. N., MAJOUMERD, M. M., BREUHAUS, P., ASSADI, M. Performance analysis of a biogas-fueled micro gas turbine using a validated thermodynamic model. **Applied Thermal Engineering.** v. 66, p. 181-190. 2014.

SUN, L., DOYLE, S., SMITH, R. Understanding steam costs for energy conservation projects (article in progress). **Applied Energy.** 9 p. 2015.

SWEDISH GAS TECHNOLOGY CENTER. **Basic Data on Biogas.** 2nd ed. Lund: Serviceförvaltningen i Lunds kommun, 2012. 23 p.

SZARGUT, J. **Exergy Method: Technical and Ecological Applications.** Boston: WIT Press, 2005. 192 p.

TSATSARONIS, G. Definitions and nomenclature in exergy analysis and exergoeconomics. **Energy.** v. 32, p. 249-253. 2007.

VESCOVO, E. O. **Capstone C200 biogás** [personal message]. Message received by <benjamin.kunte@gmail.com> on 11. Nov. 2015.

VILLELA, I. A. C. **Desenvolvimento de um modelo termoeconômico que considera os impactos ambientais** *(Development of a thermoeconomic model that considers the environmental impacts).* 151 p. Thesis (Doctor in Mechanical Engineering) – Faculty of Engineering of Guaratinguetá, São Paulo State University, Guaratinguetá, 2007 (in Portuguese).

VILLELA, I. A. C., SILVEIRA, J. L. Ecological efficiency in thermoelectric power plants. **Applied Thermal Engineering.** v. 27, p. 840-847. 2007.

WOOLCOCK, P., BROER, K. **CSET Studies Clean Syngas Production.** Iowa State University of Science and Technology, 2012. Available at: <http://old.iprt.iastate.edu/news/2011/cset_syngas.html> Accessed on 21. Oct. 2015.